

## Search and characterization of third bodies around binary systems using data from Kepler and TESS satellites

1 JEFFERSON R. P. INÁCIO,<sup>1</sup> LEONARDO A. ALMEIDA,<sup>2,1</sup> JOSÉ R. P. DA SILVA,<sup>1</sup> AND ISAAC M. MACÊDO.<sup>1</sup>

2 <sup>1</sup> Universidade do Estado do Rio Grande do Norte  
3 Mossoró, RN, Brazil

4 <sup>2</sup> Universidade Federal do Rio Grande do Norte  
5 Natal, RN, Brazil

### ABSTRACT

The study of the orbital period variation of short-period binary systems (< 10 days) has been important to understand several physical phenomena, such as the emission of gravitational waves, angular momentum loss via magnetic braking, matter transfer between the components, apsidal motion, quadrupole moment variation and presence of circumbinary bodies. In the latter scenario, the additional body could be a planet and is therefore crucial to understanding how these objects are formed and how they evolve around two parent stars. With the advent of large space missions, for example Kepler and TESS (Transiting Exoplanet Survey Satellite), an enormous amount of high precision photometric data with temporal coverage from years to decades has become available. Thus, in this work we propose to study the orbital period variation of a sample of 240 binary systems that was observed by the Kepler and TESS and, therefore, with a temporal coverage of more than 14 years. The main goal of this paper is the search and characterization of third bodies, however, all phenomena that generate the variation of the orbital period of binary systems will be investigated. Out of the sample of 240 binary star systems, 73 of them showed cyclic variation in their O-C diagrams and 167 of them have no cyclic variation in the O-C diagram detected.

**Keywords:** Exoplanets (498) — Multiple stars (1081) — Eclipsing binary stars (444) — Variable star period change (1760)

### 1. INTRODUCTION

Binary stars, which consist of two stars orbiting a common center of mass, have contributed richly to several areas in Astrophysics (). A subclass of these systems, the eclipsing binaries, which have their orbital planes in the observer's line of sight and therefore eclipse each other, are used to determine distances, and calculate fundamental parameters of stars (e.g. mass and radii) to test models of stellar evolution (e.g., Pietrzyński et al. 2012; Almeida et al. 2015, 2017).

Another topic of fundamental importance on eclipsing binary systems is the study of orbital period variation. They are used to understand various physical phenomena, e.g., emission of gravitational waves (Hulse & Taylor 1975), loss of angular momentum via magnetic braking (Tout & Hall 1991), transfer of matter between components (Tout & Hall 1991; Cehula & Pejcha 2023), apsidal motion (Gimenez & Garcia-Pelayo 1983), variation of quadrupole momentum (Applegate & Patterson 1987) and the presence of circumbinary bodies

(Correia et al. 2016). In the latter scenario, the additional bodies could be planets, and therefore, crucial to understand how these objects are formed and how they evolve around two parent stars (Martin & Triaud 2015).

Space missions, such as Kepler and TESS (*Transiting Exoplanet Survey Satellite*), have contributed significantly to the discoveries of planets around single stars and in multiple systems (). Kepler, launched by NASA (North American Space Agency), began its mission in 2009 and had as main scientific objective to detect exoplanets by the method of planetary transits, with emphasis on terrestrial planets ( $R < 2.5R_{\oplus}$ ), located within the habitable zones of Sun-like stars (Borucki et al. 2010). To continue with the mission to discover exoplanets, the TESS space telescope was launched in 2018 by NASA, and it is still in full operation with the aim of researching planets that transit bright stars and close to the Sun (Ricker et al. 2014).

Combining data from the Kepler and TESS satellites, with temporal coverage of more than 14 years of obser-

vation, provides an excellent opportunity to study long-term phenomena. In this context, this paper aims to study the orbital period variation of the eclipsing binary systems observed by the Kepler and TESS satellites. To do so, we selected a sample of 240 eclipsing binary systems reported by Conroy et al. (2014) with data of both missions. The analysis of the orbital period variation of these systems will be done through the O-C (Observed minus Calculated) diagrams, see e.g. (), and classified in cyclic and non-cyclic variations. For the systems with cyclic variations, it will be investigated if additional bodies can explain their O-C diagrams.

This paper is organized as follow. Sections 2 and 3 present the data used for our study and physical phenomena associated with the orbital period variation of binary systems, respectively. In Section 4, we present the approach of correcting the light curves, the determination of the binary orbital period, the eclipse time measurements, the construction of the O-C diagram, and the third body modelling. Finally, in Section 5 we present the results of this study and discuss them in Section 6.

## 2. DATA

The data used in this paper are from a sample of 240 close binary systems taken from Conroy et al. (2014). Sample selection was based on the criterion that the target had been observed by the Kepler and TESS satellites. Thus, temporal baseline of observations of our targets is more than 14 years. In Table 1, we list all targets with the binary's orbital period, eccentricity and orbital period of the third body found by Conroy et al. (2014).

**Aqui tem que dizer como você obteve os dados tanto do Kepler quanto do TESS da sua amostra, indicando o caminho, pagina, ect**

- Extraction of the light curve from our sample using the library *Lightkurve*;
- Light curve correction, e.g., subtraction of trends, normalization and removal of outliers, using library tools *Lightkurve*;
- Determining the orbital period of the system using the Lomb-Scargle and PyAstronomy's Stringlength<sup>1</sup> (Czesla et al. 2019) tools;
- Phasing the light curve using the orbital period obtained in the previous item;

<sup>1</sup> <https://github.com/sczesla/PyAstronomy>

- Polyfit adjustment to obtain the eclipse instants and build the O-C diagram;
- Analysis of orbital period variation using the O-C diagram. In this step, we will consider all the physical phenomena that can generate variations in the binary period: the Applegate mechanism, the apsidal movement, the emission of gravitational waves, the magnetic braking and the light travel time effect, emphasizing the disturbances generated by a third body.

**Table 1.** Table with values for the period of the inner binary ( $P_{bin}$  (days)), period for the third body ( $P_3$  (days)) and eccentricity for the third body ( $e_3$ ) derived by Conroy et al. (2014).

KIC	$P_{bin}$ days	$P_3$ days	$e_3$
(5)	(6)	(7)	(8)
2450566	1.845	$983.7 \pm 472.8$	$0.308 \pm 0.016$
3221207	0.474	$\sim 1700$	
3228863	0.731	$644.1 \pm 15.7$	$0.000 \pm 0.003$
3641446	2.100	$228.6 \pm 1.0$	$0.000 \pm 0.010$
3936357	0.369	$\sim 2400$	

NOTE—Table 1 is published in its entirety in the machine-readable format.

As we can see in the Table 1, some objects, such as KIC 3221207 and KIC 3936357, do not have values for the eccentricity of the third body; we only have an estimate period for this examples. Possibly these parameters were not determined due to the temporal coverage of the data being relatively short for the signal sought. Thus, theoretically, we can derive them in this work by implementing the TESS data together with the Kepler data.

## 3. PHYSICAL PHENOMENA ASSOCIATED WITH THE VARIATION OF THE ORBITAL PERIOD OF BINARY SYSTEMS

The variations in the periods of binary stars are not only linked to gravitational perturbations due to other bodies close to the system, they are also related to intrinsic effects to the binary. For the analysis and interpretation of these effects, we consider the relationships listed below.

137        3.1. *Applegate mechanism*

138        From the **Applegate mechanism** (Applegate 1992),  
 139 which causes changes in the distribution of angular mo-  
 140 mentum and the shape of the magnetically active star,  
 141 the following relationship derives:

$$142 \quad \frac{\Delta P}{P} = -9 \left( \frac{R}{d} \right)^2 \frac{\Delta Q}{mR^2}, \quad (1)$$

143 where  $m$  is the mass and  $R$  the radius of the active star,  
 144  $Q$  the quadrupole moment and  $d$  the orbital separation  
 145 (Applegate & Patterson 1987).

146        3.2. *Apsidal motion*

147        For the **apsidal motion**, Gimenez & Garcia-Pelayo  
 148 (1983) points out the following relation of variation of  
 149 the moments of the eclipses of the binary:

$$150 \quad t = t_c + \frac{\theta P}{2\pi} + \frac{P}{\pi} \sum_{n=1}^{\infty} (-\beta)^n \left( \frac{1}{n} + \sqrt{1-e^2} \right) \sin n\nu, \quad (2)$$

151 where  $t_c$  is the eclipse instant for  $\theta = 0$ ,  $P$  the binary  
 152 orbital period,  $\beta = \frac{e}{1+\sqrt{1-e^2}}$ ,  $e$  the eccentricity, and  $\nu$   
 153 the true anomaly.

154        3.3. *Emission of gravitational waves*

155        For a period change caused by the **emission of grav-  
 156 itational waves**, we have the following relationship, de-  
 157 rived by Hulse & Taylor (1975), for the change in the  
 158 O-C of the binary system,

$$159 \quad O - C = -\frac{1}{2P} \frac{dP}{dt} \Delta T^2, \quad (3)$$

160 where  $\Delta T$  is the interval between the observation times  
 161 and the initial epoch of the linear ephemeris.

162        3.4. *Magnetic braking*

163        For the period variations caused by **magnetic brak-  
 164 ing**, Tout & Hall (1991) derived the relation

$$165 \quad \frac{\Delta P}{P} = - \left( \frac{R_A}{d} \right)^2 \frac{m_1 + m_2}{m_1 m_2} \Delta m, \quad (4)$$

166 where  $R_A$  is Alfvén's radius,  $\Delta m$  the mass loss rate,  $m_1$   
 167 and  $m_2$  the mass of stars and  $d$  the distance between  
 168 them.

169        3.5. *Light Travel Time Effect*

170        Finally, we have the variations caused by the **light  
 171 travel time effect**, which can be characterized as fol-  
 172 lows (Irwin 1952):

$$173 \quad \tau = \frac{z}{c} = \frac{a \sin i}{c} \frac{1 - e^2}{1 + e \cos f} \sin(f + \omega), \quad (5)$$

174 where  $a$  is the semi-major axis of the binary's orbit,  $e$  its  
 175 eccentricity,  $i$  the orbital inclination with respect to the  
 176 plane of the sky,  $\omega$  the periastron argument,  $f$  its true  
 177 anomaly,  $c$  the speed of light, and  $z$  the distance from  
 178 any point in the binary's orbit a starting from the line  
 179 perpendicular to the line of sight and passing through  
 180 the center of the system.

181        4. DATA ANALYSIS

182        4.1. *Determining Eclipse Times*

183        To determine the times of eclipses of the eclipsing bi-  
 184 naries selected in our sample, we fit, like Conroy et al.  
 185 (2014), a 4-part smooth nth order polynomial chain  
 186  $P(x)$  to the data from the in-phase light curves of the  
 187 binary orbit, as described in Prša et al. (2008). Fits  
 188 are made using a computational algorithm called poly-  
 189 fit which is based on two key ideas:

- 190        (1) abandon the differentiability requirement of  $P(x)$   
 191 at nodes and thus allow the polynomial chain to  
 192 be broken, and
- 193        (2) varying the position of the nodes iteratively and  
 194 thereby relaxing the system to the nearest mini-  
 195 mum.

196        The determination of the fits is done piecewise by ap-  
 197 plying breaks at certain points (nodes) in the construc-  
 198 tion of the general solution (sum of the solutions by  
 199 intervals). Node numbers are predetermined parame-  
 200 ters in the search for the best fit, starting with four ini-  
 201 tial nodes. In the end, polyfit returns a weighted least  
 202 squares solution for a theoretical light curve with given  
 203 amplitude, minimum and maximum. For each system  
 204 we use a 2nd order polynomial with 10000 initial iter-  
 205 ations for each node search in steps, a priori, of 0.01  
 206 between them, with four input intervals for the general  
 207 solution of the average phased curve of the data ob-  
 208 tained with the adjustment. With the general solution  
 209 of the phased light curves determined by the polyfit we  
 210 calculate the time shift in each eclipse per cycle with  
 211 respect to the phased mean curve obtained, arriving at  
 212 the time variation of each system. A detailed and com-  
 213 plete formal description of the algorithm is available at  
 214 Prša et al. (2008).

215        For data analysis and, consequently, polyfit, we have  
 216 long (30 minutes) and short (2 minutes) cadence data  
 217 from Kepler and TESS data. However, the long cadence  
 218 data for the shortest binaries in the Kepler catalog, we  
 219 are using, results in significant smears and limits the  
 220 polyfit method to a minimum number of points per cycle  
 221 to determine a fit, as emphasized (Conroy et al. 2014).  
 222 This causes the detection of a third body, if it exists,

223 to be compromised as its signal would be confused by  
 224 noise. Thus, the more data points included per cycle, in  
 225 each eclipse, the better, with at least three data points  
 226 for any given eclipse; otherwise, times are not calculated  
 227 for this eclipse. Therefore, we will analyze objects that  
 228 have at least three data points per eclipse.

#### 229 4.2. Light curve correction process

230 The light curves of our targets are built using the  
 231 ([Lightkurve Collaboration et al. 2018](#)) library, developed  
 232 in Python language. This library can be used for both  
 233 Kepler and TESS mission data.

234 In this tool, `LightCurve` objects are data objects that  
 235 store the brightness of a star over time, being able to  
 236 phase this data and make its respective binning. These  
 237 objects are created by loading the light curves of the  
 238 systems we want to analyze using the `TargetPixelFile`  
 239 object, which in turn uses simple aperture photometry  
 240 for its storage. This means that all pixel points in a  
 241 predefined aperture are summed and stored in an object  
 242 of type `TargetPixelFile`. Therefore, the shape of the  
 243 mask is very important in determining the signal to be  
 244 obtained and, based on the best choice, it can reduce  
 245 the noise intensity in the data.

246 The loading of light curves for our systems  
 247 was done using the search tool `search_lightcurve`  
 248 within the [Lightkurve Collaboration et al. \(2018\)](#)  
 249 library. In addition to this, [Lightkurve Collaboration et al. \(2018\)](#) still offers two other func-  
 250 tions that facilitate the search and loading of TESS  
 252 and Kepler data products from the public data file  
 253 in MAST: `lightkurve.search_targetpixelfile` and  
 254 `lightkurve.search_tesscut`. As described in the  
 255 [Lightkurve Collaboration et al. \(2018\)](#) documentation,  
 256 this function searches the public data of MAST<sup>2</sup> looking  
 257 for a data table containing the light curve files of the ob-  
 258 ject surveyed, within a region of the sky centered around  
 259 the target's position and within a cone of a given radius.  
 260 Similarly, the function `lightkurve.search_tesscut`  
 261 searches the MAST TESSCut service<sup>3</sup> for a region of the  
 262 sky that is available as a image in TESS Full Frame.  
 263 With that, these search functions return an object of  
 264 type `SearchResult`, which provides an easy way to se-  
 265 lect, download the desired data and thus allow this data  
 266 to be filtered by exposure time using an input code from  
 267 the type `result = result[result.exptime.value <`  
 268 `100]`, for example.

269 For the light curve correction process, we use  
 270 the `flatten()` method of the `LightCurve` class

271 that removes the low frequency trend using the  
 272 Savitzky-Golay filter from Scipy (package of algo-  
 273 rithms and math functions based on Python's NumPy  
 274 extension) and normalizes the light curve. While we  
 275 apply the `flatten()` method on the light curves data,  
 276 we use the `remove_outliers()` method to remove the  
 277 points from the light curves that are very out of the av-  
 278 erage, using the sigma-clipping algorithm. This last  
 279 procedure uses the mean value and standard deviation  
 280 of each bin and excludes points outside the adopted crit-  
 281 ical range (e.g.  $1\sigma$ ,  $2\sigma$  or  $3\sigma$ ), that is, all elements of  
 282 the matrix of input,  $c$ , that satisfy both of the following  
 283 conditions:

$$284 \quad c < \bar{c} - \beta \cdot \sigma(c) \\ 285 \quad c > \bar{c} + \beta \cdot \sigma(c), \quad (6)$$

286 where  $\bar{c}$  is the mean,  $\sigma(c)$  the standard deviation and  $\beta$   
 287 is the sigma level, of the elements of the  $c$  matrix of the  
 288 data for each system studied.

#### 289 4.3. Determining the system period

290 Astronomy is a field of study that deals with the obser-  
 291 vation and analysis of celestial objects, including stars,  
 292 planets and galaxies. In this field, the study of variable  
 293 stars is of particular interest, as these objects exhibit  
 294 changes in their brightness that may be associated with  
 295 third parties, as already noted above. Thus, to better  
 296 understand the behavior of these variable stars, we often  
 297 need to analyze data from unknown periodicities ([Lomb](#)  
 298 [1976](#)) or repeating patterns observed in these objects.

299 One of the most commonly used methods for ana-  
 300 lyzing periodicities in astronomical data is the Fourier  
 301 method. This method involves breaking a signal into its  
 302 component frequencies, which can be visualized using a  
 303 graph known as a frequency spectrum. By examining  
 304 this spectrum, we can identify any regular patterns or  
 305 peaks that might be indicative of a periodic signal.

306 However, data collection in astronomy is not always  
 307 straightforward. Observations can be interrupted by  
 308 weather conditions, technical issues or other factors that  
 309 can introduce non-uniformity in the data. This non-  
 310 uniformity can result in a frequency spectrum with many  
 311 smaller peaks, which can mask the true periodicity of the  
 312 data. To overcome this problem, we use a tool known  
 313 as a frequency meter or periodogram. This tool was de-  
 314 signed to identify the true periodicity of a signal, even in  
 315 the presence of non-uniform data. By analyzing signal  
 316 strength at different frequencies, the periodogram can  
 317 identify the frequency corresponding to the true peak in  
 318 the data, allowing us to identify an underlying period-  
 319 icity in the variable star we are studying.

<sup>2</sup> <https://archive.stsci.edu/>

<sup>3</sup> <https://mast.stsci.edu/tesscut/>

320 Thus, after applying the methods of correction, nor-  
 321 malization and removal of outliers from the data us-  
 322 ing `lightkurve` tools, our next step is to deter-  
 323 mine the orbital period of the binary system through  
 324 the periodogram. Therefore, for our sample objects,  
 325 we will use the `to_periodogram()` method from the  
 326 `KeplerLightCurve` object, to create a periodogram and  
 327 identify its period, corresponding to the highest power  
 328 peak, which is likely to be associated with the orbital  
 329 period of the binary. It is worth noting that, after the  
 330 determination, we will check the phase diagram (see de-  
 331 scription below) to confirm if the period found is in fact  
 332 the reliable period of the binary.

333 The Fig. 1, shows the graph of the periodogram based  
 334 on the method of Lomb–Scargle for the KIC 2162283  
 335 (TIC 351055073) system, one of the our targets in this  
 336 research.

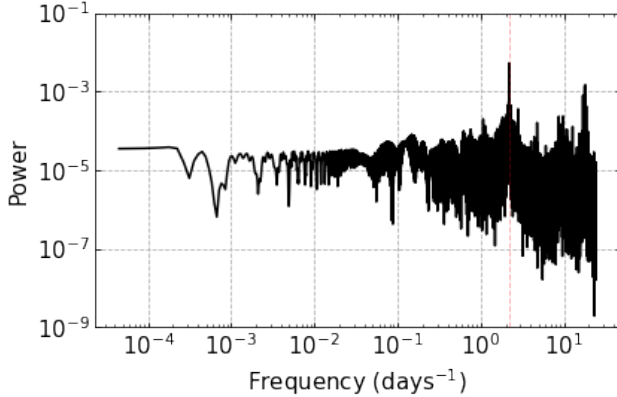


**Figure 1.** Power spectrum as a function of frequency of the KIC 2162283 object.

337 Having determined the period of the system, Fig. 1,  
 338 we use the tool `stringlength` (Fig. 2), a method of  
 339 `pyTiming` from the PyAstronomy<sup>4</sup> library (Czesla et al.  
 340 2019), for a refinement of the obtained period. This  
 341 method relies on non-sinusoidal periodic variations in  
 342 a well-ordered dataset returning a minimum as output,  
 343 see Fig. 2.

344 Finally, with the period of the system calculated, we  
 345 phase the light curve using the orbital period of the bi-  
 346 nary and apply the fitting procedure using polyfit (see  
 347 Section 4.1 for details).

348 The polynomial function derived in the polyfit fit is  
 349 a chain of four polynomials that is continuous but not  
 350 necessarily differentiable at nodes. This procedure is  
 351 optimized to find the best overall solution, as described

<sup>4</sup> <https://github.com/sczesla/PyAstronomy>

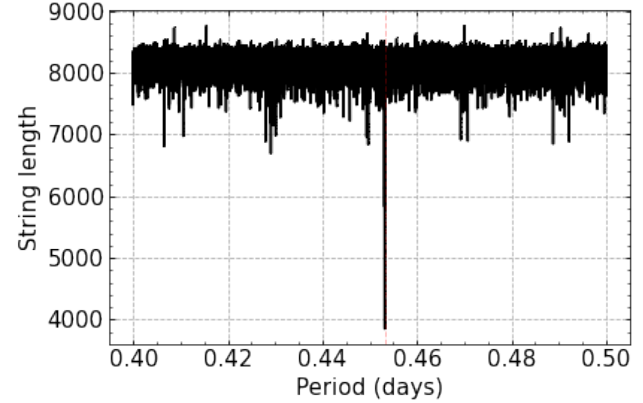


**Figure 2.** `Stringlength` used to refine the system periods. In this case, we have KIC 2162283 (TIC 351055073) object.

352 in (Conroy et al. 2014). Furthermore, this function does  
 353 not represent a physical model but, on the other hand,  
 354 analytically describes the average phased shape of the  
 355 light curve of the binary, an example that can be seen  
 356 in Fig. 3.

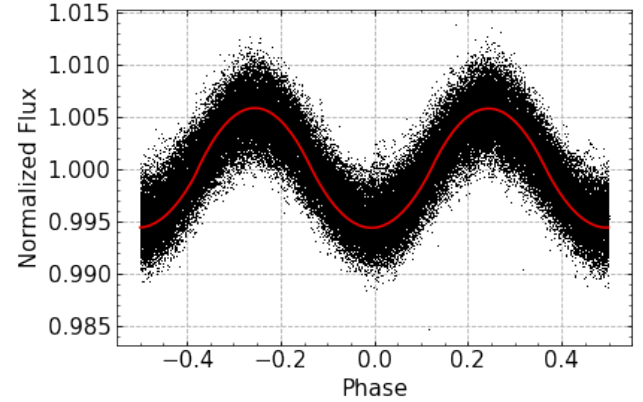


**Figure 3.** Polyfit fit (red line) to in-phase data (black dots) of the KIC 2162283 system observed by Kepler.

#### 4.4. Construction of the O-C diagram

357 The O-C diagram is a widely used method of finding  
 358 period changes and is based on the following idea: if the  
 359 primary and secondary eclipses of an eclipsing binary  
 360 star are periodic and do not change, all times between  
 361 eclipses are exactly the same and therefore, their cy-  
 362 cles can be predicted. For example, if a light curve low  
 363 occurs at, say, JD 2,450,000 and the binary period is  
 364 precisely 332 days (and never changes), the next mini-  
 365 mum will occur at JD 2,450,332. Thus, we can conclude  
 366 that there is no disturbance arising from a third body or  
 367 caused by any physical phenomenon intrinsic to the sys-  
 368 tem. Therefore, from this reasoning, observing two con-

<sup>370</sup> secutive epochs  $T_1$  and  $T_2$  indicated by Sterken (2005),  
<sup>371</sup> we can conclude that each cycle will occur following the  
<sup>372</sup> equation below:

$$\text{373} \quad T_i - T_0 = EP, \quad (7)$$

<sup>374</sup> where  $T_i$  is the times of the minima of the primary  
<sup>375</sup> eclipses,  $T_0$  is the time of the first primary eclipse,  $E$   
<sup>376</sup> is an integer and commonly called the number of cycles  
<sup>377</sup> and  $P$  is the orbital period of the system.

<sup>378</sup> With  $P$  and  $T_0$  well determined we can build the O-  
<sup>379</sup> C diagram for each Kepler system that TESS also ob-  
<sup>380</sup> served (after phasing and polynomial fitting the data,  
<sup>381</sup> Fig. 3). In this diagram, we can verify if there is any pe-  
<sup>382</sup> riodic variation in your data and, in this way, confirm, or  
<sup>383</sup> not, the existence of a possible third body, undetected,  
<sup>384</sup> and/or other physical phenomena that can generate such  
<sup>385</sup> variations. Thus, adding the Kepler observations to the  
<sup>386</sup> TESS data, in particular for objects with possible pe-  
<sup>387</sup> riodic characteristics and which could not have confir-  
<sup>388</sup> mation of a possible third body in their orbit due to  
<sup>389</sup> a time interval smaller than the orbital period of such  
<sup>390</sup> object, we are able to characterize the existence of new  
<sup>391</sup> objects to the analyzed systems, as is the case of the  
<sup>392</sup> KIC 5513861 object, see Fig. 4.

<sup>393</sup> This object makes clear the importance of the inte-  
<sup>394</sup> gration of the two missions, Kepler and TESS, showing  
<sup>395</sup> that it is possible to motorize at least one cycle for those  
<sup>396</sup> objects with incomplete orbital cycles, as is the case of  
<sup>397</sup> KIC 5513861.

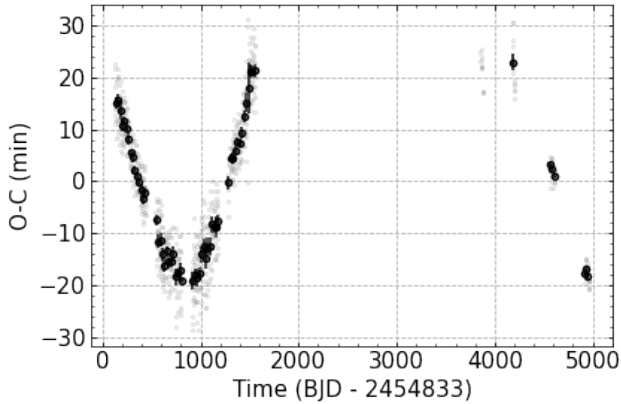


**Figure 4.** This figure shows the O-C diagram of the KIC 5513861 object with the Kepler and TESS data together. In it, we can see a certain periodicity in the data, which may be associated with the presence of a third body in the analyzed system, which would not be possible to visualize only with Kepler data.

398

#### 4.5. Third body Modelling

<sup>399</sup> After determining the O-C diagrams, we applied a  
<sup>400</sup> data binning to optimize the analysis and generate the  
<sup>401</sup> curves for the third body. After the data binning, we fit  
<sup>402</sup> the curves for a possible third body around the analyzed  
<sup>403</sup> systems using the Markov Chain Monte Carlo algorithm  
<sup>404</sup> (MCMC) through the emcee (Foreman-Mackey et al.  
<sup>405</sup> 2013) implementation in python. An example of obtain-  
<sup>406</sup> ing the curve of a third body for the object KIC 5513861  
<sup>407</sup> (O-C in Fig. 4) can be seen in Fig. 5. In the Section 5  
<sup>408</sup> we present this figure again together with the results  
<sup>409</sup> obtained in our analyses.

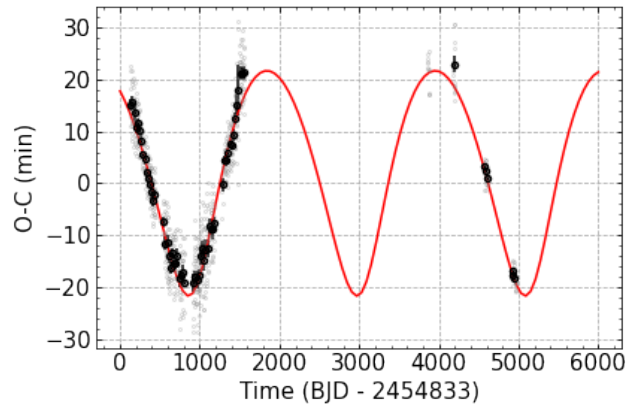


**Figure 5.** O-C diagram for the binary system KIC 5513861 (TIC 120251815). The black dots are the data binned from the original data, which are represented by gray dots. The blue curve represents the best fit.

410

## 5. RESULTS

<sup>411</sup> In this paper, we investigate the search and charac-  
<sup>412</sup> terization of third bodies around binary systems using  
<sup>413</sup> data from the Kepler and TESS satellites. Our analy-  
<sup>414</sup> sis focuses on 240 eclipsing binary systems, which were  
<sup>415</sup> examined using the methodology presented in the Sec-  
<sup>416</sup> tion 4. In this results Section, we present the general  
<sup>417</sup> results obtained through the analysis of all considered  
<sup>418</sup> binary systems.

<sup>419</sup> For an individual visualization of the systems, we list  
<sup>420</sup> in the appendix, in the Sections A, B e C, all the systems  
<sup>421</sup> with their respective parameters both for the binary sys-  
<sup>422</sup> tems and for the third bodies (if any) around it. Such  
<sup>423</sup> parameters can also be viewed in the Table 3.

### 424 5.1. Analisys of ETV's signals in the sample data

<sup>425</sup> As mentioned earlier, some objects, considering only  
<sup>426</sup> Kepler telescope data, do not have enough observation  
<sup>427</sup> times to determine possible periodic variations in their  
<sup>428</sup> eclipse times, which could show a possible third body  
<sup>429</sup> disturbing the system. However, when we add data from

the TESS satellite, increasing the observation time coverage by approximately 14 years, the periodic variation becomes clearer.

Once potential binary systems with periodic variations are identified in their O-C diagrams, it is possible to fit a Keplerian curve to the O-C's data for a third body orbiting such systems (see Eq. 5). However, the period of some of these systems may be changing with time and, therefore, may cause deformations in their O-C's diagrams. Thus, for such systems, in addition to a Keplerian curve, we adopted a linear fit, of the type  $Ax + B$ , to the data as a general solution, as illustrated in Fig. 6. In this figure, the gray dots are the O-C data, the black dots are the binned data, the red dotted line indicates the Keplerian curve, the green dashed line indicates the linear fit and the blue curve the sum of these two solutions.

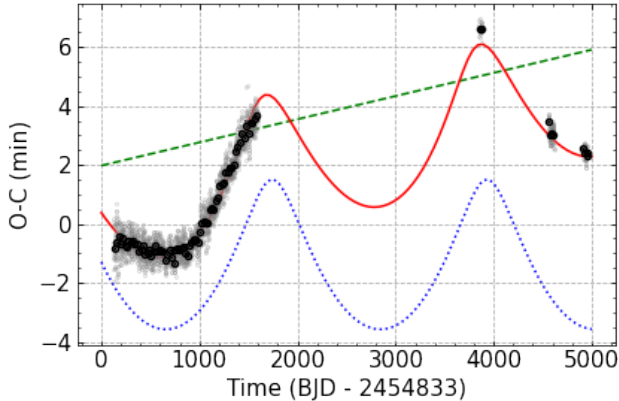


**Figure 6.** O-C diagram for the binary system KIC 3221207 (TIC 121213501). The black dots are the data binned from the original data, which are represented by gray dots. The blue curve represents the best fit using Eq. 5.

The variations in the orbital periods of the binary systems analyzed in this study can be divided into non-periodic variations, candidate periodic variations and periodic variations. In cases where we identify a periodic variation of the period through the O-C diagram, we fit to the data of these systems a Keplerian solution that describes the orbit of a third body orbiting the analyzed system. For some cases, we need to add a linear ephemeris to the Keplerian solution for a satisfactory fit due to uncertainties in the value of determining the orbital period of the binary stars analyzed.

As for variations, we have: (1) systems with non-periodic variations are defined as those that, despite having short, increasing, decreasing and/or random variations in their O-C diagrams, such variations do not represent statistical significance according to the prob-

ability of false alarm (PFA) (VanderPlas 2018) for the search and determination of the periods of these systems; (2) systems with candidate periodic variations are those that have at least half a cycle observed in their O-C diagrams; and (3) the systems denominated as periodic variations, are those that present in the O-C diagrams at least one complete cycle.

In total, 77 systems with variations in their O-C diagrams were identified, distinguishing between periodic variations and candidate periodic variations. Altogether, there are 73 binary systems with periodic variations and only 13 with periodic variations shown in their O-C diagrams. Next, we illustrate an example of each type of variation obtained in this study for the O-C diagram. In the appendices, we present all of them.

## 5.2. Binary systems with non-periodic variations on the O-C diagram

From the sample of 240 eclipsing binary systems analyzed in this work, a total of 163 have non-periodic variations in their respective O-C diagrams. That is, the possible short, increasing, decreasing and/or random variations that these systems may present in their diagrams do not represent statistical significance according to the probability of false alarm (PFA) for the search and determination of the periods of these systems. These systems require more detailed analyses, which are beyond the scope of this work, but will be carried out in future studies.

In Fig. 7 we can see one of these 163 systems that have non-periodic variations in their orbital periods.

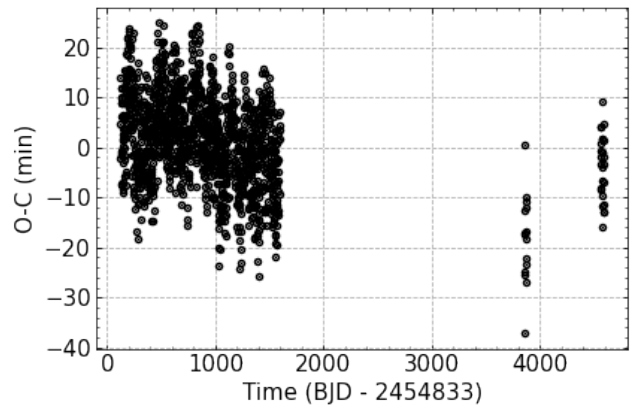


**Figure 7.** O-C diagram for the binary system KIC 2162283 (TIC 351055073).

## 5.3. Binary systems with candidate periodic variations on the O-C diagram

For systems with candidate periodic variations we have a percentage of 25% of the sample adding 60 objects with variations possibly caused by a third body. Fig. 8 illustrates one of these cases, showing the light curve, the periodogram, the stringlength, the phased light curve and its O-C diagram with and without adjustment, respectively.

#### 5.4. Binary systems with periodic variations on the O-C diagram

For systems with periodic variations in the system period characterized in their O-C diagram, we found 13 systems that satisfy this condition, equivalent to a percentage of 5.42%. These objects can be viewed individually below with their respective parameters.

Right below in the section 5.4.1 we can see an example that presents this behavior with its respective characteristics and adjusted parameters. In the appendix, in the section C, all systems with periodic variations found in our study are presented.

##### 5.4.1. KIC 2450566 (TIC 137977804) Object

The binary system KIC 2450566 has a periodic variation in its O-C diagram, as identified in Fig. 9. For a Keplerian orbit adjustable to the data of its O-C diagram points, we find for the system a period of  $P = 1059.282^{+23.443}_{-28.695}$  days, in an orbit with eccentricity  $e = 0.655^{+0.105}_{-0.066}$ , semi-major axis equal to  $a = 1487.083^{+181.846}_{-150.956}$  and periastron argument equal to  $\omega = 307.417^{+10.050}_{-17.567}$  for a third body orbiting this system.

Such parameters were derived from fitting the O-C diagram to a third body orbiting the system, as shown in Fig. 9. In Table 3 you can consult these and all other data for the 73 binary systems with periodic and candidate periodic variations presented in their O-C's diagrams analyzed here.

## 6. DISCUSSIONS

The Table 2 presents a comparison between the objects with signals from third bodies of this work and the work of (Conroy et al. 2014). The objects are divided according to the period of rotation of the third body around its respective host star. In the first part of the table, we have the objects with periods for the third body smaller than 700 days. Then, just below the objects with periods smaller than 700 days, we have the systems with periods between 700 and 1400 days of rotation for the possible third bodies. And finally, we have objects that have rotation periods greater than 1400 days.

As expected, the table only points to an estimate of the period for some objects for a possible third body derived by Conroy et al. (2014), as these systems had a temporal coverage of the database smaller than their period.

Now, with the Kepler and TESS databases combined we may be able to fit a curve to a third body, as discussed above. The table summarizes some of the parameters obtained in these adjustments for the third candidate bodies.

**Table 2.** Table with values for the period of the third body of this work ( $P_3$  (days)), period for the third body found by Conroy et al. (2014) ( $P_{3,C}$  (days)), eccentricity for the third body presented here ( $e_3$ ) and the eccentricity of the third body derived by Conroy et al. (2014) ( $e_{3,C}$ ).

KIC (1)	$P_3$ days (2)	$P_{3,C}$ days (3)	$e_3$ (4)	$e_{3,C}$ (5)
3228863	663.632	644.1	$0.224^{+0.173}_{-0.154}$	$0.000 \pm 0.003$
3641446	<b>331.383</b>	228.6	<b><math>0.930^{+0.041}_{-0.066}</math></b>	$0.000 \pm 0.010$
4909707	513.727	516.1	$0.657^{+0.029}_{-0.027}$	$0.000 \pm 0.010$
5264818	282.272	299.7	$0.436^{+0.208}_{-0.309}$	$0.421 \pm 0.306$
7690843	2714.623	74.1	$0.752^{+0.058}_{-0.152}$	$0.233 \pm 0.021$
7765894	463.815	...	$0.270^{+0.073}_{-0.088}$	...

**Table 2** *continued*

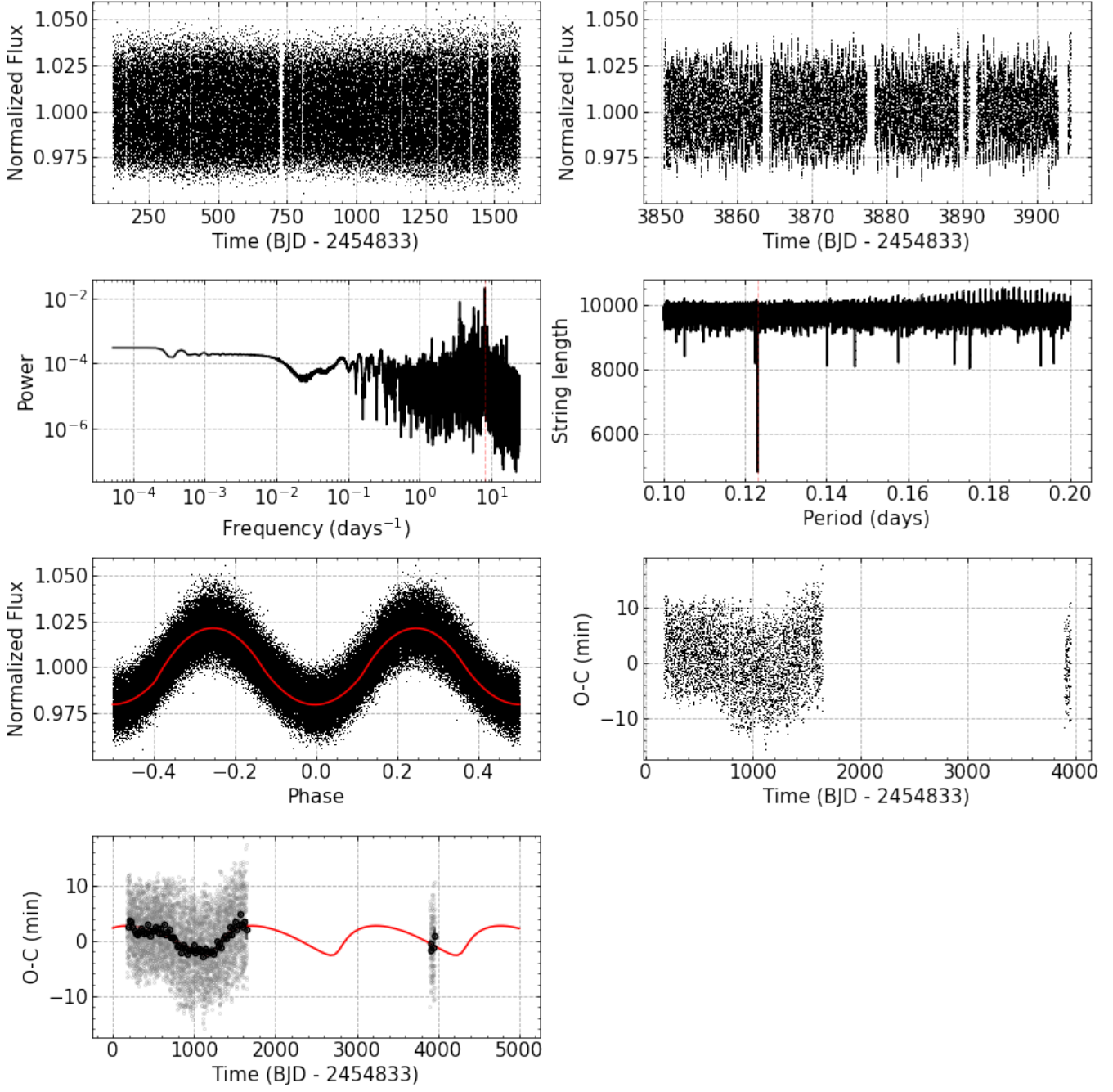


**Figure 8.** Analysis of object KIC 12216817 (TIC 122375269). First row, left panel: Light curve from Kepler in terms of Normalized Flux over Time (BJD). Right panel: Light curve from TESS in terms of Normalized Flux over Time (BJD). Second row, left panel: Periodogram analysis to obtain the system's period. Right panel: String length to refine the obtained period. Third row, left panel: Light curve in phase - black points represent the data, and the red curve represents the best fit. Right panel: O-C diagram. Fourth row, left panel: O-C diagram with its curve adjusted for the presence of a third body; the gray points are the raw data points, the black points are the binned points, and the red curve represents the best fit for the third body around the eclipsing binary system.

**Table 2** *continued*

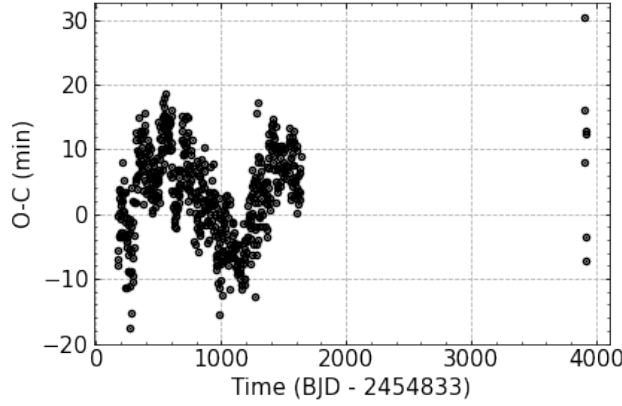


**Figure 9.** O-C diagram for the binary system KIC 2450566 (TIC 137977804).

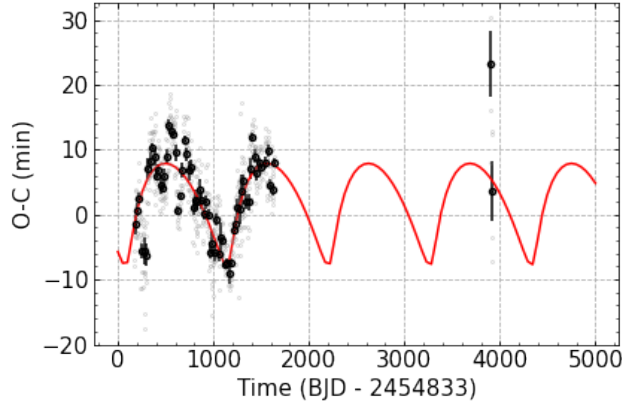


**Figure 10.** Fitting the O-C diagram of the binary system KIC 2450566 (TIC 137977804) for a third body.

**Table 2 (continued)**

KIC	$P_3$ days	$P_{3,C}$ days	$e_3$	$e_{3,C}$
(1)	(2)	(3)	(4)	(5)

**Table 2 (continued)**

KIC	$P_3$ days	$P_{3,C}$ days	$e_3$	$e_{3,C}$
(1)	(2)	(3)	(4)	(5)
8043961	422.710	478.0	$0.399^{+0.185}_{-0.121}$	$0.000 \pm 0.005$
8386865	294.267	293.9	$0.421^{+0.055}_{-0.033}$	$0.493 \pm 0.013$
9451096	<b>100.092</b>	106.8	<b><math>0.998^{+0.001}_{-0.001}</math></b>	$0.091 \pm 0.033$
10789421	455.994	...	$0.517^{+0.281}_{-0.180}$	...
10991989	<b>611.634</b>	554.8	<b><math>0.977^{+0.011}_{-0.057}</math></b>	$0.000 \pm 0.018$

**Table 2** *continued*

**Table 2** (*continued*)

KIC	$P_3$	$P_{3,C}$	$e_3$	$e_{3,C}$
	days	days		
(1)	(2)	(3)	(4)	(5)
2450566	1059.282	983.7	$0.655^{+0.105}_{-0.066}$	$0.308 \pm 0.016$
4451148	769.411	746.0	$0.466^{+0.087}_{-0.023}$	$0.293 \pm 0.004$
4647652	755.235	755.2	$0.245^{+0.290}_{-0.147}$	$0.244 \pm 0.003$
5975712	1694.123	1164.7	$0.218^{+0.001}_{-0.001}$	$0.000 \pm 0.013$
7385478	1360.065	1389.3	$0.782^{+0.148}_{-0.363}$	$0.245 \pm 0.007$
8045121	890.971	938.6	$0.349^{+0.085}_{-0.122}$	$0.000 \pm 0.001$
9365025	731.626	...	$0.969^{+0.002}_{-0.003}$	...
9612468		1264.2		$0.340 \pm 0.001$
10226388	924.443	965.3	$0.518^{+0.238}_{-0.031}$	$0.041 \pm 0.007$
10724533	1936.467	1131.4	$0.426^{+0.035}_{-0.185}$	$0.265 \pm 0.003$
2708156	1437.154	...	$0.087^{+0.167}_{-0.065}$	...
3221207	2253.652	$\sim 1700$	$0.426^{+0.048}_{-0.040}$	...
3448245	8314.481	...	$0.753^{+0.051}_{-0.014}$	...
3936357	2132.636	$\sim 2400$	$0.120^{+0.075}_{-0.061}$	...
3953981	2862.477	...	$0.223^{+0.095}_{-0.069}$	...
4450976	2546.115	...	$0.313^{+0.150}_{-0.201}$	...
4758368	2478.732	$\sim 1500$	$0.973^{+0.014}_{-0.080}$	...
4851217	2473.632	...	$0.876^{+0.083}_{-0.056}$	...
4909422	6582.935	...	$0.839^{+0.131}_{-0.096}$	...
4945588	1607.893	$\sim 1500$	$0.871^{+0.046}_{-0.045}$	...
4999260	41607.891	...	$0.895^{+0.027}_{-0.021}$	...
5022573	1826.598	...	$0.766^{+0.083}_{-0.061}$	...
5296877	4962.088	$\sim 1900$	$0.728^{+0.010}_{-0.007}$	...
5513861	2113.335	$\sim 1800$	$0.315^{+0.019}_{-0.029}$	...
5975712	1694.123	...	$0.218^{+0.001}_{-0.001}$	...
6187893	2028.925	$\sim 7800$	$0.969^{+0.004}_{-0.006}$	...
6205460	2311.862	...	$0.426^{+0.019}_{-0.071}$	...
6353203	2449.628	...	$0.575^{+0.057}_{-0.069}$	...
6462057	4926.320	...	$0.637^{+0.080}_{-0.177}$	...
7259917	4729.394	...	$0.720^{+0.063}_{-0.222}$	...
7375612	2123.456	$\sim 2100$	$0.098^{+0.074}_{-0.028}$	...
7431703	1820.383	...	$0.448^{+0.121}_{-0.158}$	...
7440742	2003.253	...	$0.983^{+0.005}_{-0.013}$	...
7457163	6255.520	...	$0.527^{+0.062}_{-0.039}$	...
7512381	6805.413	...	$0.411^{+0.040}_{-0.131}$	...
7690843	2714.623	74.1	$0.752^{+0.058}_{-0.152}$	$0.233 \pm 0.021$
7766185	1860.287	...	$0.945^{+0.015}_{-0.024}$	...
7816201	2328.001	...	$0.696^{+0.074}_{-0.124}$	...
7938870	2100.595	...	$0.627^{+0.094}_{-0.022}$	...

**Table 2** *continued*

**Table 2** (*continued*)

KIC	$P_3$	$P_{3,C}$	$e_3$	$e_{3,C}$
	days	days		
(1)	(2)	(3)	(4)	(5)
7950962	3085.157	...	$0.075^{+0.053}_{-0.055}$	...
8189196	3903.002	$\sim 8300$	$0.980^{+0.003}_{-0.004}$	...
8231231	1909.021	$\sim 1600$	$0.949^{+0.021}_{-0.033}$	...
8285349	2042.641	...	$0.522^{+0.022}_{-0.218}$	...
8397460	8112.505	...	$0.966^{+0.003}_{-0.003}$	...
8579707	1944.760	...	$0.523^{+0.090}_{-0.037}$	...
8587792	5493.004	...	$0.380^{+0.046}_{-0.040}$	...
8758161	18453.026	...	$0.908^{+0.047}_{-0.069}$	...
8894630	7635.890	...	$0.737^{+0.043}_{-0.030}$	...
9083523	2200.587	$\sim 5200$	$0.370^{+0.084}_{-0.090}$	...
9181877	1830.374	$\sim 2600$	$0.596^{+0.054}_{-0.051}$	...
9345838	2497.096	...	$0.969^{+0.013}_{-0.009}$	...
9402652	1499.321	...	$0.817^{+0.028}_{-0.034}$	...
9602595	6556.627	...	$0.762^{+0.037}_{-0.028}$	...
9657096	1829.705	$\sim 1400$	$0.607^{+0.034}_{-0.077}$	...
9760531	2984.870	...	$0.960^{+0.006}_{-0.095}$	...
9832227	6091.433	...	$0.507^{+0.028}_{-0.047}$	...
10155563	3569.345	...	$0.989^{+0.001}_{-0.002}$	...
10259530	4636.848	...	$0.561^{+0.028}_{-0.173}$	...
10389982	2300.442	...	$0.839^{+0.111}_{-0.090}$	...
10481912	4101.691	$\sim 2700$	$0.353^{+0.138}_{-0.120}$	...
10485137	5843.721	$\sim 3100$	$0.639^{+0.072}_{-0.064}$	...
10711938	6688.888	$\sim 2000$	$0.631^{+0.250}_{-0.059}$	...
10724533	1936.467	1131.4	$0.426^{+0.035}_{-0.185}$	$0.265 \pm 0.003$
10818544	1892.800	...	$0.967^{+0.011}_{-0.030}$	...
10979669	1532.272	...	$0.974^{+0.008}_{-0.013}$	...
11255667	4715.408	...	$0.269^{+0.112}_{-0.143}$	...
11409673	5483.304	...	$0.972^{+0.009}_{-0.011}$	...
11572643	2290.326	...	$0.503^{+0.314}_{-0.198}$	...
12216817	1508.869	...	$0.619^{+0.071}_{-0.084}$	...
12305537	2039.912	...	$0.736^{+0.086}_{-0.038}$	...

<sup>552</sup> *Software:* polyfit (Prša et al. 2008), lightkurve

<sup>553</sup> (Lightkurve Collaboration et al. 2018), pyastronomy

<sup>554</sup> (Czesla et al. 2019)

those with periodic variations. And, in Section D we present the table with the orbital parameters found for those systems whose variations are periodic and candidate.

#### 561 A. BINARY SYSTEMS WITH NON-PERIODIC VARIATIONS ON THE O-C DIAGRAM

562 Through the analysis of the O-C diagram of the binary systems in our sample, we were able to verify and determine  
 563 variations in certain objects, characterizing periodic variations or not in their orbital periods. Any deviations, whether  
 564 linear or periodic, in the O-C diagram could indicate changes in the orbital period over time, which could be caused  
 565 by a variety of factors, such as gravitational interactions with other stars or the presence of a third body around the  
 566 system.

567 Thus, we could observe that a percentage of approximately 68.33%, that is, 163 systems do not present non-periodic  
 568 variations in their O-C diagrams. This means that short-term variations in these systems do not represent statistically  
 569 significant deviations from the assumed orbital period, as determined by the False Alarm Probability (FAP). The FAP  
 570 is a measure of the probability that a given deviation in the O-C diagram is due to chance and not to an actual physical  
 571 effect.

572 The absence of significant variations in the O-C diagrams of these 163 systems suggests that their orbital periods  
 573 are relatively stable over time. However, it is important to note that this does not necessarily mean that these systems  
 574 are completely stable and will not show any long-term changes in their periods. Further observations and analyzes  
 575 may be necessary to confirm the stability of these systems over longer timescales.

576 Next, in the Figs. 11-12, all these systems can be visualized with their respective light curves, periodogram,  
 577 stringlength, phase light curve and their derived O-C diagram.

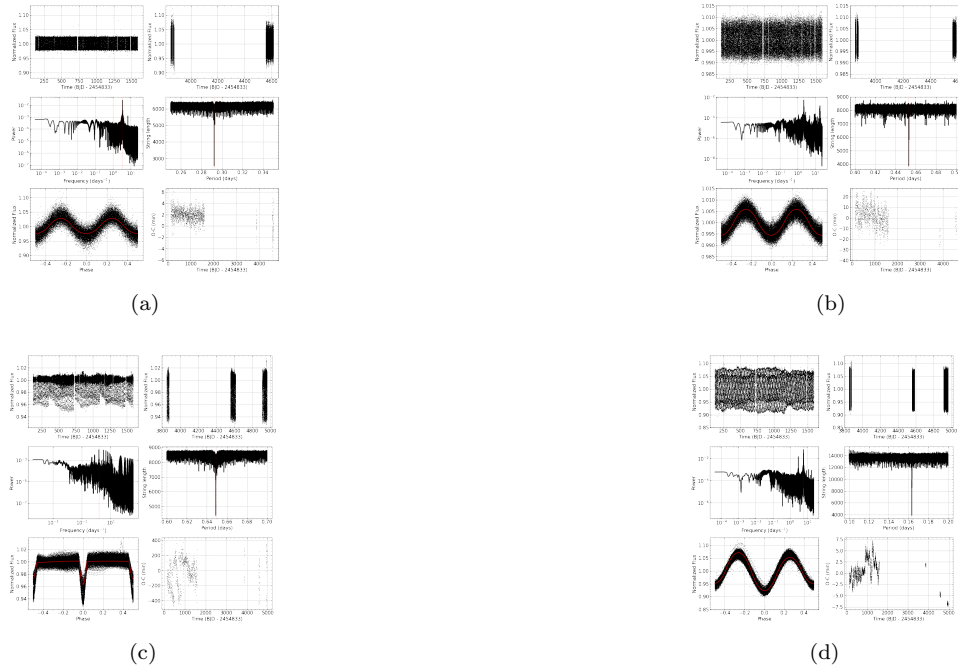


**Figure 11.** Same analyses of Fig. (8), but for (a) KIC 1868650, (b) KIC 2162283, (c) KIC 2557430, (d) KIC 2694741.

#### 578 B. BINARY SYSTEMS WITH CANDIDATE PERIODIC VARIATIONS ON THE O-C DIAGRAM

579 Binary systems with candidate periodic variations are those that present in their O-C diagram an incomplete orbital  
 580 cycle, even with the implementation of TESS data to Kepler data, adding a total of 60 eclipsing binary systems from  
 581 our sample with this characteristic. Such systems are presented below in their respective sections.

##### 582 B.1. *KIC 2708156 (TIC 122375269) Object*

583 This object presents a variation in its O-C diagram, Fig. 14, however, such variation does not present a complete  
 584 orbital cycle due to a possible third body around the binary system with a period  $P = 1437.154^{+13.913}_{-7.553}$ , in an orbit

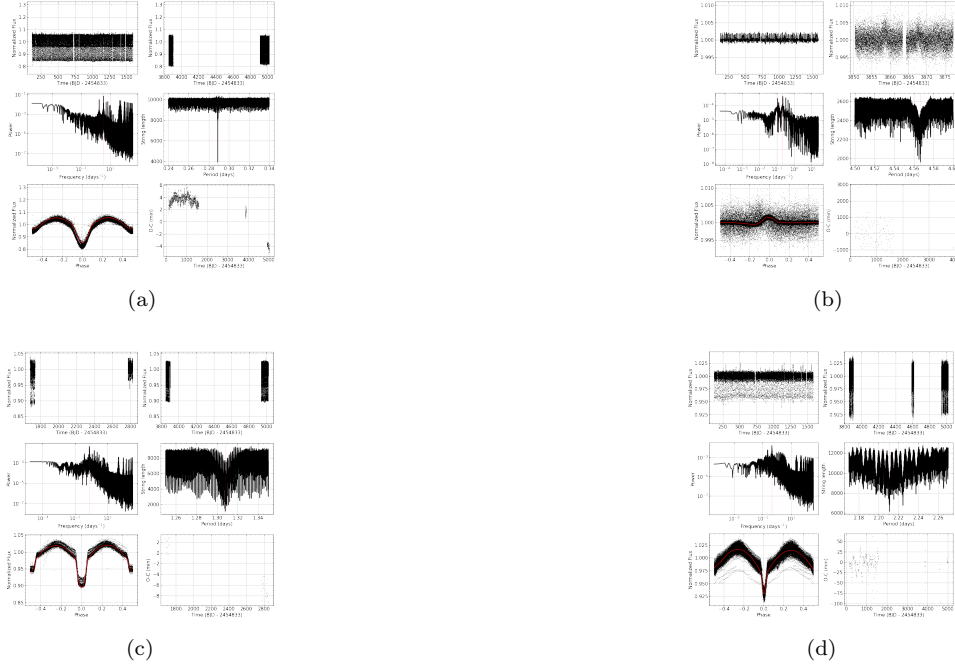


**Figure 12.** Same analyses of Fig. (8), but for (a) KIC 12157987, (b) KIC 12255108, (c) KIC 12257908, (d) KIC 12268220.

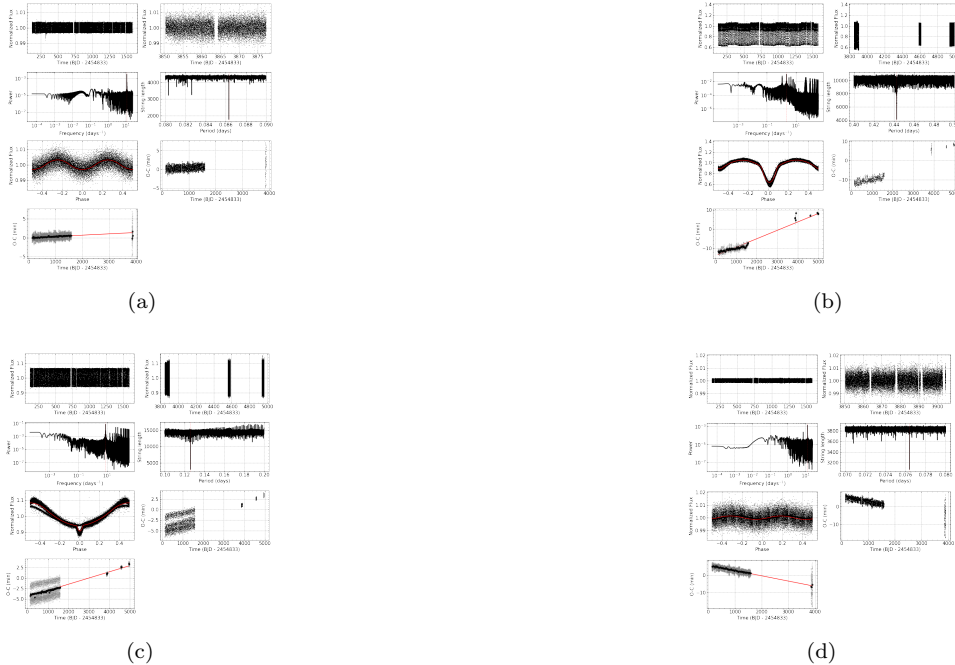


**Figure 13.** Same analyses of Fig. (8), but for (a) KIC 5872696, (b) KIC 7777443, (c) KIC 9472174.

585 with eccentricity  $e = 0.087^{+0.167}_{-0.065}$ , at a distance  $a = 3998.385^{+112.356}_{-195.565}$  from its parent stars, with its inclination axis  
586  $\omega = 186.554^{+7.738}_{-4.424}$  and linear parameters fits at  $A = -17.877^{+1.850}_{-1.752}$  and  $B = 0.007^{+0.000}_{-0.000}$ .

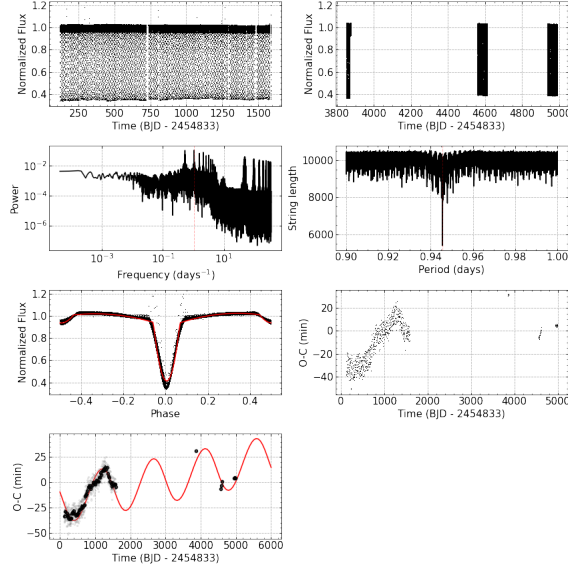


**Figure 14.** Same analyses of Fig. (8), but for KIC 2708156 (TIC 122375269).

587

### B.2. *KIC 3221207 (TIC 121213501) Object*

588 This object presents a variation in its O-C diagram, Fig. 15, however, such variation does not present a complete  
 589 orbital cycle due to a possible third body around the binary system with a period  $P = 2253.652^{+72.383}_{-62.009}$ , in an orbit  
 590 with eccentricity  $e = 0.426^{+0.048}_{-0.040}$ , at a distance  $a = 413.398^{+17.810}_{-25.905}$  from its parent stars, with its inclination axis  
 591  $\omega = 68.923^{+25.187}_{-29.382}$  and linear parameters fits at  $A = 0.711^{+0.029}_{-0.125}$  and  $B = 0.001^{+0.000}_{-0.000}$ .

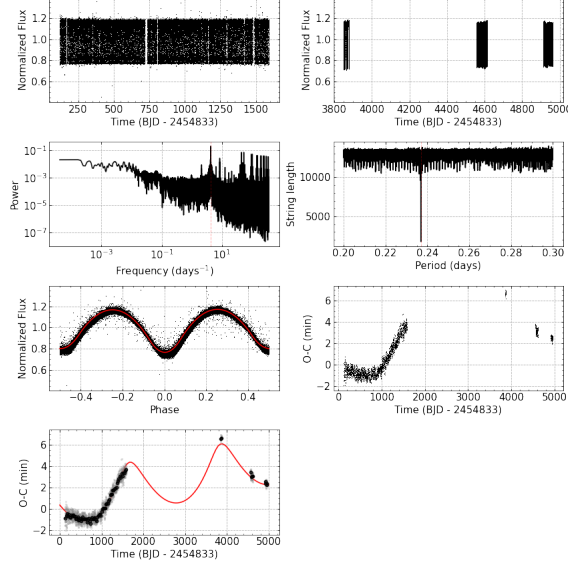


**Figure 15.** Same analyses of Fig. (8), but for KIC 3221207 (TIC 121213501).

592

### B.3. *KIC 3448245 (TIC 137687487) Object*

593 This object presents a variation in its O-C diagram, Fig. 16, however, such variation does not present a complete  
 594 orbital cycle due to a possible third body around the binary system with a period  $P = 8314.481^{+297.994}_{-89.964}$ , in an orbit  
 595 with eccentricity  $e = 0.753^{+0.051}_{-0.014}$ , at a distance  $a = 298.060^{+7.057}_{-5.386}$  from its parent stars, with its inclination axis  
 596  $\omega = 0.860^{+2.637}_{-0.683}$ .

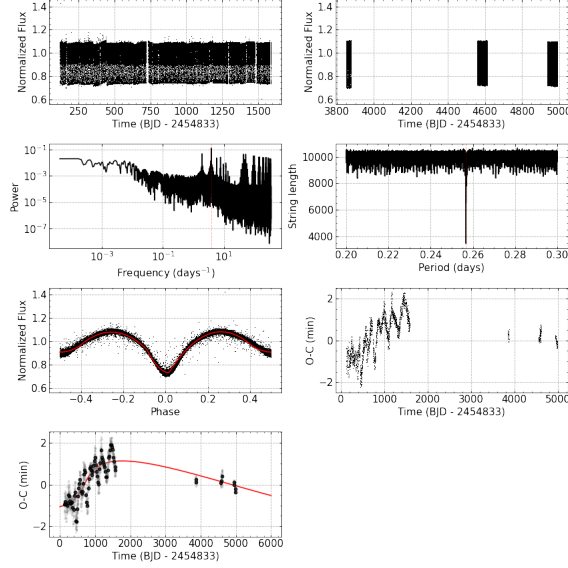


**Figure 16.** Same analyses of Fig. (8), but for KIC 3448245 (TIC 137687487).

597

#### B.4. *KIC 3936357 (TIC 120499528) Object*

This object presents a variation in its O-C diagram, Fig. 17, however, such variation does not present a complete orbital cycle due to a possible third body around the binary system with a period  $P = 2132.636^{+67.619}_{-47.151}$ , in an orbit with eccentricity  $e = 0.120^{+0.075}_{-0.061}$ , at a distance  $a = 469.656^{+18.435}_{-24.562}$  from its parent stars, with its inclination axis  $\omega = 203.482^{+26.213}_{-50.987}$  and linear parameters fits at  $A = -3.312^{+0.400}_{-0.226}$  and  $B = 0.001^{+0.000}_{-0.000}$ .

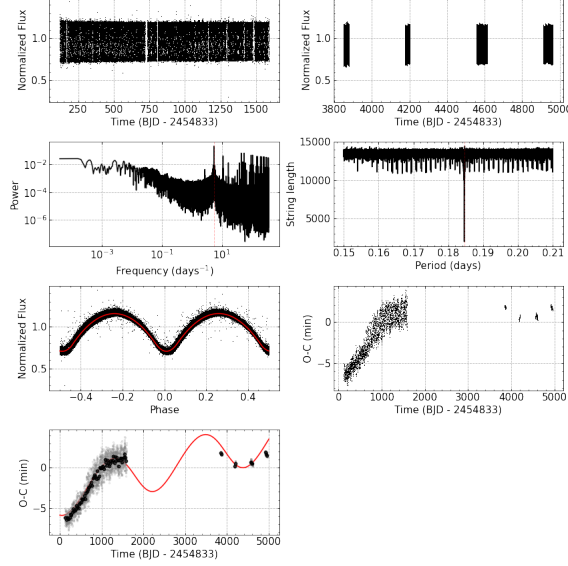


**Figure 17.** Same analyses of Fig. (8), but for KIC 3936357 (TIC 120499528).

602

#### B.5. *KIC 3953981 (TIC 137152301) Object*

This object presents a variation in its O-C diagram, Fig. 18, however, such variation does not present a complete orbital cycle due to a possible third body around the binary system with a period  $P = 2862.477^{+94.503}_{-122.901}$ , in an orbit with eccentricity  $e = 0.223^{+0.095}_{-0.069}$ , at a distance  $a = 220.574^{+19.656}_{-13.916}$  from its parent stars, with its inclination axis  $\omega = 254.738^{+28.379}_{-42.287}$  and linear parameters fits at  $A = -0.300^{+0.045}_{-0.043}$  and  $B = 0.001^{+0.000}_{-0.000}$ .

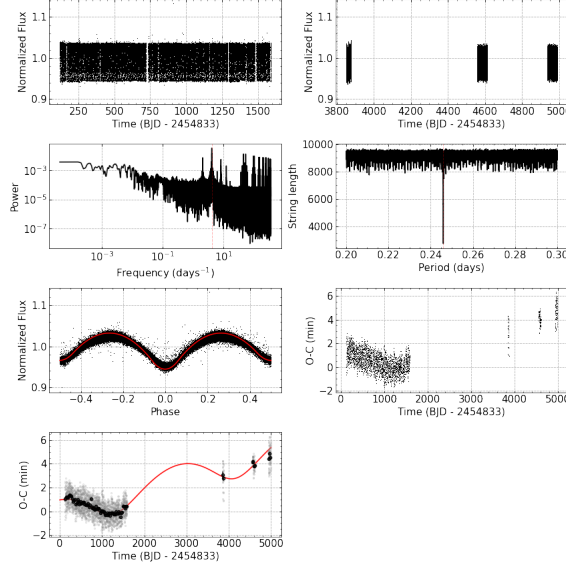


**Figure 18.** Same analyses of Fig. (8), but for KIC 3953981 (TIC 137152301).

607

#### B.6. *KIC 4450976, (TIC 121215583) Object*

608 This object presents a variation in its O-C diagram, Fig. 19, however, such variation does not present a complete  
 609 orbital cycle due to a possible third body around the binary system with a period  $P = 2546.115^{+161.201}_{-203.502}$ , in an orbit  
 610 with eccentricity  $e = 0.313^{+0.150}_{-0.201}$ , at a distance  $a = 34367.104^{+2451.117}_{-2702.057}$  from its parent stars, with its inclination axis  
 611  $\omega = 297.249^{+34.620}_{-33.954}$ .

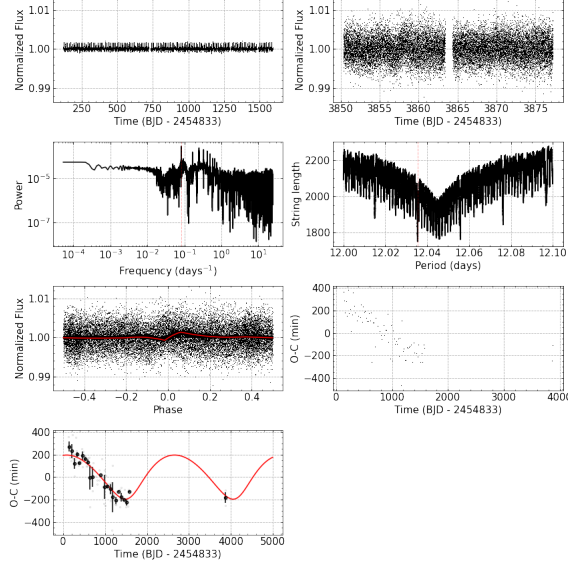


**Figure 19.** Same analyses of Fig. (8), but for KIC 4450976 (TIC 121215583).

612

#### B.7. *KIC 4851217 (TIC 184246521) Object*

613 This object presents a variation in its O-C diagram, Fig. 20, however, such variation does not present a complete  
 614 orbital cycle due to a possible third body around the binary system with a period  $P = 2473.632^{+318.289}_{-147.137}$ , in an orbit  
 615 with eccentricity  $e = 0.876^{+0.083}_{-0.056}$ , at a distance  $a = 826.152^{+98.935}_{-99.057}$  from its parent stars, with its inclination axis  
 616  $\omega = 101.987^{+13.423}_{-12.392}$  and linear parameters fits at  $A = 8.235^{+0.677}_{-0.533}$  and  $B = -0.007^{+0.001}_{-0.000}$ .

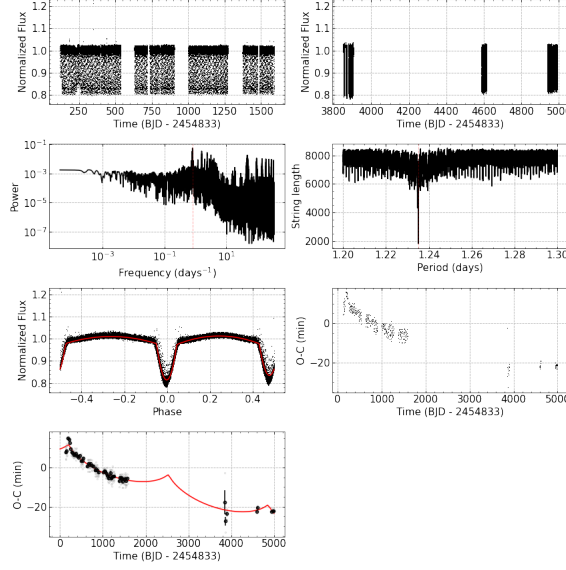


**Figure 20.** Same analyses of Fig. (8), but for KIC 4851217 (TIC 184246521).

617

#### B.8. *KIC 4909422 (TIC 121108244) Object*

618 This object presents a variation in its O-C diagram, Fig. 21, however, such variation does not present a complete  
 619 orbital cycle due to a possible third body around the binary system with a period  $P = 6582.935^{+927.321}_{-1415.082}$ , in an orbit  
 620 with eccentricity  $e = 0.839^{+0.131}_{-0.096}$ , at a distance  $a = 787.887^{+39.067}_{-99.774}$  from its parent stars, with its inclination axis  
 621  $\omega = 6.695^{+6.849}_{-4.825}$  and linear parameters fits at  $A = 6.082^{+0.732}_{-1.328}$  and  $B = -0.002^{+0.000}_{-0.000}$ .

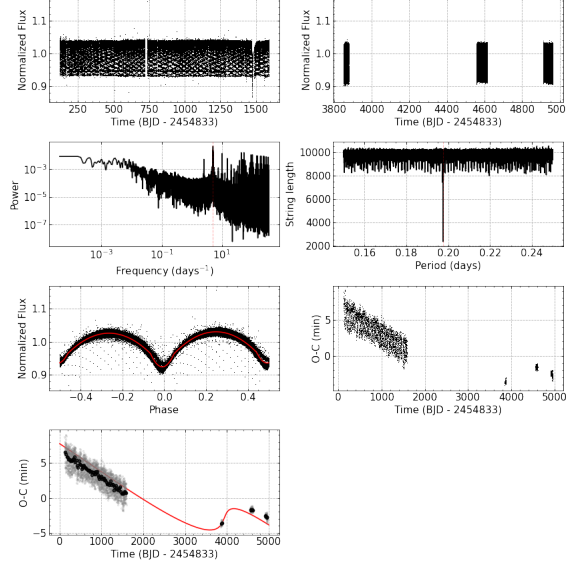


**Figure 21.** Same analyses of Fig. (8), but for KIC 4909422 (TIC 121108244).

622

#### B.9. *KIC 4945588 (TIC 169079394) Object*

623 This object presents a variation in its O-C diagram, Fig. 22, however, such variation does not present a complete  
 624 orbital cycle due to a possible third body around the binary system with a period  $P = 1607.893^{+29.331}_{-140.789}$ , in an orbit  
 625 with eccentricity  $e = 0.871^{+0.046}_{-0.045}$ , at a distance  $a = 1289.577^{+32.368}_{-66.834}$  from its parent stars, with its inclination axis  
 626  $\omega = 134.791^{+5.397}_{-6.424}$  and linear parameters fits at  $A = 9.236^{+0.291}_{-0.645}$  and  $B = -0.002^{+0.000}_{-0.000}$ .

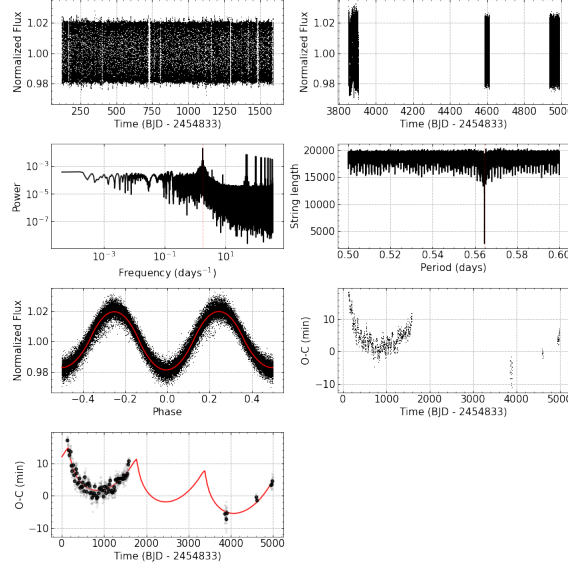


**Figure 22.** Same analyses of Fig. (8), but for KIC 4945588 (TIC 169079394).

627

#### B.10. *KIC 4999260 (TIC 121460104) Object*

628 This object presents a variation in its O-C diagram, Fig. 23, however, such variation does not present a complete  
 629 orbital cycle due to a possible third body around the binary system with a period  $P = 41607.891^{+1184.572}_{-1247.838}$ , in an orbit  
 630 with eccentricity  $e = 0.895^{+0.027}_{-0.021}$ , at a distance  $a = 1276.685^{+75.891}_{-50.225}$  from its parent stars, with its inclination axis  
 631  $\omega = 226.484^{+4.791}_{-9.178}$  and linear parameters fits at  $A = 5.785^{+0.445}_{-0.343}$  and  $B = -0.002^{+0.000}_{-0.000}$ .

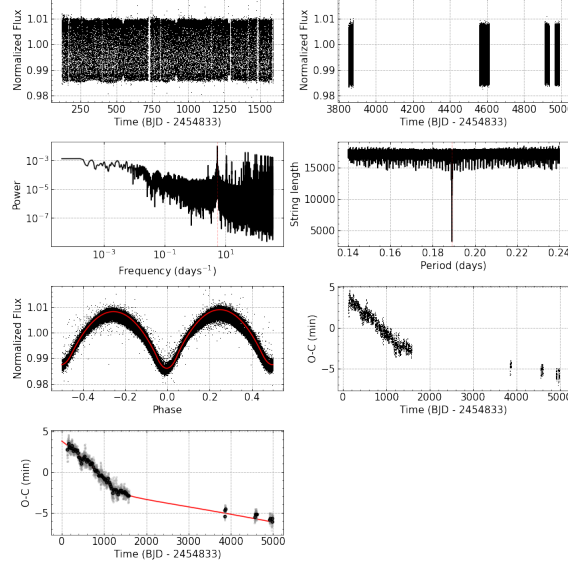


**Figure 23.** Same analyses of Fig. (8), but for KIC 4999260 (TIC 121460104).

632

#### B.11. *KIC 5022573 (TIC 138960108) Object*

633 This object presents a variation in its O-C diagram, Fig. 24, however, such variation does not present a complete  
 634 orbital cycle due to a possible third body around the binary system with a period  $P = 1826.598^{+113.755}_{-113.477}$ , in an orbit  
 635 with eccentricity  $e = 0.766^{+0.083}_{-0.061}$ , at a distance  $a = 2900.240^{+275.154}_{-298.752}$  from its parent stars, with its inclination axis  
 636  $\omega = 26.089^{+12.937}_{-10.238}$  and linear parameters fits at  $A = 2.904^{+0.122}_{-0.140}$  and  $B = -0.001^{+0.000}_{-0.000}$ .

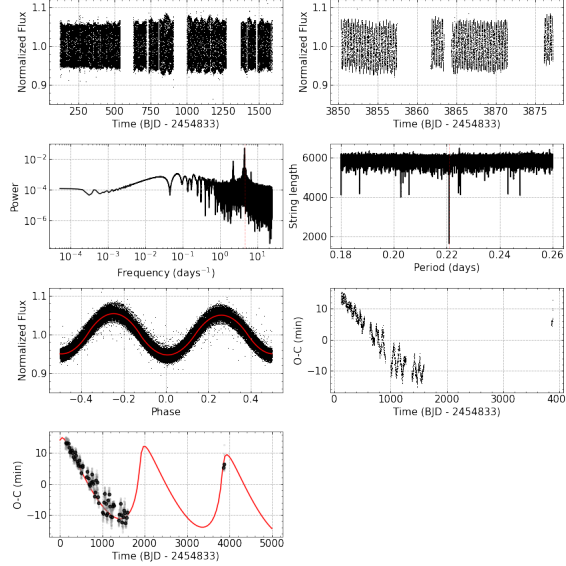


**Figure 24.** Same analyses of Fig. (8), but for KIC 5022573 (TIC 138960108).

637

#### B.12. *KIC 5296877 (TIC 169181296) Object*

638 This object presents a variation in its O-C diagram, Fig. 25, however, such variation does not present a complete  
 639 orbital cycle due to a possible third body around the binary system with a period  $P = 4962.088^{+11.012}_{-16.105}$ , in an orbit  
 640 with eccentricity  $e = 0.728^{+0.010}_{-0.007}$ , at a distance  $a = 929.247^{+4.982}_{-6.414}$  from its parent stars, with its inclination axis  
 641  $\omega = 87.015^{+0.658}_{-0.689}$ .

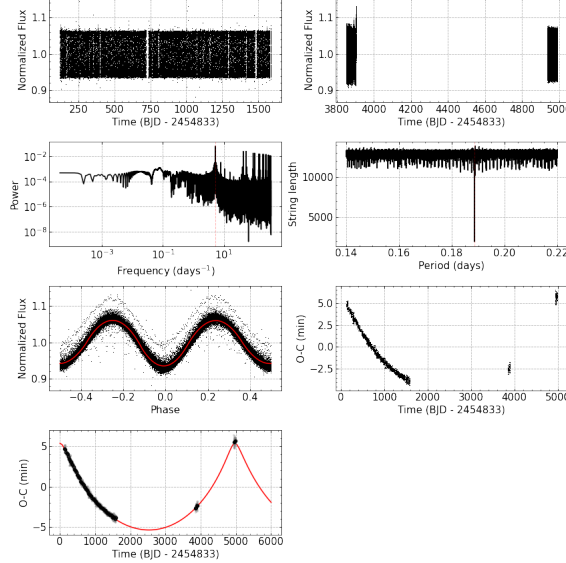


**Figure 25.** Same analyses of Fig. (8), but for KIC 5296877 (TIC 169181296).

642

#### B.13. *KIC 5513861 (TIC 120251815) Object*

643 This object presents a variation in its O-C diagram, Fig. 26, however, such variation does not present a complete  
 644 orbital cycle due to a possible third body around the binary system with a period  $P = 2113.335^{+5.927}_{-6.342}$ , in an orbit  
 645 with eccentricity  $e = 0.315^{+0.019}_{-0.029}$ , at a distance  $a = 3763.359^{+90.637}_{-88.600}$  from its parent stars, with its inclination axis  
 646  $\omega = 291.346^{+5.326}_{-5.698}$ .

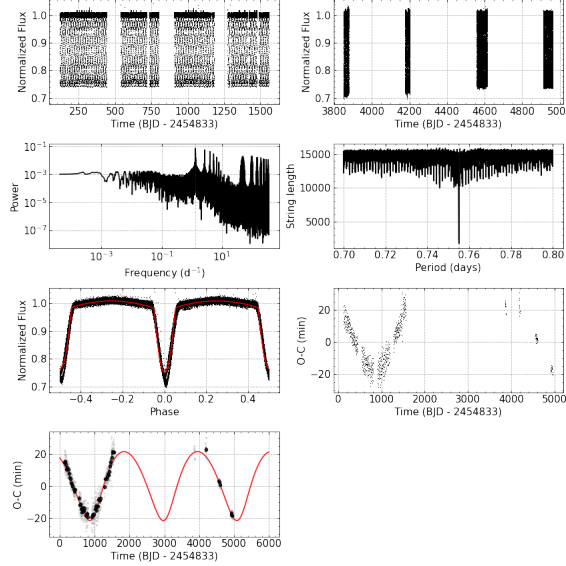


**Figure 26.** Same analyses of Fig. (8), but for KIC 5513861 (TIC 120251815).

647

#### B.14. *KIC 5975712 (TIC 184253728) Object*

648 This object presents a variation in its O-C diagram, Fig. 27, however, such variation does not present a complete  
 649 orbital cycle due to a possible third body around the binary system with a period  $P = 1694.123^{+2.155}_{-1.001}$ , in an orbit  
 650 with eccentricity  $e = 0.218^{+0.001}_{-0.001}$ , at a distance  $a = 1718.050^{+0.840}_{-1.923}$  from its parent stars, with its inclination axis  
 651  $\omega = 262.220^{+0.376}_{-0.450}$  and linear parameters fits at  $A = 25.815^{+0.036}_{-0.014}$  and  $B = -0.012^{+0.000}_{-0.000}$ .

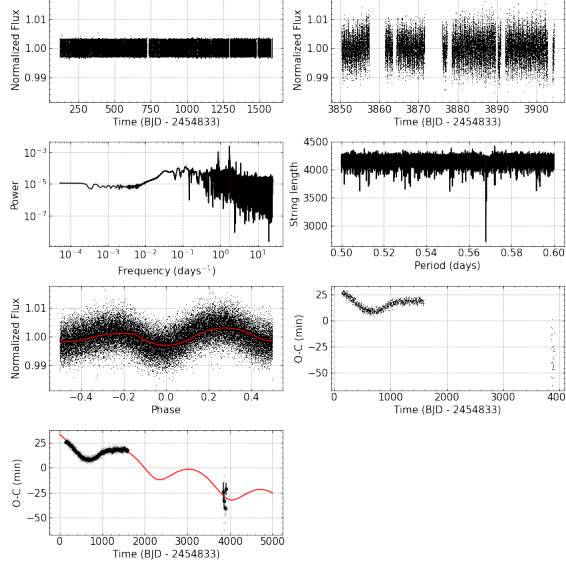


**Figure 27.** Same analyses of Fig. (8), but for KIC 5975712 (TIC 184253728).

652

#### B.15. *KIC 6187893 (TIC 120576722) Object*

653 This object presents a variation in its O-C diagram, Fig. 28, however, such variation does not present a complete  
 654 orbital cycle due to a possible third body around the binary system with a period  $P = 2028.925^{+5.819}_{-5.788}$ , in an orbit  
 655 with eccentricity  $e = 0.969^{+0.004}_{-0.006}$ , at a distance  $a = 15566.140^{+1116.612}_{-1159.858}$  from its parent stars, with its inclination axis  
 656  $\omega = 354.398^{+0.646}_{-0.703}$ .

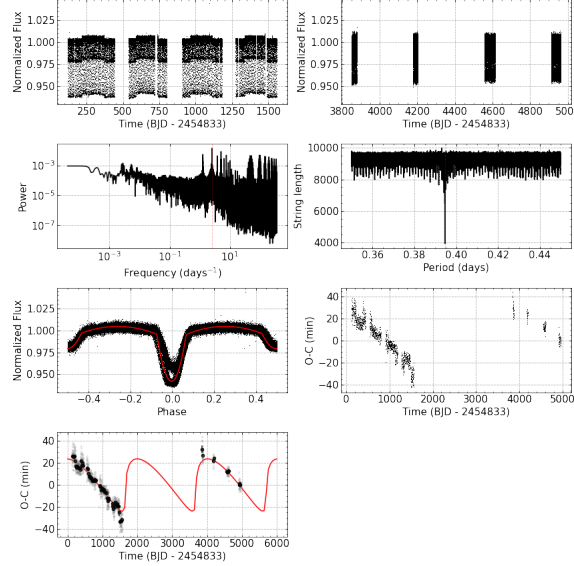


**Figure 28.** Same analyses of Fig. (8), but for KIC 6187893 (TIC 120576722).

657

#### B.16. *KIC 6205460 (TIC 137408317) Object*

658 This object presents a variation in its O-C diagram, Fig. 29, however, such variation does not present a complete  
 659 orbital cycle due to a possible third body around the binary system with a period  $P = 2311.862^{+83.952}_{-29.020}$ , in an orbit  
 660 with eccentricity  $e = 0.426^{+0.019}_{-0.071}$ , at a distance  $a = 37561.143^{+214.540}_{-973.443}$  from its parent stars, with its inclination axis  
 661  $\omega = 233.491^{+4.345}_{-1.748}$ .

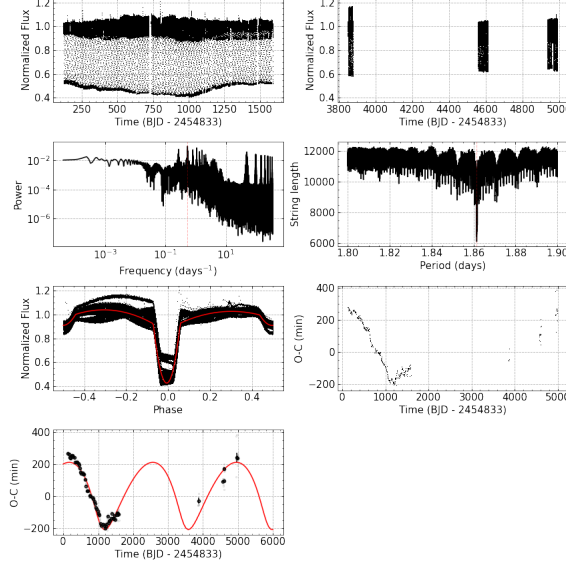


**Figure 29.** Same analyses of Fig. (8), but for KIC 6205460 (TIC 137408317).

662

#### B.17. *KIC 6353203 (TIC 121463130) Object*

663 This object presents a variation in its O-C diagram, Fig. 30, however, such variation does not present a complete  
 664 orbital cycle due to a possible third body around the binary system with a period  $P = 2449.628^{+19.370}_{-7.118}$ , in an orbit  
 665 with eccentricity  $e = 0.575^{+0.057}_{-0.069}$ , at a distance  $a = 2535.311^{+140.257}_{-264.969}$  from its parent stars, with its inclination axis  
 666  $\omega = 33.826^{+9.897}_{-2.290}$ .

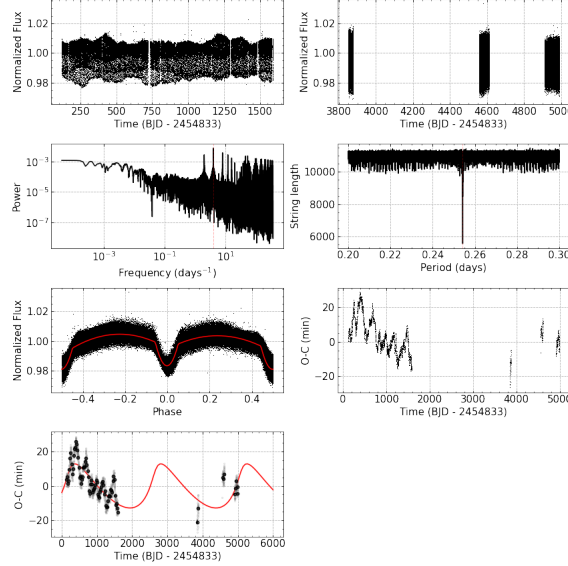


**Figure 30.** Same analyses of Fig. (8), but for KIC 6353203 (TIC 121463130).

667

#### B.18. *KIC 6462057 (TIC 169175441) Object*

668 This object presents a variation in its O-C diagram, Fig. 31, however, such variation does not present a complete  
 669 orbital cycle due to a possible third body around the binary system with a period  $P = 4926.320^{+359.711}_{-147.307}$ , in an orbit  
 670 with eccentricity  $e = 0.637^{+0.080}_{-0.177}$ , at a distance  $a = 410.767^{+31.402}_{-42.634}$  from its parent stars, with its inclination axis  
 671  $\omega = 76.324^{+18.082}_{-11.176}$  and linear parameters fits at  $A = 1.690^{+0.111}_{-0.211}$  and  $B = -0.001^{+0.000}_{-0.000}$ .

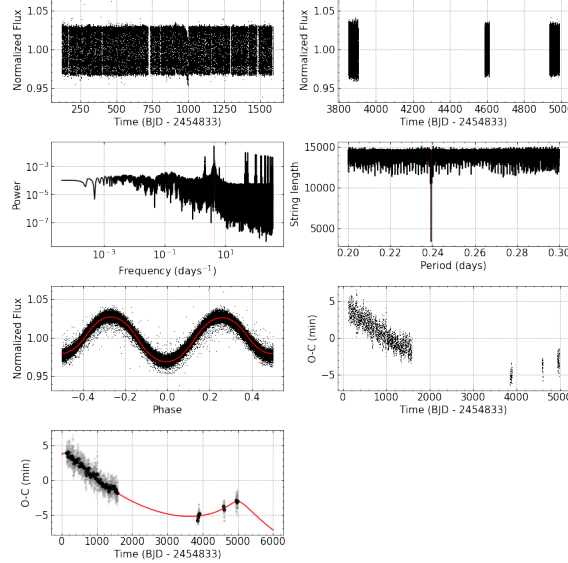


**Figure 31.** Same analyses of Fig. (8), but for KIC 6462057 (TIC 169175441).

672

#### B.19. *KIC 7259917 (TIC 164463075) Object*

673 This object presents a variation in its O-C diagram, Fig. 32, however, such variation does not present a complete  
 674 orbital cycle due to a possible third body around the binary system with a period  $P = 4729.394^{+441.635}_{-196.787}$ , in an orbit  
 675 with eccentricity  $e = 0.720^{+0.063}_{-0.222}$ , at a distance  $a = 794.232^{+124.608}_{-171.657}$  from its parent stars, with its inclination axis  
 676  $\omega = 223.241^{+21.873}_{-16.910}$  and linear parameters fits at  $A = 5.809^{+0.837}_{-0.721}$  and  $B = 0.001^{+0.000}_{-0.000}$ .

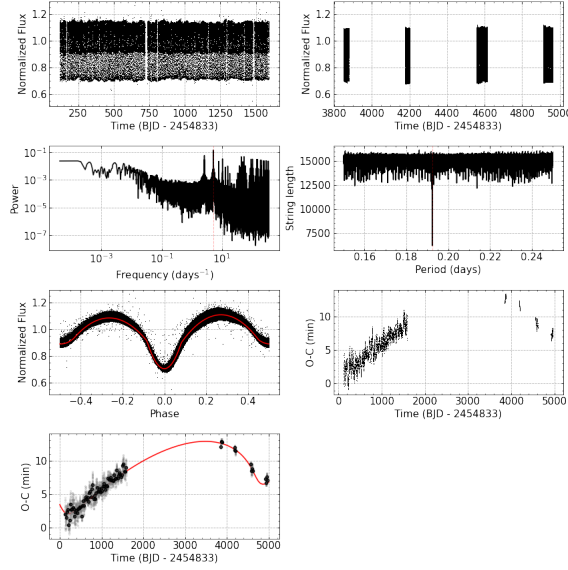


**Figure 32.** Same analyses of Fig. (8), but for KIC 7259917 (TIC 164463075).

677

#### B.20. *KIC 7375612 (TIC 271671189) Object*

678 This object presents a variation in its O-C diagram, Fig. 33, however, such variation does not present a complete  
 679 orbital cycle due to a possible third body around the binary system with a period  $P = 2123.456^{+15.279}_{-7.569}$ , in an orbit  
 680 with eccentricity  $e = 0.098^{+0.074}_{-0.028}$ , at a distance  $a = 1221.564^{+45.153}_{-18.592}$  from its parent stars, with its inclination axis  
 681  $\omega = 302.775^{+39.354}_{-19.329}$ .

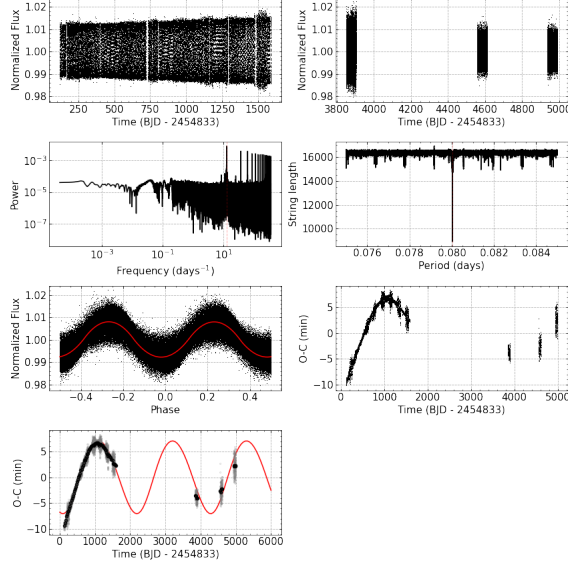


**Figure 33.** Same analyses of Fig. (8), but for KIC 7375612 (TIC 271671189).

682

#### B.21. *KIC 7385478 (TIC 273501820) Object*

683 This object presents a variation in its O-C diagram, Fig. 34, however, such variation does not present a complete  
 684 orbital cycle due to a possible third body around the binary system with a period  $P = 1360.065^{+76.397}_{-101.476}$ , in an orbit  
 685 with eccentricity  $e = 0.782^{+0.148}_{-0.363}$ , at a distance  $a = 2892.213^{+287.804}_{-627.328}$  from its parent stars, with its inclination axis  
 686  $\omega = 59.734^{+24.105}_{-25.564}$  and linear parameters fits at  $A = 8.118^{+1.161}_{-2.345}$  and  $B = -0.002^{+0.000}_{-0.001}$ .

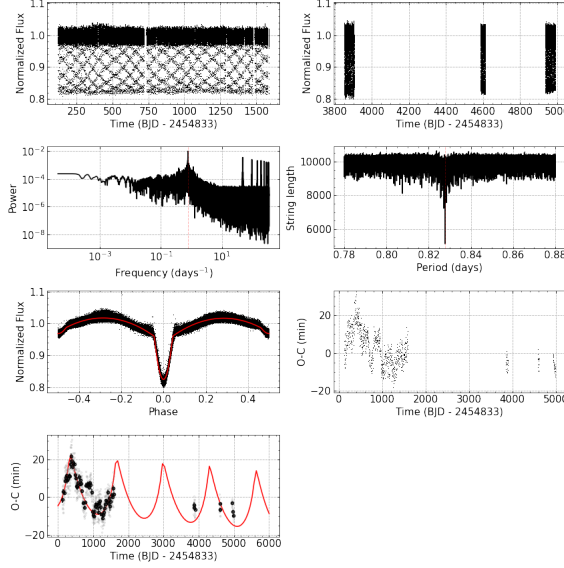


**Figure 34.** Same analyses of Fig. (8), but for KIC 7385478 (TIC 273501820).

687

### B.22. *KIC 7431703 (TIC 158431889) Object*

688 This object presents a variation in its O-C diagram, Fig. 35, however, such variation does not present a complete  
 689 orbital cycle due to a possible third body around the binary system with a period  $P = 1820.383^{+42.684}_{-105.177}$ , in an orbit  
 690 with eccentricity  $e = 0.448^{+0.121}_{-0.158}$ , at a distance  $a = 193.698^{+45.269}_{-23.174}$  from its parent stars, with its inclination axis  
 691  $\omega = 133.419^{+48.678}_{-38.020}$ .

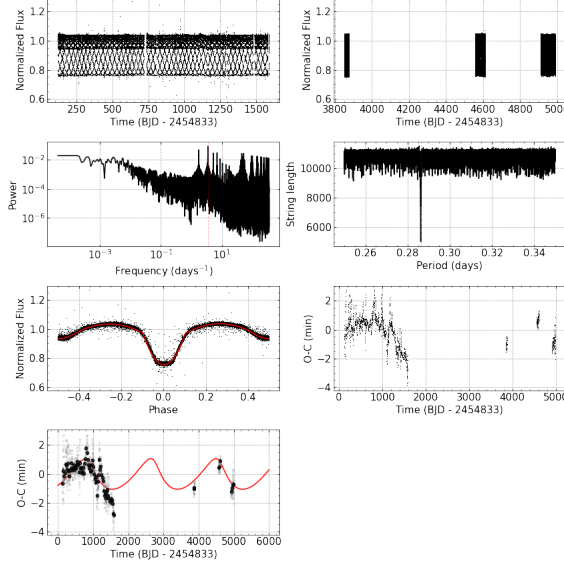


**Figure 35.** Same analyses of Fig. (8), but for KIC 7431703 (TIC 158431889).

692

### B.23. *KIC 7440742 (TIC 159444225) Object*

693 This object presents a variation in its O-C diagram, Fig. 36, however, such variation does not present a complete  
 694 orbital cycle due to a possible third body around the binary system with a period  $P = 2003.253^{+133.920}_{-126.183}$ , in an orbit  
 695 with eccentricity  $e = 0.983^{+0.005}_{-0.013}$ , at a distance  $a = 3175.282^{+129.578}_{-270.423}$  from its parent stars, with its inclination axis  
 696  $\omega = 11.419^{+1.766}_{-3.858}$  and linear parameters fits at  $A = 3.956^{+0.521}_{-0.421}$  and  $B = 0.007^{+0.000}_{-0.000}$ .

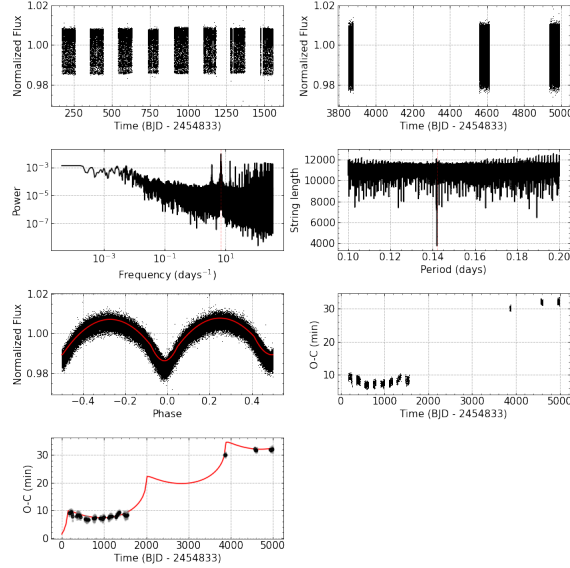


**Figure 36.** Same analyses of Fig. (8), but for KIC 7440742 (TIC 159444225).

697

#### B.24. *KIC 7457163 (TIC 271539287) Object*

This object presents a variation in its O-C diagram, Fig. 37, however, such variation does not present a complete orbital cycle due to a possible third body around the binary system with a period  $P = 6255.520^{+135.002}_{-193.789}$ , in an orbit with eccentricity  $e = 0.527^{+0.062}_{-0.039}$ , at a distance  $a = 2751.917^{+61.453}_{-41.633}$  from its parent stars, with its inclination axis  $\omega = 278.115^{+8.270}_{-3.766}$ .

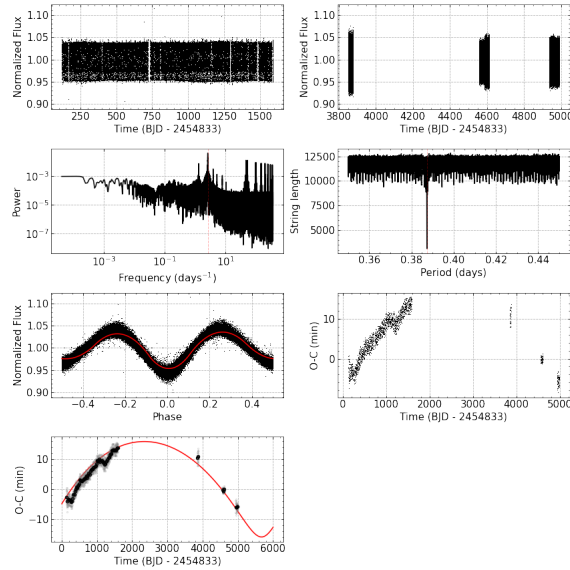


**Figure 37.** Same analyses of Fig. (8), but for KIC 7457163 (TIC 271539287).

702

#### B.25. *KIC 7512381 (TIC 158218818) Object*

This object presents a variation in its O-C diagram, Fig. 38, however, such variation does not present a complete orbital cycle due to a possible third body around the binary system with a period  $P = 6805.413^{+249.021}_{-135.070}$ , in an orbit with eccentricity  $e = 0.411^{+0.040}_{-0.131}$ , at a distance  $a = 1298.333^{+127.638}_{-41.743}$  from its parent stars, with its inclination axis  $\omega = 340.888^{+7.394}_{-5.227}$ .

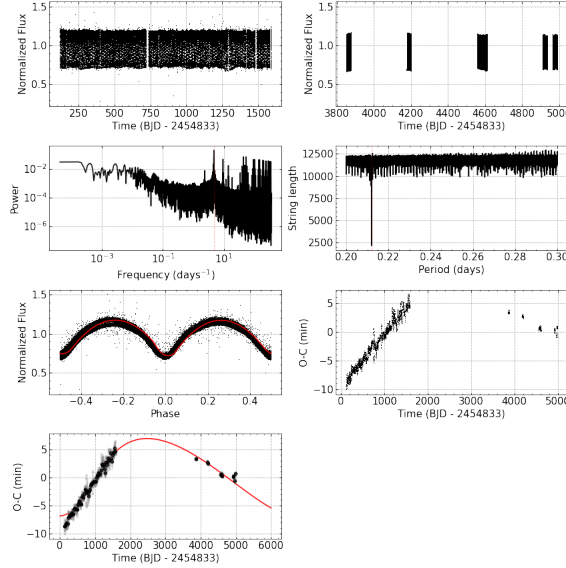


**Figure 38.** Same analyses of Fig. (8), but for KIC 7512381 (TIC 158218818).

#### B.26. *KIC 7690843 (TIC 271158877) Object*

This object presents a variation in its O-C diagram, Fig. 39, however, such variation does not present a complete orbital cycle due to a possible third body around the binary system with a period  $P = 2714.623^{+60.236}_{-72.170}$ , in an orbit with eccentricity  $e = 0.752^{+0.058}_{-0.152}$ , at a distance  $a = 2435.466^{+384.915}_{-494.907}$  from its parent stars, with its inclination axis  $\omega = 340.293^{+7.820}_{-10.974}$  and linear parameters fits at  $A = -0.752^{+0.125}_{-0.158}$  and  $B = -0.000^{+0.000}_{-0.000}$ .

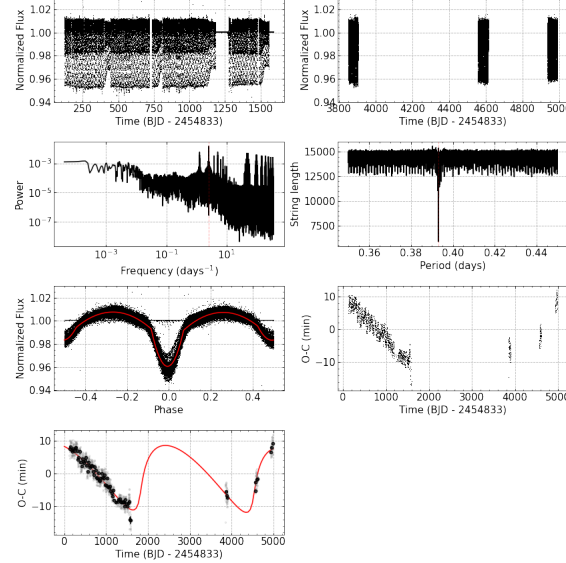


**Figure 39.** Same analyses of Fig. (8), but for KIC 7690843 (TIC 271158877).

#### B.27. *KIC 7766185 (TIC 272176884) Object*

This object presents a variation in its O-C diagram, Fig. 40, however, such variation does not present a complete orbital cycle due to a possible third body around the binary system with a period  $P = 1860.287^{+99.837}_{-87.249}$ , in an orbit with eccentricity  $e = 0.945^{+0.015}_{-0.024}$ , at a distance  $a = 88.601^{+10.424}_{-12.943}$  from its parent stars, with its inclination axis  $\omega = 353.253^{+5.047}_{-9.173}$  and linear parameters fits at  $A = 1.442^{+0.046}_{-0.043}$  and  $B = -0.001^{+0.000}_{-0.000}$ .

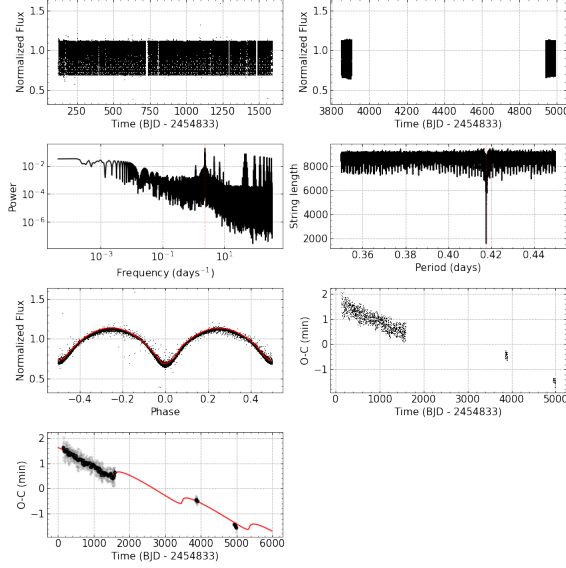


**Figure 40.** Same analyses of Fig. (8), but for KIC 7766185 (TIC 272176884).

717

#### B.28. *KIC 7816201 (TIC 159105713) Object*

This object presents a variation in its O-C diagram, Fig. 41, however, such variation does not present a complete orbital cycle due to a possible third body around the binary system with a period  $P = 2328.001^{+209.934}_{-397.908}$ , in an orbit with eccentricity  $e = 0.696^{+0.074}_{-0.124}$ , at a distance  $a = 320.107^{+17.816}_{-22.707}$  from its parent stars, with its inclination axis  $\omega = 61.045^{+35.826}_{-26.856}$  and linear parameters fits at  $A = 4.540^{+0.222}_{-0.501}$  and  $B = -0.001^{+0.000}_{-0.000}$ .

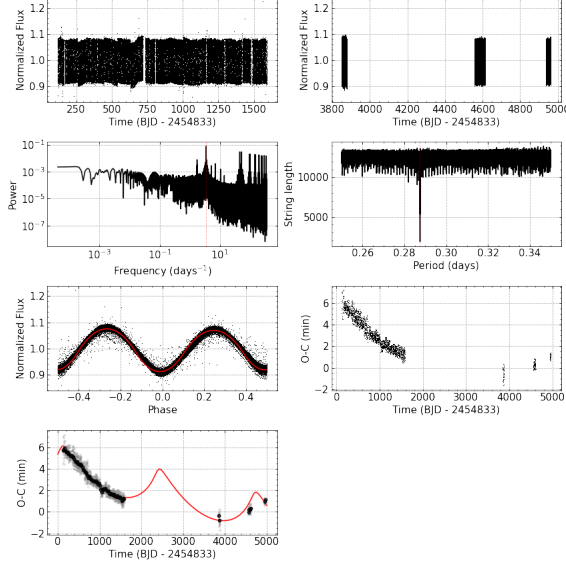


**Figure 41.** Same analyses of Fig. (8), but for KIC 7816201 (TIC 159105713).

722

#### B.29. *KIC 7938870 (TIC 123416563) Object*

This object presents a variation in its O-C diagram, Fig. 42, however, such variation does not present a complete orbital cycle due to a possible third body around the binary system with a period  $P = 2100.595^{+31.818}_{-32.686}$ , in an orbit with eccentricity  $e = 0.627^{+0.094}_{-0.022}$ , at a distance  $a = 486.852^{+41.826}_{-14.625}$  from its parent stars, with its inclination axis  $\omega = 302.126^{+8.472}_{-6.225}$  and linear parameters fits at  $A = -7.672^{+0.155}_{-0.219}$  and  $B = 0.002^{+0.000}_{-0.000}$ .

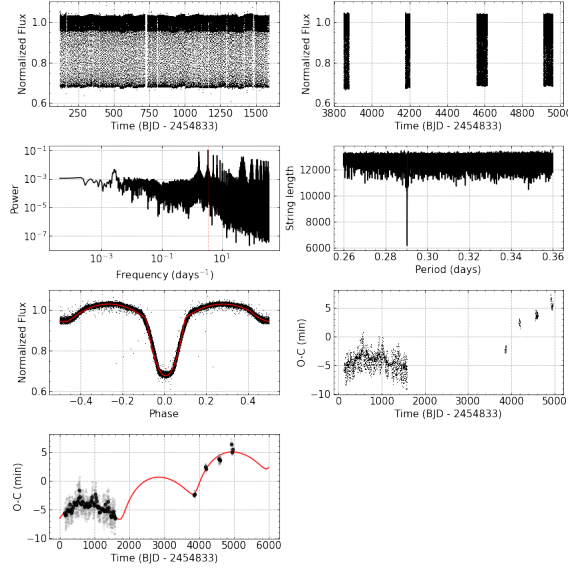


**Figure 42.** O-C diagram for the binary system KIC 7938870 (TIC 123416563).

727

### B.30. *KIC 7950962 (TIC 158726046) Object*

728 This object presents a variation in its O-C diagram, Fig. 43, however, such variation does not present a complete  
 729 orbital cycle due to a possible third body around the binary system with a period  $P = 3085.157^{+100.353}_{-116.633}$ , in an orbit  
 730 with eccentricity  $e = 0.075^{+0.053}_{-0.055}$ , at a distance  $a = 309.409^{+18.086}_{-30.892}$  from its parent stars, with its inclination axis  
 731  $\omega = 172.259^{+3.845}_{-5.776}$  and linear parameters fits at  $A = 1.990^{+0.130}_{-0.175}$  and  $B = 0.002^{+0.000}_{-0.000}$ .

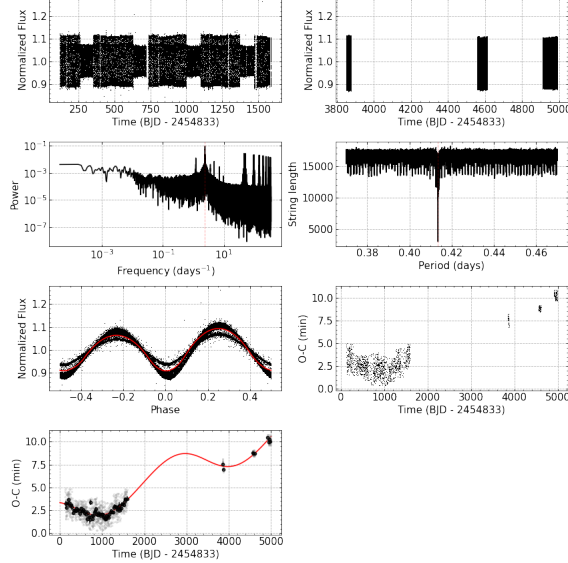


**Figure 43.** Same analyses of Fig. (8), but for KIC 7950962 (TIC 158726046).

732

### B.31. *KIC 8189196 (TIC 268302473) Object*

733 This object presents a variation in its O-C diagram, Fig. 44, however, such variation does not present a complete  
 734 orbital cycle due to a possible third body around the binary system with a period  $P = 3903.002^{+24.689}_{-30.695}$ , in an orbit  
 735 with eccentricity  $e = 0.980^{+0.003}_{-0.004}$ , at a distance  $a = 12579.602^{+931.164}_{-840.971}$  from its parent stars, with its inclination axis  
 736  $\omega = 352.082^{+0.671}_{-0.857}$ .

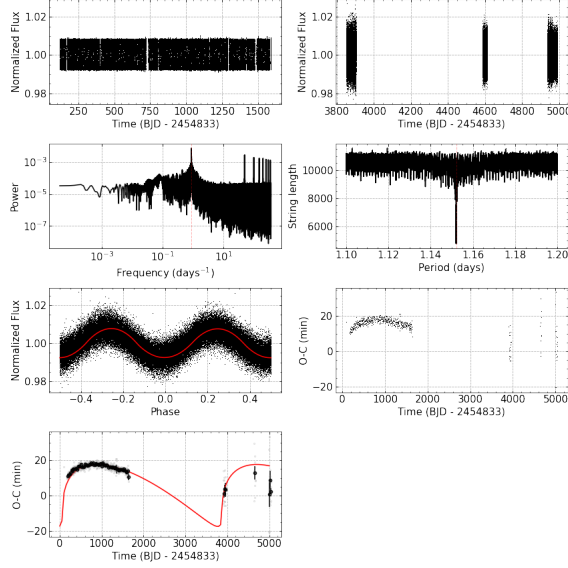


**Figure 44.** Same analyses of Fig. (8), but for KIC 8189196 (TIC 268302473).

737

### B.32. *KIC 8231231 (TIC 159578658) Object*

This object presents a variation in its O-C diagram, Fig. 45, however, such variation does not present a complete orbital cycle due to a possible third body around the binary system with a period  $P = 1909.021^{+50.390}_{-54.438}$ , in an orbit with eccentricity  $e = 0.949^{+0.021}_{-0.033}$ , at a distance  $a = 2930.266^{+110.526}_{-401.530}$  from its parent stars, with its inclination axis  $\omega = 17.464^{+4.268}_{-4.281}$  and linear parameters fits at  $A = 3.187^{+0.745}_{-0.630}$  and  $B = 0.009^{+0.001}_{-0.001}$ .

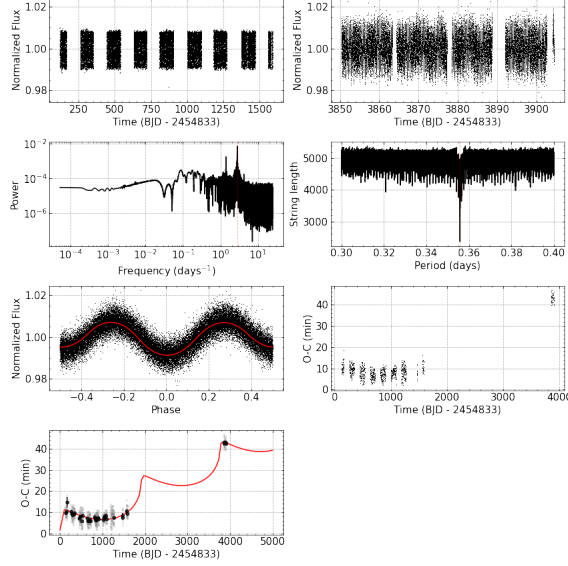


**Figure 45.** Same analyses of Fig. (8), but for KIC 8231231 (TIC 159578658).

742

### B.33. *KIC 8285349 (TIC 352012002) Object*

This object presents a variation in its O-C diagram, Fig. 46, however, such variation does not present a complete orbital cycle due to a possible third body around the binary system with a period  $P = 2042.641^{+16.160}_{-55.476}$ , in an orbit with eccentricity  $e = 0.522^{+0.022}_{-0.218}$ , at a distance  $a = 1553.753^{+36.747}_{-102.809}$  from its parent stars, with its inclination axis  $\omega = 0.246^{+0.658}_{-0.195}$ .

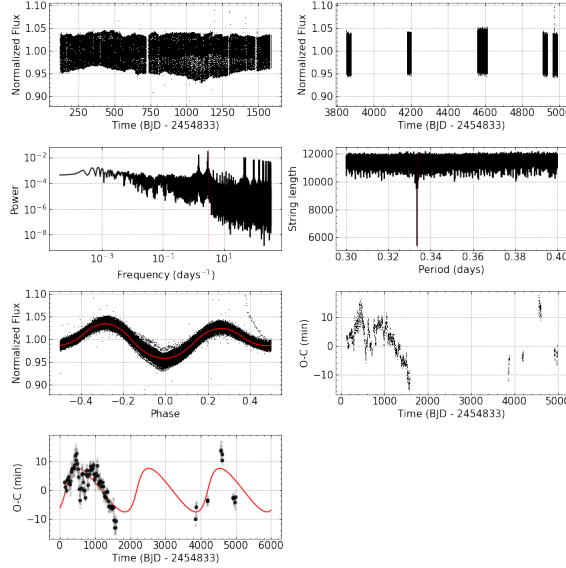


**Figure 46.** Same analyses of Fig. (8), but for KIC 8285349 (TIC 352012002).

747

#### B.34. *KIC 8397460 (TIC 185286922) Object*

This object presents a variation in its O-C diagram, Fig. 47, however, such variation does not present a complete orbital cycle due to a possible third body around the binary system with a period  $P = 8112.505^{+509.919}_{-443.186}$ , in an orbit with eccentricity  $e = 0.966^{+0.003}_{-0.003}$ , at a distance  $a = 17859.920^{+1277.042}_{-1093.353}$  from its parent stars, with its inclination axis  $\omega = 184.634^{+3.200}_{-3.526}$  and linear parameters fits at  $A = -2.969^{+0.807}_{-0.626}$  and  $B = 0.003^{+0.000}_{-0.000}$ .

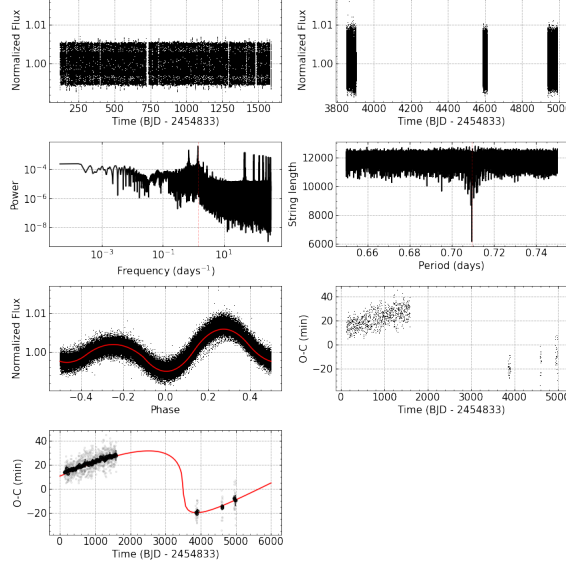


**Figure 47.** Same analyses of Fig. (8), but for KIC 8397460 (TIC 185286922).

752

#### B.35. *KIC 8579707 (TIC 273865522) Object*

This object presents a variation in its O-C diagram, Fig. 48, however, such variation does not present a complete orbital cycle due to a possible third body around the binary system with a period  $P = 1944.760^{+203.672}_{-24.784}$ , in an orbit with eccentricity  $e = 0.523^{+0.090}_{-0.037}$ , at a distance  $a = 767.345^{+60.336}_{-22.646}$  from its parent stars, with its inclination axis  $\omega = 274.445^{+12.220}_{-27.352}$ .

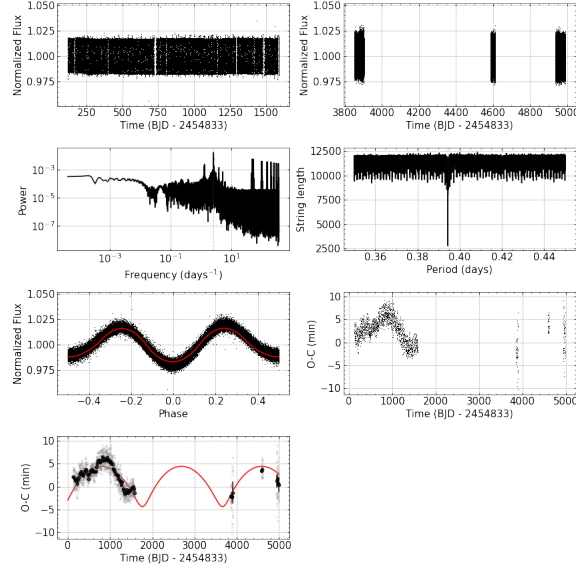


**Figure 48.** Same analyses of Fig. (8), but for KIC 8579707 (TIC 273865522).

#### B.36. *KIC 8587792 (TIC 239290086) Object*

This object presents a variation in its O-C diagram, Fig. 49, however, such variation does not present a complete orbital cycle due to a possible third body around the binary system with a period  $P = 5493.004^{+294.492}_{-278.158}$ , in an orbit with eccentricity  $e = 0.380^{+0.046}_{-0.040}$ , at a distance  $a = 1206.681^{+74.433}_{-72.220}$  from its parent stars, with its inclination axis  $\omega = 320.376^{+8.325}_{-6.775}$  and linear parameters fits at  $A = 0.202^{+0.201}_{-0.160}$  and  $B = 0.000^{+0.000}_{-0.000}$ .

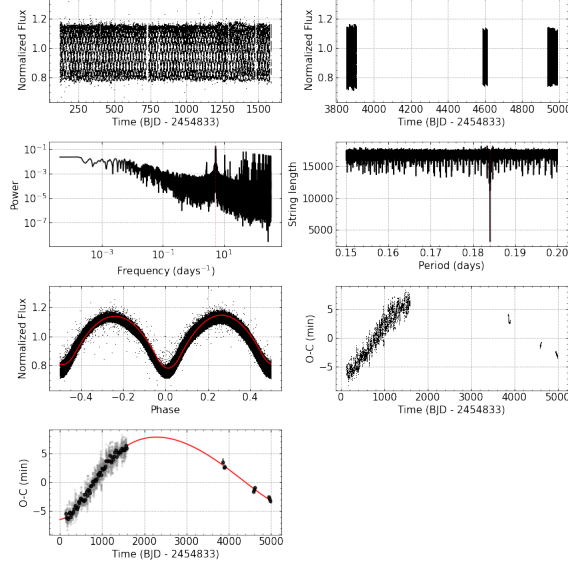


**Figure 49.** Same analyses of Fig. (8), but for KIC 8587792 (TIC 239290086).

#### B.37. *KIC 8758161 (TIC 270615728) Object*

This object presents a variation in its O-C diagram, Fig. 50, however, such variation does not present a complete orbital cycle due to a possible third body around the binary system with a period  $P = 18453.026^{+3264.951}_{-3355.454}$ , in an orbit with eccentricity  $e = 0.908^{+0.047}_{-0.069}$ , at a distance  $a = 8615.186^{+1034.901}_{-1451.131}$  from its parent stars, with its inclination axis  $\omega = 8.511^{+9.509}_{-4.650}$ .

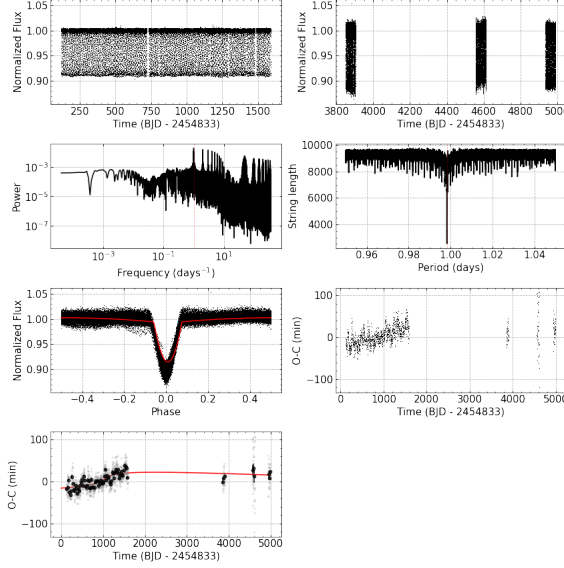


**Figure 50.** Same analyses of Fig. (8), but for KIC 8758161 (TIC 270615728).

767

### B.38. *KIC 8894630 (TIC 271352011) Object*

768 This object presents a variation in its O-C diagram, Fig. 51, however, such variation does not present a complete  
 769 orbital cycle due to a possible third body around the binary system with a period  $P = 7635.890^{+351.320}_{-315.610}$ , in an orbit  
 770 with eccentricity  $e = 0.737^{+0.043}_{-0.030}$ , at a distance  $a = 5539.682^{+502.895}_{-297.206}$  from its parent stars, with its inclination axis  
 771  $\omega = 14.359^{+4.427}_{-4.471}$ .

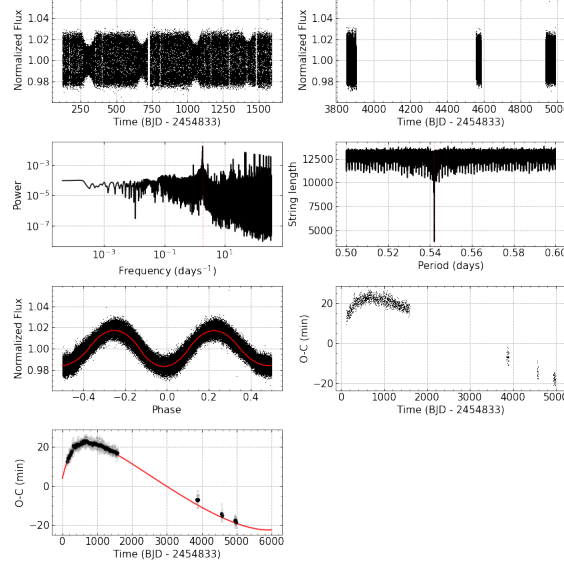


**Figure 51.** Same analyses of Fig. (8), but for KIC 8894630 (TIC 271352011).

772

### B.39. *KIC 9083523 (TIC 159169838) Object*

773 This object presents a variation in its O-C diagram, Fig. 52, however, such variation does not present a complete  
 774 orbital cycle due to a possible third body around the binary system with a period  $P = 2200.587^{+36.070}_{-16.377}$ , in an orbit  
 775 with eccentricity  $e = 0.370^{+0.084}_{-0.090}$ , at a distance  $a = 621.439^{+29.266}_{-30.823}$  from its parent stars, with its inclination axis  
 776  $\omega = 202.850^{+10.495}_{-7.422}$ .

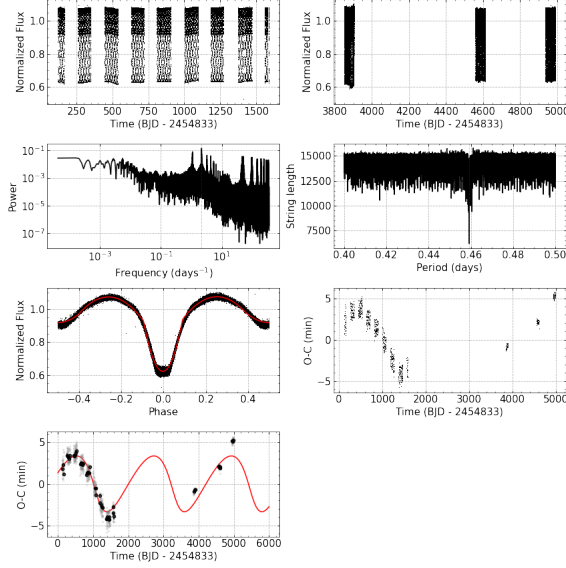


**Figure 52.** Same analyses of Fig. (8), but for KIC 9083523 (TIC 159169838).

#### B.40. *KIC 9181877 (TIC 239309691) Object*

This object presents a variation in its O-C diagram, Fig. 53, however, such variation does not present a complete orbital cycle due to a possible third body around the binary system with a period  $P = 1830.374^{+20.089}_{-49.420}$ , in an orbit with eccentricity  $e = 0.596^{+0.054}_{-0.051}$ , at a distance  $a = 2570.357^{+286.471}_{-143.622}$  from its parent stars, with its inclination axis  $\omega = 44.869^{+9.228}_{-9.783}$  and linear parameters fits at  $A = 4.696^{+0.304}_{-0.491}$  and  $B = -0.001^{+0.000}_{-0.000}$ .

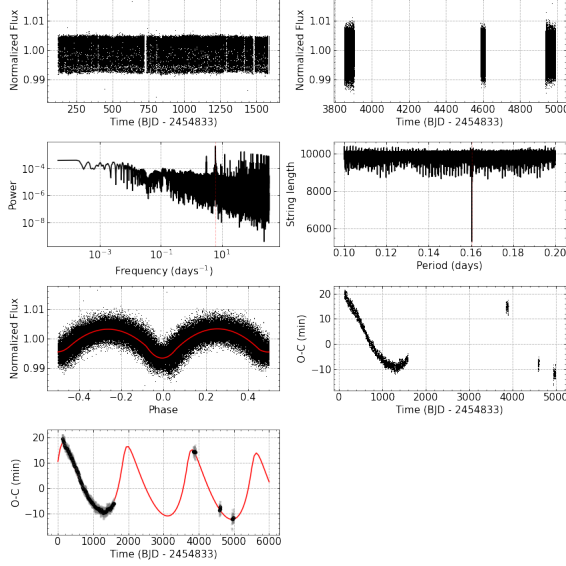


**Figure 53.** Same analyses of Fig. (8), but for KIC 9181877 (TIC 239309691).

#### B.41. *KIC 9345838 (TIC 275575030) Object*

This object presents a variation in its O-C diagram, Fig. 54, however, such variation does not present a complete orbital cycle due to a possible third body around the binary system with a period  $P = 2497.096^{+5.248}_{-7.119}$ , in an orbit with eccentricity  $e = 0.969^{+0.013}_{-0.009}$ , at a distance  $a = 3366.064^{+932.765}_{-754.234}$  from its parent stars, with its inclination axis  $\omega = 6.993^{+0.821}_{-1.239}$ .

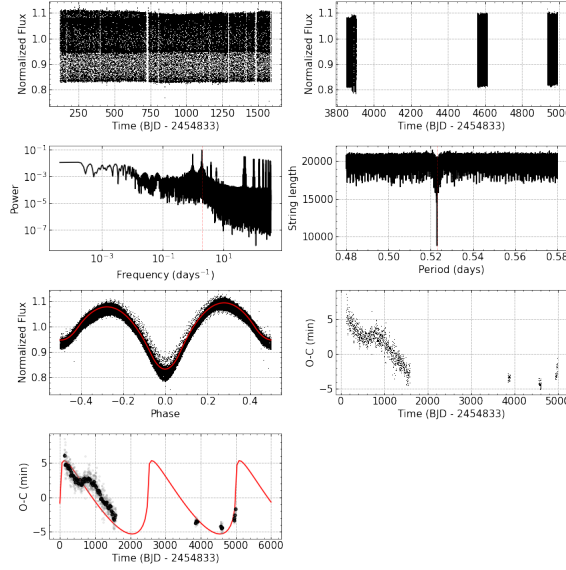


**Figure 54.** Same analyses of Fig. (8), but for KIC 9345838 (TIC 275575030).

787

#### B.42. *KIC 9402652 (TIC 159723646) Object*

This object presents a variation in its O-C diagram, Fig. 55, however, such variation does not present a complete orbital cycle due to a possible third body around the binary system with a period  $P = 1499.321^{+2.076}_{-2.039}$ , in an orbit with eccentricity  $e = 0.817^{+0.028}_{-0.034}$ , at a distance  $a = 1473.178^{+38.354}_{-37.486}$  from its parent stars, with its inclination axis  $\omega = 263.772^{+1.795}_{-2.034}$  and linear parameters fits at  $A = -12.516^{+0.311}_{-0.189}$  and  $B = 0.003^{+0.000}_{-0.000}$ .

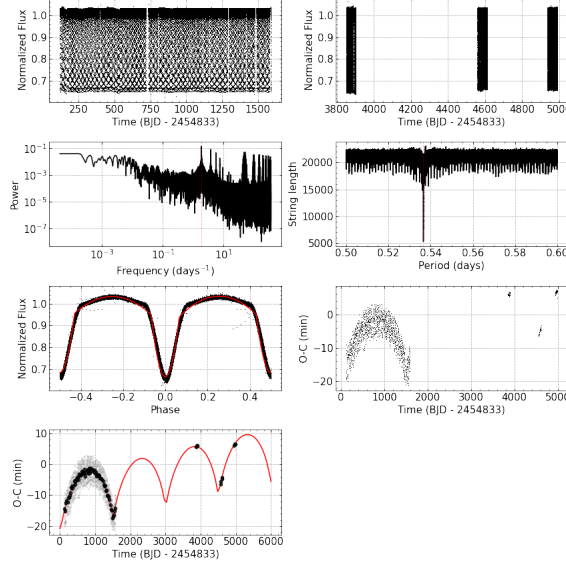


**Figure 55.** Same analyses of Fig. (8), but for KIC 9402652 (TIC 159723646).

792

#### B.43. *KIC 9602595 (TIC 273043307) Object*

This object presents a variation in its O-C diagram, Fig. 56, however, such variation does not present a complete orbital cycle due to a possible third body around the binary system with a period  $P = 6556.627^{+175.520}_{-624.070}$ , in an orbit with eccentricity  $e = 0.762^{+0.037}_{-0.028}$ , at a distance  $a = 37057.818^{+1690.472}_{-1659.916}$  from its parent stars, with its inclination axis  $\omega = 191.337^{+7.883}_{-4.892}$ .

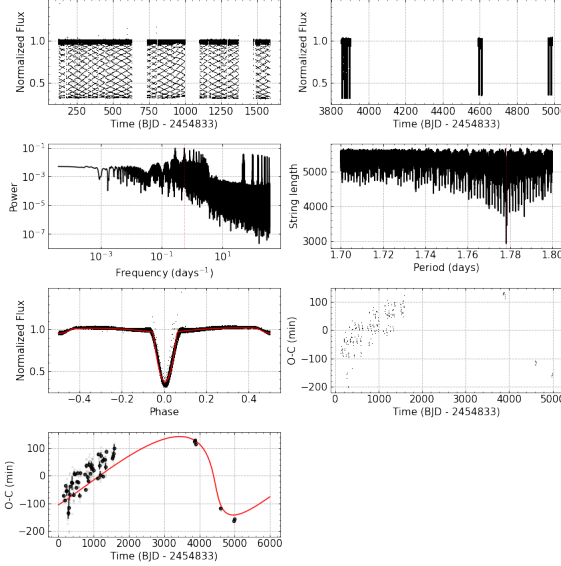


**Figure 56.** Same analyses of Fig. (8), but for KIC 9602595 (TIC 273043307).

#### B.44. *KIC 9657096 (TIC 271354390) Object*

This object presents a variation in its O-C diagram, Fig. 57, however, such variation does not present a complete orbital cycle due to a possible third body around the binary system with a period  $P = 1829.705^{+96.740}_{-26.635}$ , in an orbit with eccentricity  $e = 0.607^{+0.034}_{-0.077}$ , at a distance  $a = 1929.070^{+47.691}_{-45.751}$  from its parent stars, with its inclination axis  $\omega = 132.949^{+8.377}_{-4.699}$  and linear parameters fits at  $A = 6.868^{+0.166}_{-0.249}$  and  $B = -0.001^{+0.000}_{-0.000}$ .

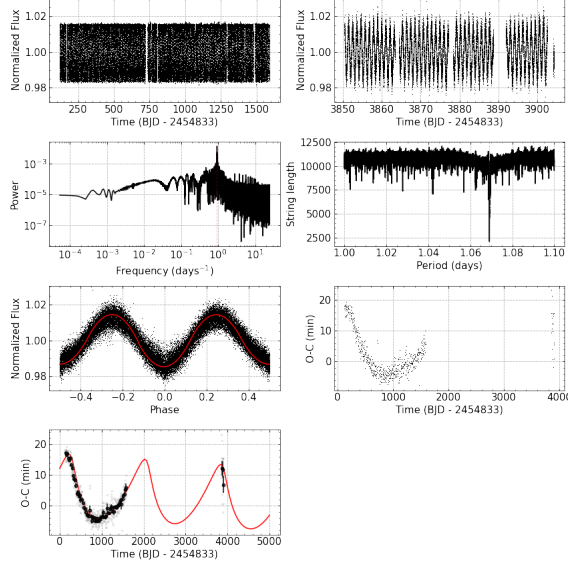


**Figure 57.** Same analyses of Fig. (8), but for KIC 9657096 (TIC 271354390).

#### B.45. *KIC 9760531 (TIC 158321712) Object*

This object presents a variation in its O-C diagram, Fig. 58, however, such variation does not present a complete orbital cycle due to a possible third body around the binary system with a period  $P = 2984.870^{+23.366}_{-31.904}$ , in an orbit with eccentricity  $e = 0.960^{+0.006}_{-0.095}$ , at a distance  $a = 886.002^{+45.537}_{-122.871}$  from its parent stars, with its inclination axis  $\omega = 15.153^{+18.866}_{-4.047}$  and linear parameters fits at  $A = 3.328^{+1.061}_{-0.176}$  and  $B = -0.001^{+0.000}_{-0.000}$ .

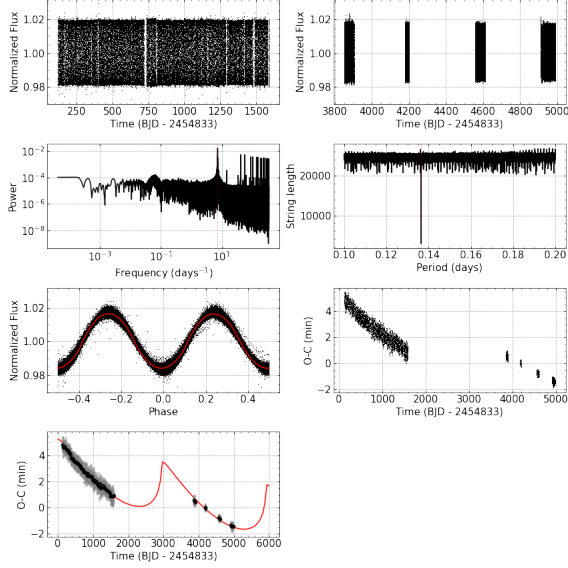


**Figure 58.** Same analyses of Fig. (8), but for KIC 9760531 (TIC 158321712).

#### B.46. *KIC 9832227 (TIC 63205800) Object*

This object presents a variation in its O-C diagram, Fig. 59, however, such variation does not present a complete orbital cycle due to a possible third body around the binary system with a period  $P = 6091.433^{+142.763}_{-115.053}$ , in an orbit with eccentricity  $e = 0.507^{+0.028}_{-0.047}$ , at a distance  $a = 4066.124^{+32.655}_{-168.895}$  from its parent stars, with its inclination axis  $\omega = 313.916^{+1.271}_{-5.992}$ .

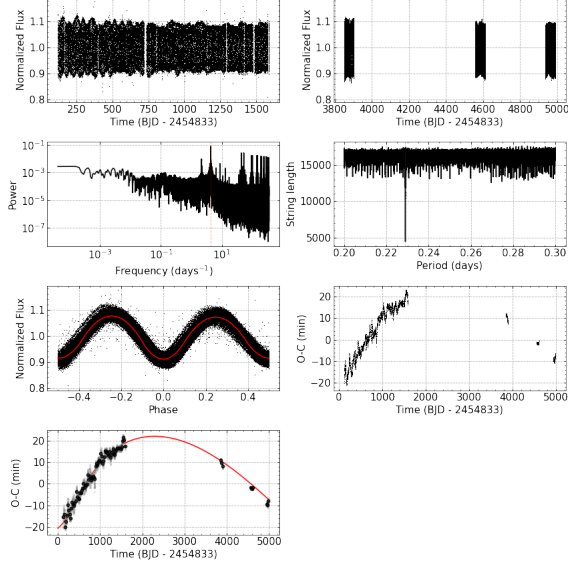


**Figure 59.** Same analyses of Fig. (8), but for KIC 9832227 (TIC 63205800).

#### B.47. *KIC 10155563 (TIC 63205800) Object*

This object presents a variation in its O-C diagram, Fig. 60, however, such variation does not present a complete orbital cycle due to a possible third body around the binary system with a period  $P = 3569.345^{+16.637}_{-16.118}$ , in an orbit with eccentricity  $e = 0.989^{+0.001}_{-0.002}$ , at a distance  $a = 1719.462^{+363.269}_{-295.336}$  from its parent stars, with its inclination axis  $\omega = 218.980^{+10.329}_{-6.680}$ .

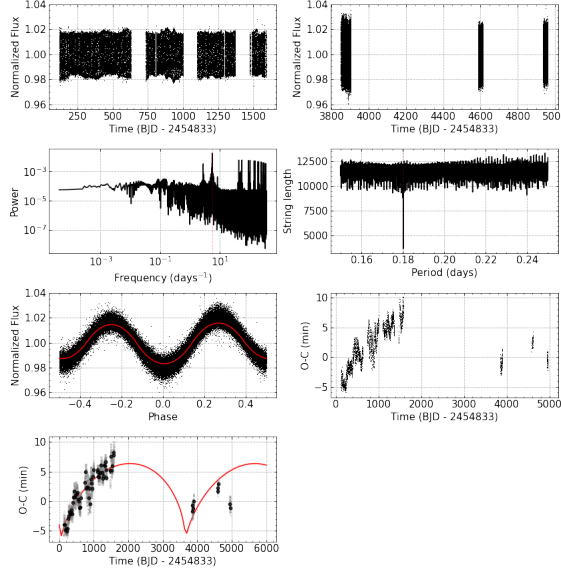


**Figure 60.** Same analyses of Fig. (8), but for KIC 10155563 (TIC 63205800).

817

#### B.48. *KIC 10259530 (TIC 164833847) Object*

This object presents a variation in its O-C diagram, Fig. 61, however, such variation does not present a complete orbital cycle due to a possible third body around the binary system with a period  $P = 4636.848^{+95.939}_{-92.547}$ , in an orbit with eccentricity  $e = 0.561^{+0.028}_{-0.173}$ , at a distance  $a = 381.542^{+18.713}_{-25.245}$  from its parent stars, with its inclination axis  $\omega = 100.245^{+11.074}_{-21.152}$  and linear parameters fits at  $A = 2.821^{+0.126}_{-0.411}$  and  $B = -0.001^{+0.000}_{-0.000}$ .

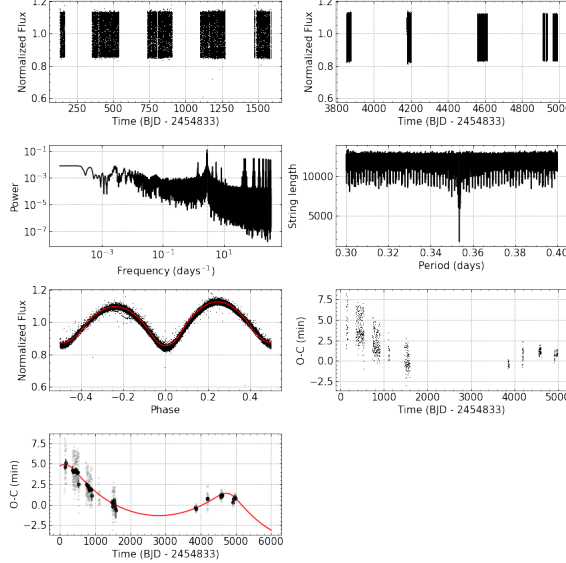


**Figure 61.** Same analyses of Fig. (8), but for KIC 10259530 (TIC 164833847).

822

#### B.49. *KIC 10389982 (TIC 164782264) Object*

This object presents a variation in its O-C diagram, Fig. 62, however, such variation does not present a complete orbital cycle due to a possible third body around the binary system with a period  $P = 2300.442^{+103.102}_{-37.377}$ , in an orbit with eccentricity  $e = 0.839^{+0.111}_{-0.090}$ , at a distance  $a = 239.080^{+8.393}_{-14.645}$  from its parent stars, with its inclination axis  $\omega = 330.594^{+20.678}_{-14.730}$  and linear parameters fits at  $A = 5.085^{+0.228}_{-0.217}$  and  $B = -0.001^{+0.000}_{-0.000}$ .

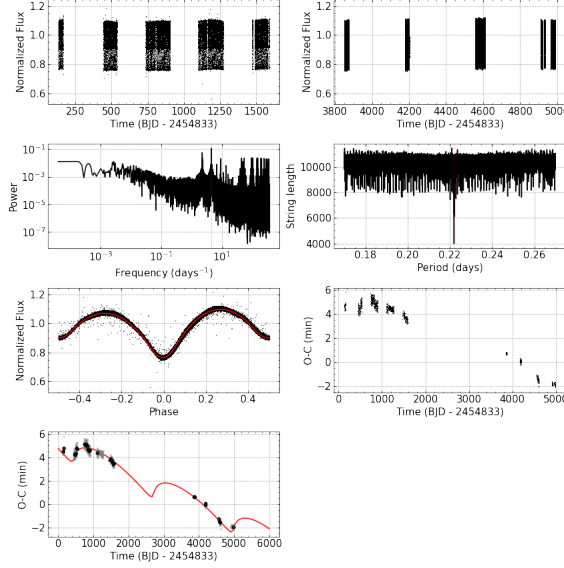


**Figure 62.** Same analyses of Fig. (8), but for KIC 10389982 (TIC 164782264).

827

#### B.50. *KIC 10481912 (TIC 272079818) Object*

This object presents a variation in its O-C diagram, Fig. 63, however, such variation does not present a complete orbital cycle due to a possible third body around the binary system with a period  $P = 4101.691^{+96.134}_{-510.167}$ , in an orbit with eccentricity  $e = 0.353^{+0.138}_{-0.120}$ , at a distance  $a = 543.619^{+43.615}_{-42.953}$  from its parent stars, with its inclination axis  $\omega = 56.372^{+36.062}_{-30.249}$  and linear parameters fits at  $A = 4.864^{+0.512}_{-0.339}$  and  $B = -0.002^{+0.000}_{-0.000}$ .

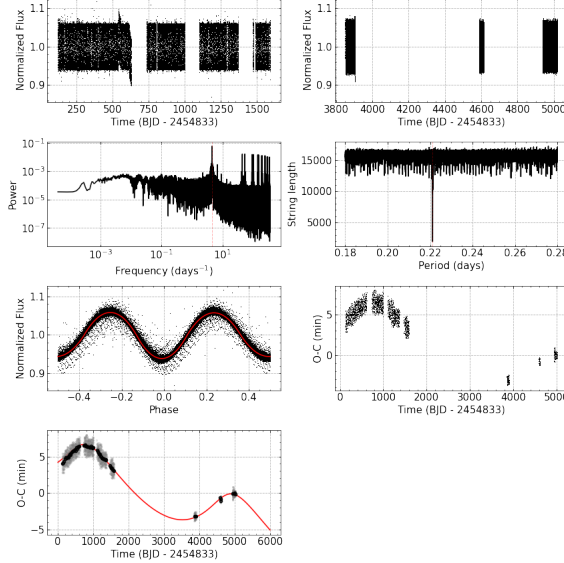


**Figure 63.** Same analyses of Fig. (8), but for KIC 10481912 (TIC 272079818).

832

#### B.51. *KIC 10485137 (TIC 272841995) Object*

This object presents a variation in its O-C diagram, Fig. 64, however, such variation does not present a complete orbital cycle due to a possible third body around the binary system with a period  $P = 5843.721^{+412.625}_{-144.971}$ , in an orbit with eccentricity  $e = 0.639^{+0.072}_{-0.064}$ , at a distance  $a = 1209.034^{+122.158}_{-7.875}$  from its parent stars, with its inclination axis  $\omega = 129.134^{+6.999}_{-2.731}$ .

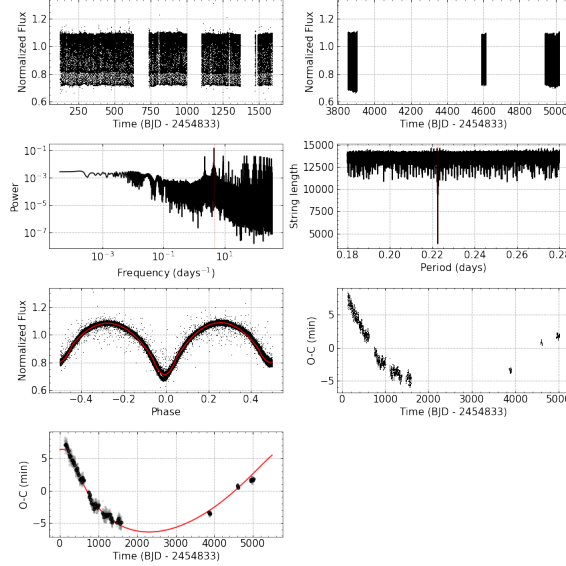


**Figure 64.** Same analyses of Fig. (8), but for KIC 10485137 (TIC 272841995).

837

### B.52. *KIC 10711938 (TIC 48189126) Object*

This object presents a variation in its O-C diagram, Fig. 65, however, such variation does not present a complete orbital cycle due to a possible third body around the binary system with a period  $P = 6688.888^{+261.034}_{-315.892}$ , in an orbit with eccentricity  $e = 0.631^{+0.250}_{-0.059}$ , at a distance  $a = 1187.255^{+320.546}_{-199.144}$  from its parent stars, with its inclination axis  $\omega = 18.743^{+20.175}_{-10.691}$ .

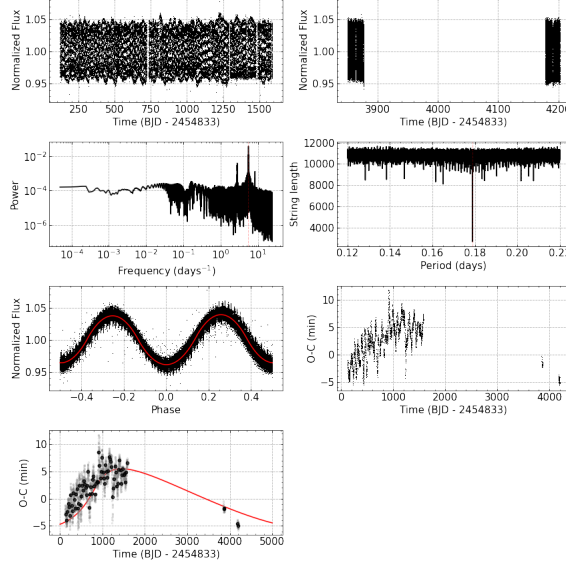


**Figure 65.** Same analyses of Fig. (8), but for KIC 10711938 (TIC 48189126).

842

### B.53. *KIC 10724533 (TIC 299156852) Object*

This object presents a variation in its O-C diagram, Fig. 66, however, such variation does not present a complete orbital cycle due to a possible third body around the binary system with a period  $P = 1936.467^{+52.152}_{-28.855}$ , in an orbit with eccentricity  $e = 0.426^{+0.035}_{-0.185}$ , at a distance  $a = 539.967^{+20.384}_{-38.284}$  from its parent stars, with its inclination axis  $\omega = 218.297^{+7.611}_{-178.969}$  and linear parameters fits at  $A = 7.412^{+0.985}_{-0.230}$  and  $B = -0.002^{+0.000}_{-0.000}$ .

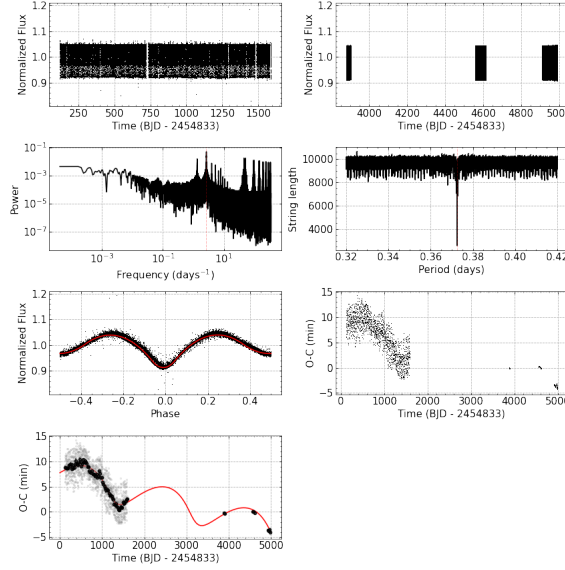


**Figure 66.** Same analyses of Fig. (8), but for KIC 10724533 (TIC 299156852).

847

#### B.54. *KIC 10818544 (TIC 416528957) Object*

This object presents a variation in its O-C diagram, Fig. 67, however, such variation does not present a complete orbital cycle due to a possible third body around the binary system with a period  $P = 1892.800^{+120.088}_{-78.434}$ , in an orbit with eccentricity  $e = 0.967^{+0.011}_{-0.030}$ , at a distance  $a = 1050.905^{+160.062}_{-328.243}$  from its parent stars, with its inclination axis  $\omega = 356.844^{+2.560}_{-3.514}$  and linear parameters fits at  $A = 1.808^{+0.153}_{-0.093}$  and  $B = 0.000^{+0.000}_{-0.000}$ .

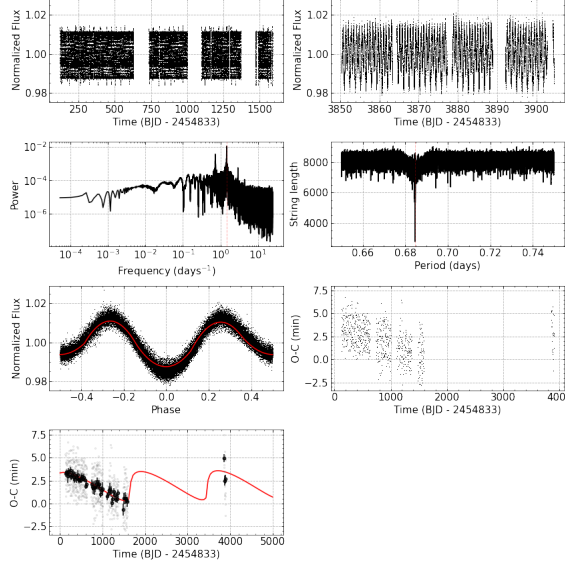


**Figure 67.** Same analyses of Fig. (8), but for KIC 10818544 (TIC 416528957).

852

#### B.55. *KIC 10979669 (TIC 26962050) Object*

This object presents a variation in its O-C diagram, Fig. 68, however, such variation does not present a complete orbital cycle due to a possible third body around the binary system with a period  $P = 1532.272^{+54.987}_{-20.992}$ , in an orbit with eccentricity  $e = 0.974^{+0.008}_{-0.013}$ , at a distance  $a = 1995.936^{+218.291}_{-463.016}$  from its parent stars, with its inclination axis  $\omega = 356.030^{+1.424}_{-2.425}$  and linear parameters fits at  $A = -0.022^{+0.008}_{-0.002}$  and  $B = 0.000^{+0.000}_{-0.000}$ .

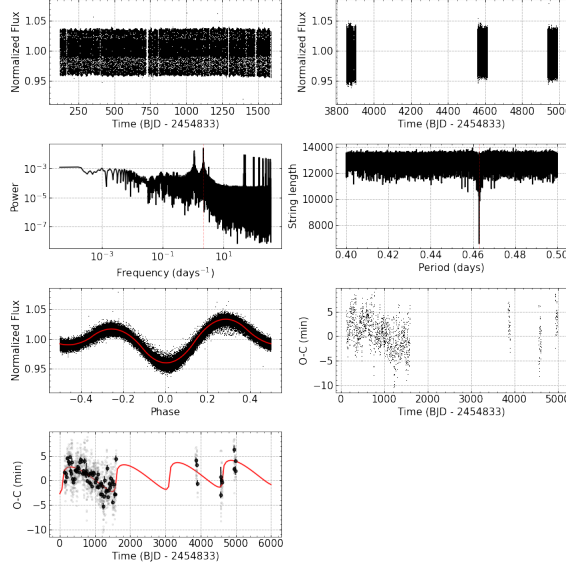


**Figure 68.** Same analyses of Fig. (8), but for KIC 10979669 (TIC 26962050).

#### B.56. *KIC 11255667 (TIC 27914890) Object*

This object presents a variation in its O-C diagram, Fig. 69, however, such variation does not present a complete orbital cycle due to a possible third body around the binary system with a period  $P = 4715.408^{+411.622}_{-203.023}$ , in an orbit with eccentricity  $e = 0.269^{+0.112}_{-0.143}$ , at a distance  $a = 674.638^{+58.702}_{-38.804}$  from its parent stars, with its inclination axis  $\omega = 331.369^{+16.426}_{-9.484}$  and linear parameters fits at  $A = 2.895^{+0.342}_{-0.914}$  and  $B = -0.002^{+0.000}_{-0.000}$ .

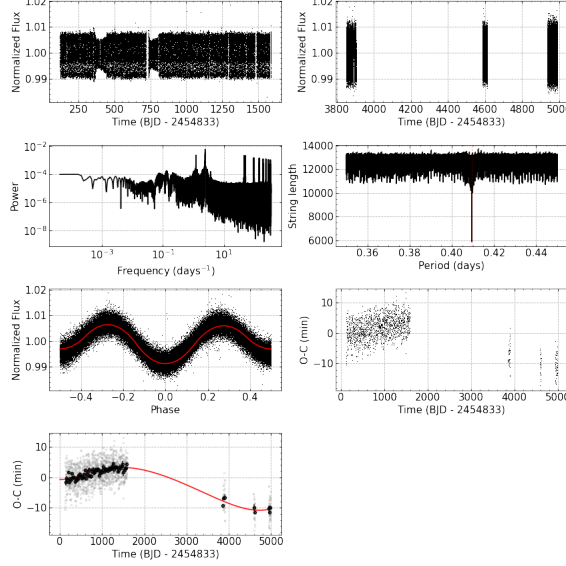


**Figure 69.** Same analyses of Fig. (8), but for KIC 11255667 (TIC 27914890).

#### B.57. *KIC 11409673 (TIC 27395746) Object*

This object presents a variation in its O-C diagram, Fig. 70, however, such variation does not present a complete orbital cycle due to a possible third body around the binary system with a period  $P = 5483.304^{+199.637}_{-143.780}$ , in an orbit with eccentricity  $e = 0.972^{+0.009}_{-0.011}$ , at a distance  $a = 1566216.412^{+259342.620}_{-189283.693}$  from its parent stars, with its inclination axis  $\omega = 182.402^{+1.092}_{-1.396}$ .

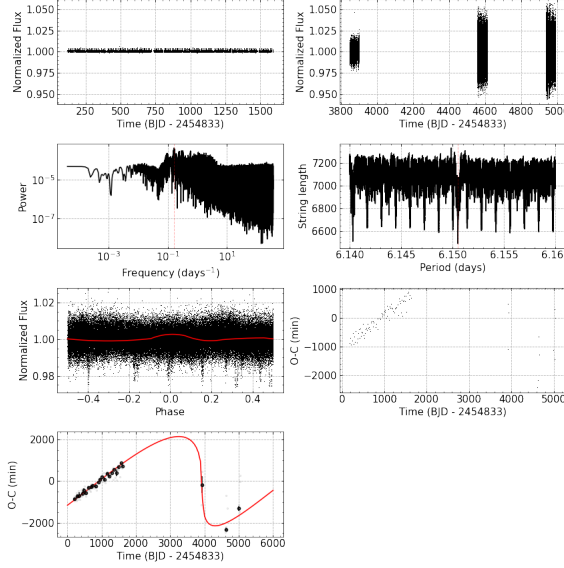


**Figure 70.** Same analyses of Fig. (8), but for KIC 11409673 (TIC 27395746).

867

#### B.58. *KIC 11572643 (TIC 28306907) Object*

868 This object presents a variation in its O-C diagram, Fig. 71, however, such variation does not present a complete  
 869 orbital cycle due to a possible third body around the binary system with a period  $P = 2290.326^{+48.331}_{-46.637}$ , in an orbit  
 870 with eccentricity  $e = 0.503^{+0.314}_{-0.198}$ , at a distance  $a = 1129.003^{+56.179}_{-112.310}$  from its parent stars, with its inclination axis  
 871  $\omega = 15.912^{+39.195}_{-14.694}$ .

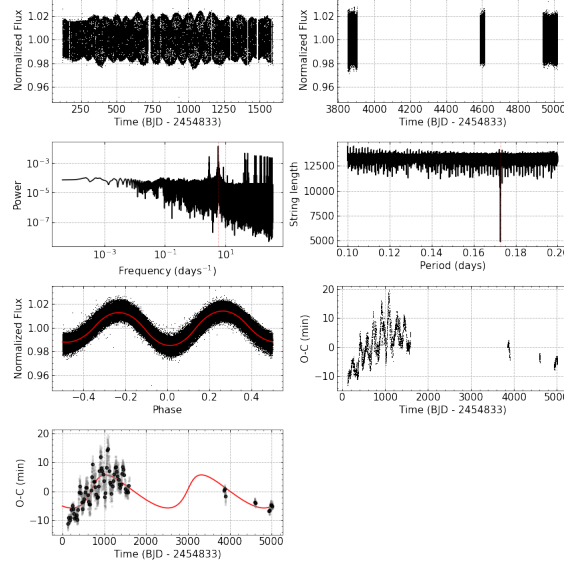


**Figure 71.** Same analyses of Fig. (8), but for KIC 11572643 (TIC 28306907).

872

#### B.59. *KIC 12216817 (TIC 27639466) Object*

873 This object presents a variation in its O-C diagram, Fig. 72, however, such variation does not present a complete  
 874 orbital cycle due to a possible third body around the binary system with a period  $P = 1508.869^{+27.582}_{-41.085}$ , in an orbit  
 875 with eccentricity  $e = 0.619^{+0.071}_{-0.084}$ , at a distance  $a = 533.169^{+48.895}_{-41.912}$  from its parent stars, with its inclination axis  
 876  $\omega = 323.187^{+7.506}_{-10.828}$ .

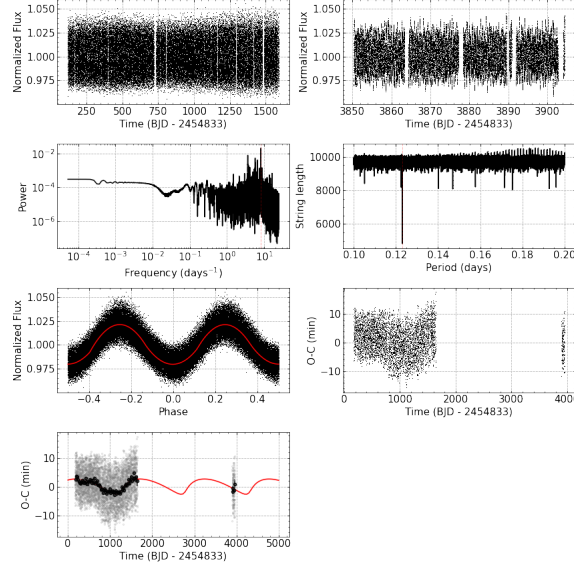


**Figure 72.** Same analyses of Fig. (8), but for KIC 12216817 (TIC 27639466).

#### B.60. *KIC 12305537 (TIC 406951407) Object*

This object presents a variation in its O-C diagram, Fig. 73, however, such variation does not present a complete orbital cycle due to a possible third body around the binary system with a period  $P = 2039.912^{+9.942}_{-11.011}$ , in an orbit with eccentricity  $e = 0.736^{+0.086}_{-0.038}$ , at a distance  $a = 2946.364^{+654.431}_{-207.403}$  from its parent stars, with its inclination axis  $\omega = 5.025^{+1.976}_{-2.009}$  and linear parameters fits at  $A = -0.757^{+0.015}_{-0.025}$  and  $B = 0.001^{+0.000}_{-0.000}$ .

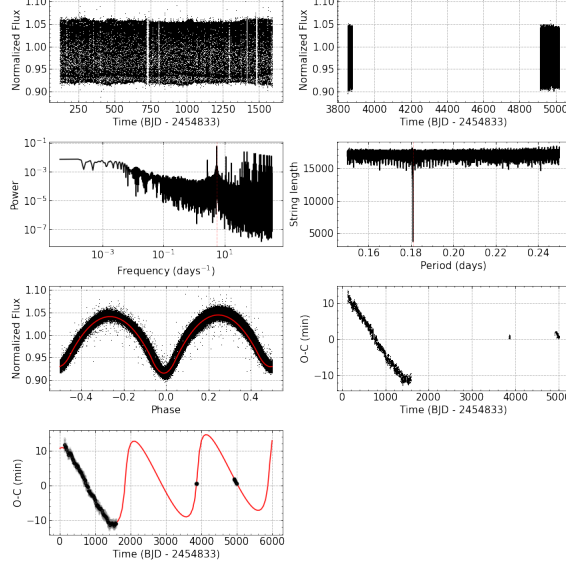


**Figure 73.** Same analyses of Fig. (8), but for KIC 12305537 (TIC 406951407).

### C. BINARY SYSTEMS WITH PERIODIC VARIATIONS ON THE O-C DIAGRAM

Of the 240 binary systems in our sample, a total of 13 systems, 5.42% of the sample, have periodic variations shown in their O-C diagrams. In the following subsections we present each system with its respective characteristics for the possible third bodies orbiting its respective binary system. For each object we derive, by adjusting for a third body, its orbital period  $P$ , its eccentricity  $e$ , semi-major axis  $a$  and periastron argument  $\omega$ .

887

### C.1. KIC 2450566 (TIC 137977804) Object

This object presents a periodic variation in its O-C diagram, Fig. 74, intuiting the presence of a third body around the binary system with a period  $P = 1059.282^{+23.443}_{-28.695}$ , in an orbit with eccentricity  $e = 0.655^{+0.105}_{-0.066}$ , at a distance  $a = 1487.083^{+181.846}_{-150.956}$  from its parent stars, with its inclination axis  $\omega = 307.417^{+10.050}_{-17.567}$ .

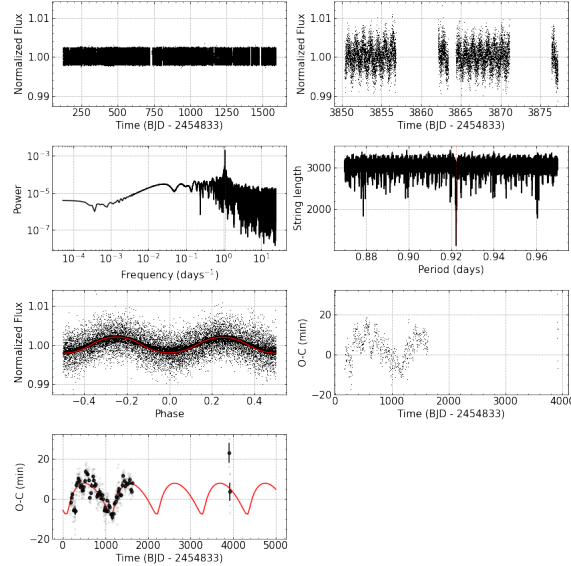


**Figure 74.** Same analyses of Fig. (8), but for KIC 2450566 (TIC 137977804).

891

### C.2. KIC 3228863 (TIC 394179296) Object

This object presents a periodic variation in its O-C diagram, Fig. 14, intuiting the presence of a third body around the binary system with a period  $P = 663.632^{+6.202}_{-15.304}$ , in an orbit with eccentricity  $e = 0.224^{+0.173}_{-0.154}$ , at a distance  $a = 659.632^{+27.744}_{-56.636}$  from its parent stars, with its inclination axis  $\omega = 260.622^{+23.252}_{-4.142}$ .

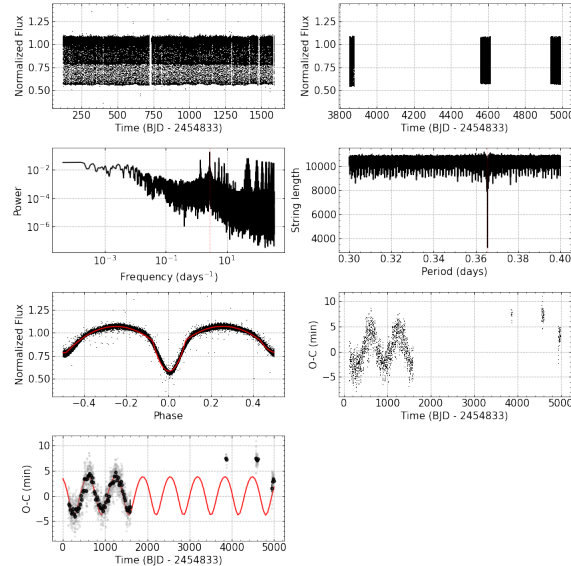


**Figure 75.** Same analyses of Fig. (8), but for KIC 3228863 (TIC 394179296).

### C.3. KIC 4451148 (TIC 121274442) Object

This object presents a periodic variation in its O-C diagram, Fig. 76, intuiting the presence of a third body around the binary system with a period  $P = 769.411^{+6.770}_{-10.758}$ , in an orbit with eccentricity  $e = 0.466^{+0.087}_{-0.023}$ , at a distance  $a = 909.084^{+315.158}_{-185.851}$  from its parent stars, with its inclination axis  $\omega = 165.080^{+1.177}_{-7.611}$ .

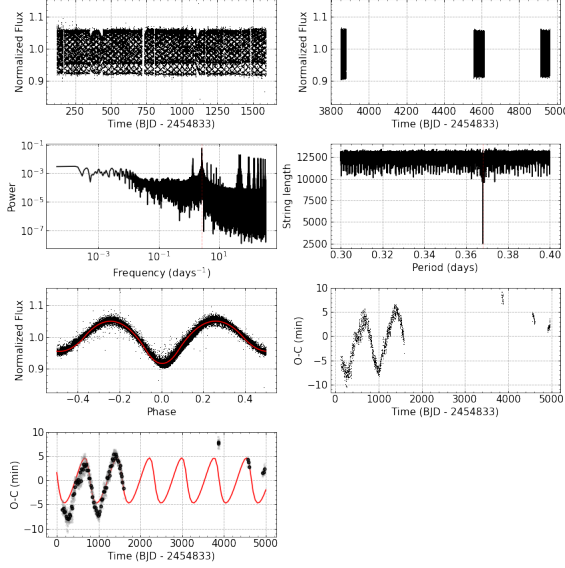


**Figure 76.** Same analyses of Fig. (8), but for KIC 4451148 (TIC 121274442).

### C.4. KIC 4647652 (TIC 122070918) Object

This object presents a periodic variation in its O-C diagram, Fig. 77, intuiting the presence of a third body around the binary system with a period  $P = 755.235^{+19.495}_{-13.418}$ , in an orbit with eccentricity  $e = 0.245^{+0.290}_{-0.147}$ , at a distance  $a = 636.222^{+147.225}_{-143.015}$  from its parent stars, with its inclination axis  $\omega = 239.394^{+58.689}_{-21.004}$ .

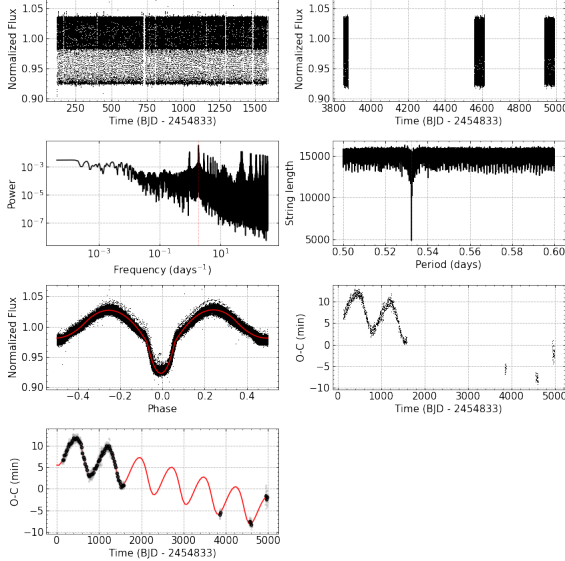


**Figure 77.** Same analyses of Fig. (8), but for KIC 4647652 (TIC 122070918).

903

### C.5. KIC 4909707 (TIC 121119758) Object

This object presents a periodic variation in its O-C diagram, Fig. 78, intuiting the presence of a third body around the binary system with a period  $P = 513.727^{+0.617}_{-0.517}$ , in an orbit with eccentricity  $e = 0.657^{+0.029}_{-0.027}$ , at a distance  $a = 2066.938^{+71.794}_{-65.971}$  from its parent stars, with its inclination axis  $\omega = 358.498^{+1.114}_{-1.642}$  and linear parameters fits at  $A = -6.858^{+0.110}_{-0.107}$  and  $B = 0.003^{+0.000}_{-0.000}$ .

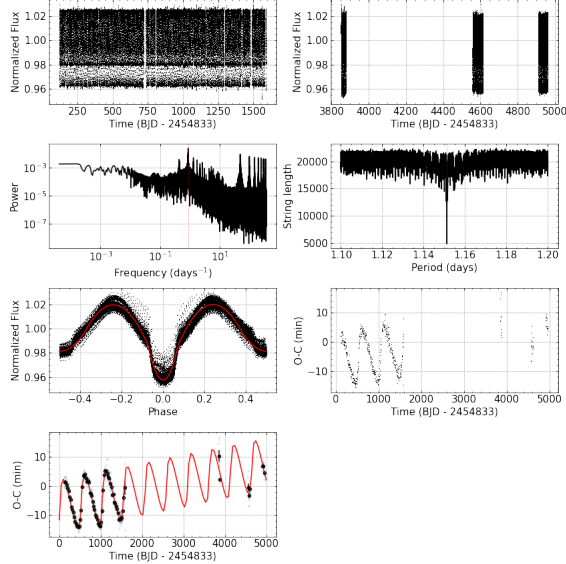


**Figure 78.** Same analyses of Fig. (8), but for KIC 4909707 (TIC 121119758).

908

### C.6. KIC 5264818 (TIC 121732964) Object

This object presents a periodic variation in its O-C diagram, Fig. 79, intuiting the presence of a third body around the binary system with a period  $P = 282.272^{+2.898}_{-4.298}$ , in an orbit with eccentricity  $e = 0.436^{+0.208}_{-0.309}$ , at a distance  $a = 486.055^{+59.249}_{-177.430}$  from its parent stars, with its inclination axis  $\omega = 342.066^{+13.325}_{-45.838}$  and linear parameters fits at  $A = 3.680^{+0.351}_{-0.301}$  and  $B = -0.000^{+0.000}_{-0.000}$ .

913

### C.7. KIC 7765894 (TIC 271967202) Object

This object presents a periodic variation in its O-C diagram, Fig. 80, intuiting the presence of a third body around the binary system with a period  $P = 463.815^{+3.584}_{-5.356}$ , in an orbit with eccentricity  $e = 0.270^{+0.073}_{-0.088}$ , at a distance  $a = 3831.739^{+874.241}_{-406.815}$  from its parent stars, with its inclination axis  $\omega = 142.982^{+33.786}_{-16.853}$ .

917

### C.8. KIC 8043961 (TIC 272609309) Object

This object presents a periodic variation in its O-C diagram, Fig. 81, intuiting the presence of a third body around the binary system with a period  $P = 422.710^{+1.645}_{-1.526}$ , in an orbit with eccentricity  $e = 0.399^{+0.185}_{-0.121}$ , at a distance  $a = 585.481^{+74.753}_{-59.217}$  from its parent stars, with its inclination axis  $\omega = 232.003^{+21.284}_{-26.824}$ .

921

### C.9. KIC 8045121 (TIC 272941454) Object

This object presents a periodic variation in its O-C diagram, Fig. 82, intuiting the presence of a third body around the binary system with a period  $P = 890.971^{+14.033}_{-17.999}$ , in an orbit with eccentricity  $e = 0.349^{+0.085}_{-0.122}$ , at a distance  $a = 856.664^{+130.413}_{-86.810}$  from its parent stars, with its inclination axis  $\omega = 178.152^{+31.503}_{-31.898}$  and linear parameters fits at  $A = 0.755^{+0.138}_{-0.066}$  and  $B = 0.003^{+0.001}_{-0.001}$ .

926

### C.10. KIC 8386865 (TIC 274024023) Object

This object presents a periodic variation in its O-C diagram, Fig. 83, intuiting the presence of a third body around the binary system with a period  $P = 294.267^{+0.998}_{-0.874}$ , in an orbit with eccentricity  $e = 0.421^{+0.055}_{-0.033}$ , at a distance  $a = 543.508^{+17.373}_{-19.167}$  from its parent stars, with its inclination axis  $\omega = 141.070^{+7.028}_{-6.075}$ .

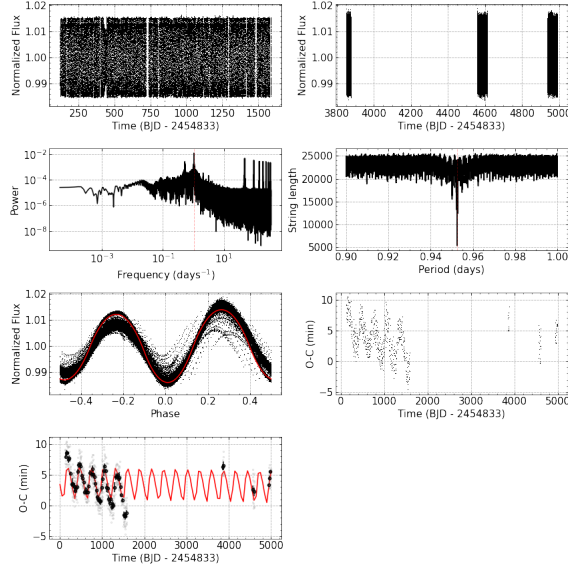


**Figure 79.** Same analyses of Fig. (8), but for KIC 5264818 (TIC 121732964).

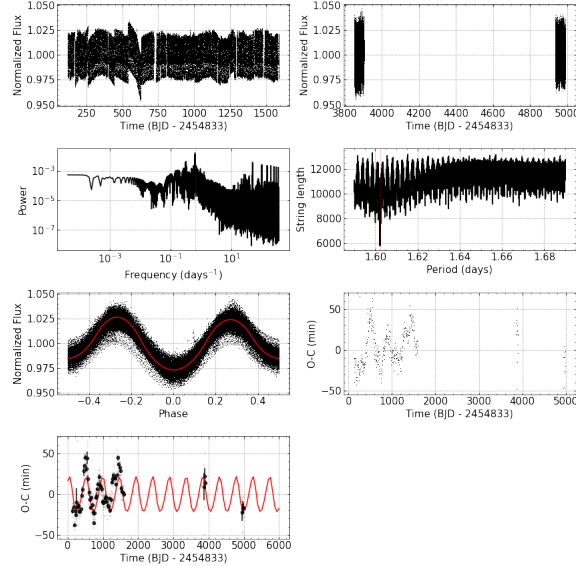


**Figure 80.** Same analyses of Fig. (8), but for KIC 7765894 (TIC 271967202).

### C.11. KIC 9365025 (TIC 268711288) Object

This object presents a periodic variation in its O-C diagram, Fig. 84, intuiting the presence of a third body around the binary system with a period  $P = 731.626^{+3.616}_{-2.190}$ , in an orbit with eccentricity  $e = 0.969^{+0.002}_{-0.003}$ , at a distance  $a = 3666.195^{+37.781}_{-17.177}$  from its parent stars, with its inclination axis  $\omega = 4.144^{+0.547}_{-0.347}$ .

### C.12. KIC 10226388 (TIC 273872891) Object

This object presents a periodic variation in its O-C diagram, Fig. 85, intuiting the presence of a third body around the binary system with a period  $P = 924.443^{+9.411}_{-1.880}$ , in an orbit with eccentricity  $e = 0.518^{+0.238}_{-0.031}$ , at a distance  $a = 1402.755^{+308.527}_{-174.692}$  from its parent stars, with its inclination axis  $\omega = 73.461^{+5.698}_{-11.645}$ .

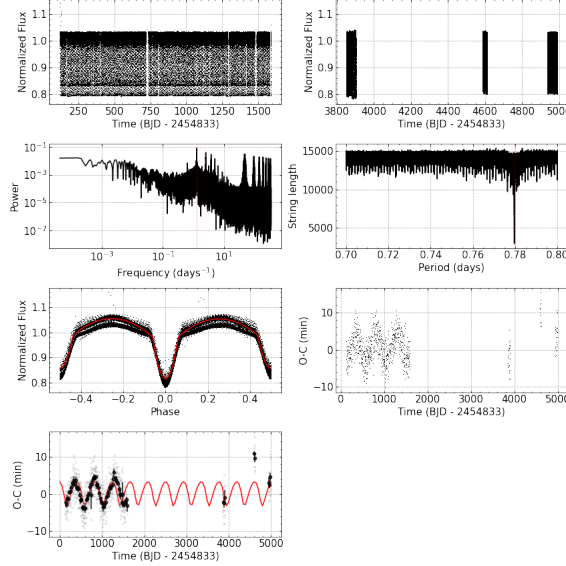


**Figure 81.** Same analyses of Fig. (8), but for KIC 8043961 (TIC 272609309).

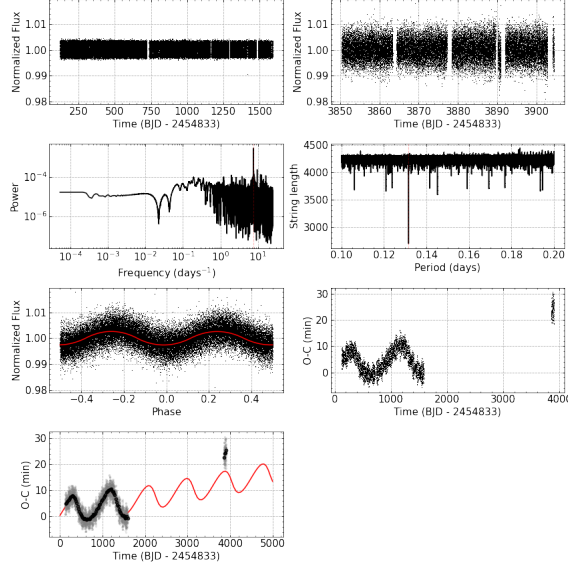


**Figure 82.** Same analyses of Fig. (8), but for KIC 8045121 (TIC 272941454).

### C.13. *KIC 10789421 (TIC 299032481) Object*

This object presents a periodic variation in its O-C diagram, Fig. 86, intuiting the presence of a third body around the binary system with a period  $P = 455.994^{+10.275}_{-18.197}$ , in an orbit with eccentricity  $e = 0.517^{+0.281}_{-0.180}$ , at a distance  $a = 903.600^{+184.665}_{-97.340}$  from its parent stars, with its inclination axis  $\omega = 8.881^{+17.913}_{-7.311}$  and linear parameters fits at  $A = 9.258^{+0.345}_{-0.448}$  and  $B = -0.010^{+0.001}_{-0.000}$ .

938

### D. FULL TABLE OF THE SAMPLE

943

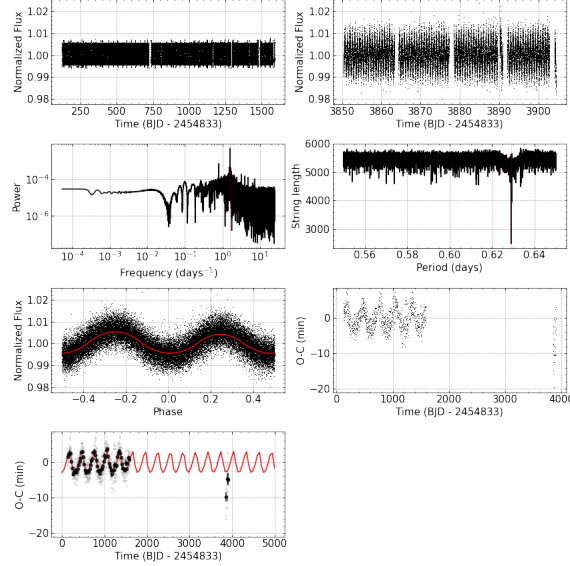


**Figure 83.** Same analyses of Fig. (8), but for KIC 8386865 (TIC 274024023).

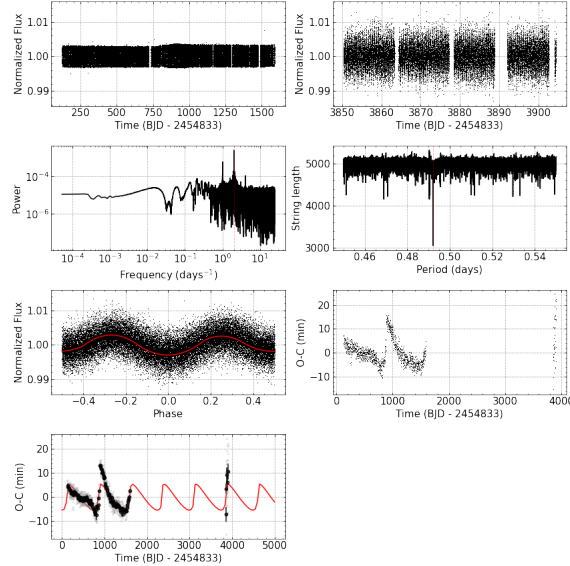


**Figure 84.** Same analyses of Fig. (8), but for KIC 9365025 (TIC 268711288).

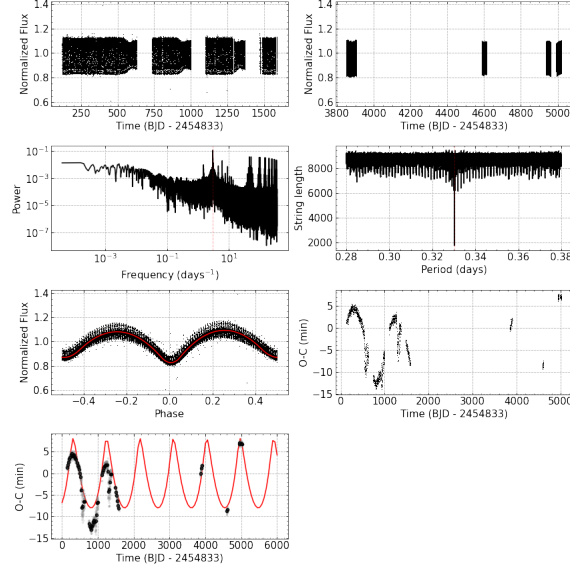


**Figure 85.** Same analyses of Fig. (8), but for KIC 10226388 (TIC 273872891).

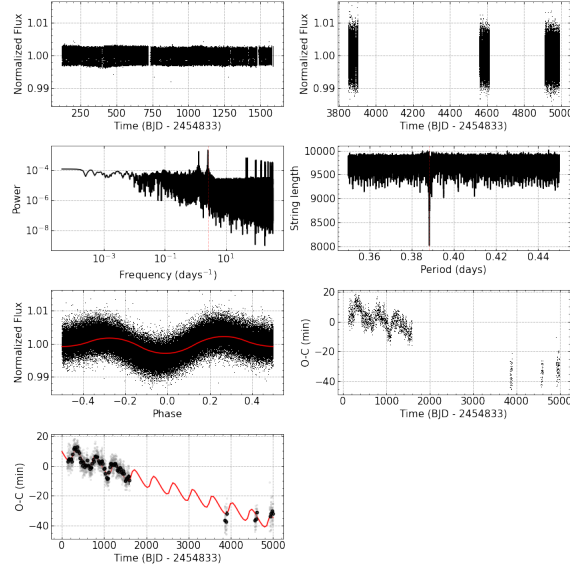


**Figure 86.** Same analyses of Fig. (8), but for KIC 10789421 (TIC 299032481).

**Table 3.** Physical and geometric parameters derived from the binary systems of our sample taken from Conroy et al. (2014). \*Our values are indicated in bold

KIC	$P_{bin}$	$P_3$	$e_3$	$P_3^*$	$e_3^*$	$a^*$	$\omega^*$	A	B
	(days)	(days)		(days)		(min)			
1868650	...	...	...	...	...	...	...	...	...
2162283	...	...	...	...	...	...	...	...	...
2450566	1.845	983.7 ± 472.8	0.308 ± 0.016	1059.282 <sup>+23.443</sup> <sub>-28.695</sub>	0.655 <sup>+0.105</sup> <sub>-0.066</sub>	1487.083 <sup>+181.846</sup> <sub>-150.956</sub>	307.417 <sup>+10.050</sup> <sub>-17.567</sub>	...	...
2557430	...	...	...	...	...	...	...	...	...
2694741	...	...	...	...	...	...	...	...	...
2708156	...	...	...	...	1437.154 <sup>+13.913</sup> <sub>-7.53</sub>	0.087 <sup>+0.167</sup> <sub>-0.065</sub>	3998.385 <sup>+112.356</sup> <sub>-195.565</sub>	1.86.554 <sup>+7.738</sup> <sub>-4.424</sub>	-17.877 <sup>+1.850</sup> <sub>-0.752</sub>
3221207	0.474	~1700	...	...	2253.652 <sup>+72.009</sup> <sub>-72.383</sub>	0.426 <sup>-0.040</sup> <sub>-0.048</sub>	413.398 <sup>+25.905</sup> <sub>-27.744</sub>	68.923 <sup>+25.382</sup> <sub>-23.252</sub>	0.001 <sup>+0.000</sup> <sub>-0.000</sub>
3228863	0.731	644.1 ± 15.7	0.000 ± 0.003	663.632 <sup>+6.209</sup> <sub>-15.304</sub>	0.224 <sup>+0.173</sup> <sub>-0.154</sub>	659.632 <sup>-56.636</sup>	260.622 <sup>+29.325</sup> <sub>-4.142</sub>	0.711 <sup>+0.125</sup> <sub>-0.125</sub>	0.001 <sup>+0.000</sup> <sub>-0.000</sub>
3431321	...	...	...	...	...	...	...	...	...
3443519	...	...	...	...	...	...	...	...	...
3448245	...	...	...	...	8314.481 <sup>+297.994</sup> <sub>-89.964</sub>	0.753 <sup>+0.051</sup> <sub>-0.014</sub>	298.060 <sup>+7.057</sup> <sub>-5.386</sub>	0.860 <sup>+2.637</sup> <sub>-0.683</sub>	...
3547874	...	...	...	...	...	...	...	...	...
3558822	...	...	...	...	...	...	...	...	...
3641446	2.100	228.6 ± 1.0	0.000 ± 0.010	...	...	...	...	...	...
3729724	...	...	...	...	...	...	...	...	...
3735597	...	...	...	...	...	...	...	...	...
3749404	...	...	...	...	...	...	...	...	...
3850086	...	...	...	...	...	...	...	...	...
3936357	0.369	~2400	...	2132.636 <sup>+67.619</sup> <sub>-47.151</sub>	0.120 <sup>+0.075</sup> <sub>-0.061</sub>	469.656 <sup>+18.435</sup> <sub>-24.562</sub>	203.482 <sup>+26.213</sup> <sub>-55.974</sub>	-3.312 <sup>+0.400</sup> <sub>-0.226</sub>	0.001 <sup>+0.000</sup> <sub>-0.000</sub>
3953981	...	...	...	2862.477 <sup>+14.503</sup> <sub>-122.901</sub>	0.223 <sup>+0.095</sup> <sub>-0.069</sub>	220.574 <sup>+19.636</sup> <sub>-13.916</sub>	254.738 <sup>+29.749</sup> <sub>-42.287</sub>	-0.300 <sup>+0.045</sup> <sub>-0.043</sub>	0.001 <sup>+0.000</sup> <sub>-0.000</sub>
3957477	...	...	...	...	...	...	...	...	...
4245897	...	...	...	...	...	...	...	...	...
4247791	...	...	...	...	...	...	...	...	...
4248941	...	...	...	...	...	...	...	...	...
4450976	...	...	...	2546.115 <sup>+161.201</sup> <sub>-203.502</sub>	0.313 <sup>+0.150</sup> <sub>-0.201</sub>	34367.104 <sup>+2451.117</sup> <sub>-2702.157</sub>	297.249 <sup>+34.620</sup> <sub>-33.954</sub>	...	...
4451148	0.736	746.0 ± 52.1	0.293 ± 0.004	769.411 <sup>+10.758</sup> <sub>-10.758</sub>	0.466 <sup>-0.037</sup> <sub>-0.039</sub>	909.084 <sup>+185.831</sup> <sub>-185.831</sub>	165.080 <sup>+7.611</sup> <sub>-7.611</sub>	...	...
4647652	1.065	755.2 ± 44.3	0.244 ± 0.003	755.235 <sup>+13.418</sup> <sub>-13.418</sub>	0.245 <sup>+0.030</sup> <sub>-0.147</sub>	636.222 <sup>-143.015</sup>	239.394 <sup>+58.689</sup> <sub>-42.004</sub>	...	...
4729553	...	...	...	...	...	...	...	...	...
4743626	...	...	...	...	...	...	...	...	...
4758368	3.750	~1500	...	...	...	...	...	...	...
4761060	...	...	...	...	...	...	...	...	...
4850874	...	...	...	...	...	...	...	...	...
4851217	...	...	...	2473.632 <sup>+318.289</sup> <sub>-194.321</sub>	0.876 <sup>+0.083</sup> <sub>-0.058</sub>	826.152 <sup>+98.935</sup> <sub>-98.057</sub>	101.987 <sup>+13.423</sup> <sub>-12.392</sub>	8.235 <sup>+0.677</sup> <sub>-0.532</sub>	-0.007 <sup>+0.001</sup> <sub>-0.000</sub>
4909422	...	...	...	6582.935 <sup>+141.982</sup> <sub>-141.982</sub>	0.839 <sup>+0.056</sup> <sub>-0.056</sub>	787.887 <sup>+97.744</sup> <sub>-99.067</sub>	6.695 <sup>-4.852</sup> <sub>-4.852</sub>	6.082 <sup>+0.328</sup> <sub>-0.328</sub>	-0.002 <sup>+0.000</sup> <sub>-0.000</sub>
4909707	2.302	516.1 ± 16.1	0.686 ± 0.006	513.727 <sup>-0.517</sup>	0.657 <sup>+0.029</sup> <sub>-0.027</sub>	2063.938 <sup>+71.94</sup> <sub>-65.971</sub>	358.498 <sup>+1.114</sup> <sub>-1.642</sub>	3.588 <sup>+0.110</sup> <sub>-0.107</sub>	0.003 <sup>+0.000</sup> <sub>-0.000</sub>

**Table 3** continued

Table 3 (continued)

KIC	$P_{bin}$ (days)	$P_3$ (days)	$e_3$	$P_3^*$ (days)	$e_3^*$	$a^*$ (min)	$\omega^*$	A	B
4945588	1.129	~1500	...	1607.893 <sup>+29.331</sup> <sub>-140.789</sub>	0.871 <sup>+0.046</sup> <sub>-0.045</sub>	1289.577 <sup>+32.368</sup> <sub>-66.834</sub>	1.34.791 <sup>+5.397</sup> <sub>-6.424</sub>	9.236 <sup>+0.291</sup> <sub>-0.645</sub>	-0.002 <sup>+0.000</sup> <sub>-0.000</sub>
4949194	...	...	...	...	...	...	...	...	...
4954113	...	...	...	41607.891 <sup>+11.84.572</sup> <sub>-1247.838</sub>	0.895 <sup>+0.027</sup> <sub>-0.021</sub>	1276.685 <sup>+75.891</sup> <sub>-50.225</sub>	226.484 <sup>+4.791</sup> <sub>-9.178</sub>	5.785 <sup>+0.445</sup> <sub>-0.343</sub>	-0.002 <sup>+0.000</sup> <sub>-0.000</sub>
4999260	...	...	...	1826.598 <sup>+113.477</sup> <sub>-113.477</sub>	0.766 <sup>+0.083</sup> <sub>-0.061</sub>	2900.240 <sup>+275.554</sup> <sub>-298.752</sub>	26.089 <sup>+12.937</sup> <sub>-10.238</sub>	2.904 <sup>+0.122</sup> <sub>-0.140</sub>	-0.001 <sup>+0.000</sup> <sub>-0.000</sub>
5022573	...	...	...	...	...	...	...	...	...
5090937	...	...	...	...	...	...	...	...	...
5123176	...	...	...	...	...	...	...	...	...
5197256	...	...	...	...	...	...	...	...	...
5264818	1.905	299.7 ± 107.5	0.421 ± 0.306	282.272 <sup>+2.898</sup> <sub>-4.988</sub>	0.436 <sup>+0.208</sup> <sub>-0.390</sub>	486.055 <sup>+59.249</sup> <sub>-77.680</sub>	342.066 <sup>+13.325</sup> <sub>-45.898</sub>	3.680 <sup>+0.351</sup> <sub>-0.301</sub>	-0.000 <sup>+0.000</sup> <sub>-0.000</sub>
5296877	0.377	~1900	...	4962.088 <sup>+1.012</sup> <sub>-16.105</sub>	0.728 <sup>+0.100</sup> <sub>-0.007</sub>	929.247 <sup>+4.982</sup> <sub>-6.414</sub>	87.015 <sup>+0.358</sup> <sub>-0.689</sub>	...	...
5398002	...	...	...	...	...	...	...	...	...
5444392	...	...	...	...	...	...	...	...	...
5455880	...	...	...	...	...	...	...	...	...
5471619	...	...	...	...	...	...	...	...	...
5511076	...	...	...	...	...	...	...	...	...
5533861	1.510	~1800	...	2113.335 <sup>+5.927</sup> <sub>-6.342</sub>	0.315 <sup>+0.019</sup> <sub>-0.029</sub>	3763.359 <sup>+90.637</sup> <sub>-88.600</sub>	291.346 <sup>+5.326</sup> <sub>-5.698</sub>	...	...
5598639	...	...	...	...	...	...	...	...	...
5703230	...	...	...	...	...	...	...	...	...
5733384	...	...	...	...	...	...	...	...	...
5771961	...	...	...	...	...	...	...	...	...
5802834	...	...	...	...	...	...	...	...	...
5818706	...	...	...	...	...	...	...	...	...
5821050	...	...	...	...	...	...	...	...	...
5872696	...	...	...	...	...	...	...	...	...
5952403	...	...	...	...	...	...	...	...	...
5975712	1.136	1164.7 ± 964.3	0.000 ± 0.013	1694.123 <sup>+2.155</sup> <sub>-1.001</sub>	0.218 <sup>+0.001</sup> <sub>-0.001</sub>	1718.050 <sup>+0.840</sup> <sub>-1.923</sub>	262.220 <sup>+0.376</sup> <sub>-0.450</sub>	25.815 <sup>+0.036</sup> <sub>-0.014</sub>	-0.012 <sup>+0.000</sup> <sub>-0.000</sub>
5985314	...	...	...	...	...	...	...	...	...
5988465	...	...	...	...	...	...	...	...	...
6026204	...	...	...	...	...	...	...	...	...
6072195	...	...	...	...	...	...	...	...	...
6105491	...	...	...	...	...	...	...	...	...
6187893	0.789	~7800	...	2028.925 <sup>+5.819</sup> <sub>-8.788</sub>	0.969 <sup>+0.004</sup> <sub>-0.006</sub>	15566.140 <sup>+1116.612</sup> <sub>-1159.558</sub>	354.398 <sup>+0.646</sup> <sub>-0.703</sub>	...	...
6205460	...	...	...	2311.862 <sup>+8.952</sup> <sub>-19.020</sub>	0.426 <sup>+0.019</sup> <sub>-0.071</sub>	37561.143 <sup>+214.540</sup> <sub>-973.443</sub>	233.491 <sup>+4.345</sup> <sub>-1.748</sub>	...	...
6353203	...	...	...	2449.628 <sup>+19.370</sup> <sub>-7.118</sub>	0.575 <sup>+0.057</sup> <sub>-0.069</sub>	2535.311 <sup>+140.357</sup> <sub>-264.969</sub>	33.826 <sup>+3.897</sup> <sub>-2.290</sub>	...	...
6370558	...	...	...	...	...	...	...	...	...
6443392	...	...	...	...	...	...	...	...	...
6447430	...	...	...	...	...	...	...	...	...
6462057	...	...	...	4926.320 <sup>+359.711</sup> <sub>-147.307</sub>	0.637 <sup>+0.080</sup> <sub>-0.177</sub>	410.767 <sup>+31.402</sup> <sub>-42.634</sub>	76.324 <sup>+18.082</sup> <sub>-11.176</sub>	1.690 <sup>+0.111</sup> <sub>-0.211</sub>	-0.001 <sup>+0.000</sup> <sub>-0.000</sub>

Table 3 continued

Table 3 (continued)

KIC	$P_{bin}$ (days)	$P_3$ (days)	$e_3$	$P_3^*$ (days)	$e_3^*$	$a^*$ (min)	$\omega^*$	$A$	$B$
6669809	...	...	...	...	...	...	...	...	...
6670812	...	...	...	...	...	...	...	...	...
6695510	...	...	...	...	...	...	...	...	...
6699679	...	...	...	...	...	...	...	...	...
6803335	...	...	...	...	...	...	...	...	...
6833229	...	...	...	...	...	...	...	...	...
7023917	...	...	...	...	...	...	...	...	...
7097571	...	...	...	...	...	...	...	...	...
7259917	...	...	...	4729.394 $^{+441.635}_{-196.787}$	0.720 $^{+0.063}_{-0.222}$	794.232 $^{+124.608}_{-171.657}$	223.241 $^{+21.873}_{-16.910}$	5.809 $^{+0.837}_{-0.721}$	0.001 $^{+0.000}_{-0.000}$
7284688	...	...	...	...	...	...	...	...	...
7335517	...	...	...	...	...	...	...	...	...
7335713	...	...	...	...	...	...	...	...	...
7350038	...	...	...	...	...	...	...	...	...
7373255	...	...	...	...	...	...	...	...	...
7375612	0.160	~2100	...	2123.456 $^{+15.279}_{-7.569}$	0.098 $^{+0.074}_{-0.028}$	1221.564 $^{+45.153}_{-18.592}$	302.775 $^{+39.354}_{-19.329}$	...	...
7382250	...	...	...	...	...	...	...	...	...
7385478	1.655	1389.3 $\pm$ 795.2	0.245 $\pm$ 0.007	1360.065 $^{+76.397}_{-101.476}$	0.782 $^{+0.148}_{-0.363}$	2892.213 $^{+287.804}_{-627.328}$	59.734 $^{+24.105}_{-25.564}$	8.118 $^{+1.161}_{-2.345}$	-0.002 $^{+0.000}_{-0.001}$
7387296	...	...	...	...	...	...	...	...	...
7431703	...	...	...	1820.383 $^{+42.684}_{-105.177}$	0.448 $^{+0.121}_{-0.158}$	193.698 $^{+45.269}_{-23.174}$	133.419 $^{+48.678}_{-38.020}$	...	...
7440742	...	...	...	2003.253 $^{+133.920}_{-135.182}$	0.983 $^{+0.005}_{-0.005}$	3175.282 $^{+239.578}_{-261.423}$	11.419 $^{+0.521}_{-3.852}$	0.007 $^{+0.000}_{-0.000}$	0.007 $^{+0.000}_{-0.000}$
7457163	...	...	...	6255.520 $^{+135.802}_{-135.789}$	0.527 $^{+0.032}_{-0.032}$	2751.917 $^{+40.423}_{-41.743}$	278.115 $^{+3.827}_{-3.827}$	...	...
7512381	...	...	...	6805.413 $^{+249.789}_{-135.070}$	0.411 $^{+0.040}_{-0.131}$	1298.333 $^{+127.933}_{-41.743}$	340.888 $^{+7.94}_{-5.227}$	...	...
7542091	...	...	...	...	...	...	...	...	...
7591456	...	...	...	...	...	...	...	...	...
7630690	...	...	...	...	...	...	...	...	...
7672068	...	...	...	...	...	...	...	...	...
7690843	0.786	74.1 $\pm$ 0.1	0.233 $\pm$ 0.021	2714.623 $^{+60.236}_{-72.170}$	0.752 $^{+0.058}_{-0.152}$	2435.466 $^{+384.915}_{-494.907}$	340.293 $^{+7.820}_{-10.974}$	-0.752 $^{+0.125}_{-0.158}$	0.000 $^{+0.000}_{-0.000}$
7740302	...	...	...	...	...	...	...	...	...
7765894	...	...	...	463.815 $^{+3.584}_{-5.356}$	0.270 $^{+0.073}_{-0.088}$	3831.739 $^{+874.241}_{-406.845}$	142.982 $^{+33.786}_{-16.853}$	...	...
7766185	...	...	...	1860.287 $^{+95.837}_{-87.249}$	0.945 $^{+0.015}_{-0.024}$	88.601 $^{+106.424}_{-12.943}$	353.253 $^{+5.047}_{-9.173}$	1.442 $^{+0.046}_{-0.043}$	-0.001 $^{+0.000}_{-0.000}$
7777443	...	...	...	...	...	...	...	...	...
7816201	...	...	...	2328.001 $^{+209.934}_{-397.908}$	0.696 $^{+0.074}_{-0.124}$	320.107 $^{+17.816}_{-22.707}$	61.045 $^{+35.826}_{-26.856}$	4.540 $^{+0.222}_{-0.501}$	-0.001 $^{+0.000}_{-0.000}$
7830460	...	...	...	...	...	...	...	...	...
7884842	...	...	...	...	...	...	...	...	...
7885570	...	...	...	...	...	...	...	...	...
7887124	...	...	...	...	...	...	...	...	...
7897952	...	...	...	2100.595 $^{+31.818}_{-32.686}$	0.627 $^{+0.094}_{-0.022}$	486.852 $^{+41.826}_{-14.625}$	302.126 $^{+8.472}_{-6.225}$	-7.672 $^{+0.155}_{-0.219}$	0.002 $^{+0.000}_{-0.000}$
7938870	...	...	...	...	...	...	...	...	...

Table 3 continued

Table 3 (continued)

KIC	$P_{bin}$	$P_3$	$e_3$	$P_3^*$	$e_3^*$	$a^*$	$\omega^*$	A	B
	(days)	(days)		(days)		(min)			
7950962	...	...	...	3085.157 $^{+100.353}_{-116.633}$	0.075 $^{+0.053}_{-0.055}$	309.409 $^{+18.086}_{-30.892}$	172.259 $^{+3.845}_{-5.776}$	1.990 $^{+0.130}_{-0.175}$	0.002 $^{+0.000}_{-0.000}$
7975824	...	...	...	...	...	...	...	...	...
7976783	...	...	...	...	...	...	...	...	...
8027591	...	...	...	422.710 $^{+1.645}_{-1.403}$	0.399 $^{+0.185}_{-0.126}$	585.481 $^{+74.753}_{-59.217}$	232.003 $^{+21.284}_{-26.824}$	0.755 $^{+0.138}_{-0.066}$	0.003 $^{+0.001}_{-0.001}$
8043961	1.559	478.0 $\pm$ 10.4	0.000 $\pm$ 0.005	890.971 $^{+1.799}_{-1.799}$	0.349 $^{+0.122}_{-0.122}$	856.664 $^{+86.810}_{-86.810}$	178.152 $^{+31.898}_{-31.898}$	3.187 $^{+0.745}_{-0.630}$	0.009 $^{+0.001}_{-0.001}$
8045121	0.263	938.6 $\pm$ 25.8	0.000 $\pm$ 0.001	890.971 $^{+1.799}_{-1.799}$	0.349 $^{+0.122}_{-0.122}$	12579.602 $^{+931.164}_{-840.971}$	352.082 $^{+0.671}_{-0.857}$	1.7464 $^{+4.281}_{-4.281}$	0.246 $^{+0.658}_{-0.195}$
8098728	...	...	...	3903.002 $^{+24.689}_{-30.695}$	0.980 $^{+0.003}_{-0.003}$	2930.266 $^{+110.526}_{-401.530}$	...	...	...
8189196	2.304	$\sim$ 8300	...	1909.021 $^{+30.390}_{-54.438}$	0.949 $^{+0.031}_{-0.033}$	2042.641 $^{+16.160}_{-55.476}$	0.522 $^{+0.022}_{-0.218}$	1553.753 $^{+36.747}_{-102.809}$	1.41.070 $^{+7.028}_{-6.075}$
8231231	0.712	$\sim$ 1600	...	...	...	...	...	...	...
8262223	...	...	...	2042.641 $^{+16.160}_{-55.476}$	0.522 $^{+0.022}_{-0.218}$	1553.753 $^{+36.747}_{-102.809}$	0.246 $^{+0.658}_{-0.195}$	0.246 $^{+0.658}_{-0.195}$	0.246 $^{+0.658}_{-0.195}$
8285349	...	...	...	294.267 $^{+0.998}_{-0.874}$	0.421 $^{+0.055}_{-0.033}$	543.508 $^{+17.373}_{-19.167}$	...	...	...
8382182	...	...	...	8112.505 $^{+509.919}_{-443.186}$	0.966 $^{+0.003}_{-0.003}$	17859.920 $^{+1277.042}_{-1093.553}$	1.84.634 $^{+3.200}_{-3.526}$	-2.969 $^{+0.807}_{-0.626}$	0.003 $^{+0.000}_{-0.000}$
8386865	1.258	293.9 $\pm$ 2.8	0.493 $\pm$ 0.013	294.267 $^{+0.998}_{-0.874}$	0.421 $^{+0.055}_{-0.033}$	543.508 $^{+17.373}_{-19.167}$	1.41.070 $^{+7.028}_{-6.075}$	1.41.070 $^{+7.028}_{-6.075}$	1.41.070 $^{+7.028}_{-6.075}$
8386982	...	...	...	...	...	...	...	...	...
8397460	...	...	...	...	...	...	...	...	...
8523194	...	...	...	...	...	...	...	...	...
8545456	...	...	...	...	...	...	...	...	...
8579707	...	...	...	1944.760 $^{+203.672}_{-247.784}$	0.523 $^{+0.090}_{-0.077}$	767.345 $^{+60.336}_{-72.433}$	274.445 $^{+12.220}_{-22.646}$	...	...
8587792	...	...	...	5493.004 $^{+294.992}_{-278.158}$	0.380 $^{+0.046}_{-0.040}$	1206.681 $^{+74.433}_{-72.220}$	320.376 $^{+8.325}_{-6.775}$	0.202 $^{+0.201}_{-0.160}$	0.000 $^{+0.000}_{-0.000}$
8590527	...	...	...	...	...	...	...	...	...
8654097	...	...	...	...	...	...	...	...	...
8685306	...	...	...	...	...	...	...	...	...
8696442	...	...	...	...	...	...	...	...	...
8719324	...	...	...	...	...	...	...	...	...
8758161	...	...	...	18453.026 $^{+3264.951}_{-3355.454}$	0.908 $^{+0.047}_{-0.069}$	8615.186 $^{+1034.901}_{-1451.131}$	8.511 $^{+9.509}_{-4.650}$	...	...
8841616	...	...	...	...	...	...	...	...	...
8848288	...	...	...	...	...	...	...	...	...
8868650	...	...	...	...	...	...	...	...	...
8892722	...	...	...	...	...	...	...	...	...
8894630	...	...	...	7635.890 $^{+351.320}_{-315.610}$	0.737 $^{+0.043}_{-0.030}$	5539.682 $^{+502.895}_{-297.206}$	14.359 $^{+4.427}_{-4.471}$	...	...
8912468	...	...	...	...	...	...	...	...	...
9002076	...	...	...	...	...	...	...	...	...
9007918	...	...	...	...	...	...	...	...	...
9083523	0.918	$\sim$ 5200	...	2200.587 $^{+36.070}_{-16.377}$	0.370 $^{+0.084}_{-0.090}$	621.439 $^{+29.266}_{-30.823}$	202.850 $^{+10.495}_{-7.422}$	...	...
9108579	...	...	...	...	...	...	...	...	...
9159301	...	...	...	1830.374 $^{+20.089}_{-49.420}$	0.596 $^{+0.054}_{-0.051}$	2570.357 $^{+286.471}_{-143.622}$	44.869 $^{+9.228}_{-9.783}$	4.696 $^{+0.304}_{-0.491}$	-0.001 $^{+0.000}_{-0.000}$

Table 3 continued

Table 3 (*continued*)

KIC	$P_{bin}$ (days)	$P_3$ (days)	$e_3$	$P_3^*$ (days)	$e_3^*$	$a^*$ (min)	$\omega^*$	A	B
9220600	...	...	...	...	...	...	...	...	...
9228778	...	...	...	...	...	...	...	...	...
9345838	...	...	...	2497.096 $^{+5.248}_{-7.119}$	0.969 $^{+0.013}_{-0.009}$	3366.064 $^{+932.765}_{-754.234}$	6.993 $^{+0.821}_{-1.239}$	...	...
9357275	...	...	...	...	...	...	...	...	...
9365025	...	...	...	731.626 $^{+3.616}_{-2.190}$	0.969 $^{+0.002}_{-0.003}$	3666.195 $^{+37.781}_{-17.177}$	4.144 $^{+0.547}_{-0.347}$	...	...
9392682	...	...	...	...	...	...	...	...	...
9394601	...	...	...	...	...	...	...	...	...
9402652	...	...	...	1499.321 $^{+2.076}_{-2.039}$	0.817 $^{+0.028}_{-0.034}$	1473.178 $^{+38.354}_{-37.486}$	263.772 $^{+1.795}_{-2.034}$	-12.516 $^{+0.311}_{-0.189}$	0.003 $^{+0.000}_{-0.000}$
9451096	1.250	106.8 $\pm$ 0.1	0.091 $\pm$ 0.033	...	...	...	...	...	...
9470054	...	...	...	...	...	...	...	...	...
9472174	...	...	...	...	...	...	...	...	...
9480977	...	...	...	...	...	...	...	...	...
9512958	...	...	...	...	...	...	...	...	...
9592855	...	...	...	6556.627 $^{+175.520}_{-624.070}$	0.762 $^{+0.037}_{-0.028}$	37057.818 $^{+1690.472}_{-1659.916}$	191.337 $^{+7.832}_{-4.892}$	...	...
9602595	...	...	...	...	...	...	...	...	...
9612468	0.133	1264.2 $\pm$ 233.2	0.340 $\pm$ 0.001	...	...	...	...	...	...
9655187	...	...	...	...	...	...	...	...	...
9657096	2.138	$\sim$ 1400	...	1829.705 $^{+96.740}_{-26.635}$	0.607 $^{+0.034}_{-0.077}$	1929.070 $^{+47.691}_{-45.751}$	132.949 $^{+8.377}_{-4.699}$	6.868 $^{+0.166}_{-0.249}$	-0.001 $^{+0.000}_{-0.000}$
9716456	...	...	...	...	...	...	...	...	...
9790531	...	...	...	2984.870 $^{+23.366}_{-31.904}$	0.960 $^{+0.006}_{-0.095}$	886.002 $^{+45.537}_{-122.871}$	15.153 $^{+18.866}_{-4.047}$	3.328 $^{+1.061}_{-0.176}$	-0.001 $^{+0.000}_{-0.000}$
9784371	...	...	...	...	...	...	...	...	...
9786017	...	...	...	...	...	...	...	...	...
9788113	...	...	...	...	...	...	...	...	...
9827122	...	...	...	...	...	...	...	...	...
9839227	...	...	...	6091.433 $^{+142.763}_{-115.053}$	0.507 $^{+0.028}_{-0.047}$	4066.124 $^{+32.655}_{-168.895}$	313.916 $^{+1.271}_{-5.992}$	...	...
9848190	...	...	...	...	...	...	...	...	...
9851944	...	...	...	...	...	...	...	...	...
9898401	...	...	...	...	...	...	...	...	...
9899216	...	...	...	...	...	...	...	...	...
9899416	...	...	...	...	...	...	...	...	...
9906590	...	...	...	...	...	...	...	...	...
9953894	...	...	...	...	...	...	...	...	...
9970937	...	...	...	...	...	...	...	...	...
10000490	...	...	...	...	...	...	...	...	...
10014536	...	...	...	...	...	...	...	...	...
10119517	...	...	...	...	...	...	...	...	...
10149845	...	...	...	...	...	...	...	...	...
10155563	...	...	...	3569.345 $^{+16.637}_{-16.118}$	0.989 $^{+0.001}_{-0.002}$	1719.462 $^{+363.269}_{-295.336}$	218.980 $^{+10.329}_{-6.680}$	...	...

Table 3 *continued*

Table 3 (continued)

KIC	$P_{bin}$ (days)	$P_3$ (days)	$e_3$	$P_3^*$ (days)	$e_3^*$	$a^*$ (min)	$\omega^*$	A	B
10191056	...	...	...	...	...	...	...	...	...
10206340	...	...	...	...	...	...	...	...	...
10221886	...	...	...	...	...	...	...	...	...
10226388	0.661	965.3 ± 183.8	0.041 ± 0.007	924.443 <sup>+9.411</sup> <sub>-1.880</sub>	0.518 <sup>+0.238</sup> <sub>-0.031</sub>	1402.755 <sup>+308.527</sup> <sub>-174.692</sub>	73.461 <sup>+5.698</sup> <sub>-11.645</sub>	-0.001 <sup>+0.000</sup> <sub>-0.000</sub>	
10253421	...	...	...	...	...	...	...	...	...
10259330	...	...	...	4636.848 <sup>+95.939</sup> <sub>-92.547</sub>	0.561 <sup>+0.028</sup> <sub>-0.173</sub>	381.542 <sup>+18.713</sup> <sub>-25.245</sub>	100.245 <sup>+11.074</sup> <sub>-21.152</sub>	2.821 <sup>+0.126</sup> <sub>-0.411</sub>	-0.001 <sup>+0.000</sup> <sub>-0.000</sub>
10274218	...	...	...	...	...	...	...	...	...
10291683	...	...	...	...	...	...	...	...	...
10389982	...	...	...	2300.442 <sup>+103.102</sup> <sub>-37.377</sub>	0.839 <sup>+0.111</sup> <sub>-0.090</sub>	239.080 <sup>+8.393</sup> <sub>-14.645</sub>	330.594 <sup>+20.678</sup> <sub>-14.730</sub>	5.085 <sup>+0.228</sup> <sub>-0.217</sub>	-0.001 <sup>+0.000</sup> <sub>-0.000</sub>
10417986	...	...	...	4101.691 <sup>+96.134</sup> <sub>-51.067</sub>	0.353 <sup>+0.138</sup> <sub>-0.020</sub>	543.619 <sup>+43.615</sup> <sub>-42.953</sub>	56.372 <sup>+36.062</sup> <sub>-30.639</sub>	4.864 <sup>+0.512</sup> <sub>-0.339</sub>	-0.002 <sup>+0.000</sup> <sub>-0.000</sub>
10481912	0.442	~ 2700	...	5843.721 <sup>+412.167</sup> <sub>-412.157</sub>	0.639 <sup>+0.072</sup> <sub>-0.064</sub>	1209.034 <sup>+122.58</sup> <sub>-7.875</sub>	129.134 <sup>+6.99</sup> <sub>-2.731</sub>	...	...
10485137	0.445	~ 3100	...	...	...	...	...	...	...
10556068	...	...	...	...	...	...	...	...	...
10619109	...	...	...	...	...	...	...	...	...
10661783	...	...	...	...	...	...	...	...	...
10684673	...	...	...	...	...	...	...	...	...
10711938	0.358	~ 2000	...	6688.888 <sup>+261.034</sup> <sub>-315.892</sub>	0.631 <sup>+0.250</sup> <sub>-0.050</sub>	1187.255 <sup>+320.546</sup> <sub>-139.144</sub>	18.743 <sup>+20.175</sup> <sub>-19.691</sub>	-0.002 <sup>+0.000</sup> <sub>-0.000</sub>	-0.002 <sup>+0.000</sup> <sub>-0.000</sub>
10724533	0.745	1131.4 ± 197.7	0.265 ± 0.003	1936.467 <sup>+72.152</sup> <sub>-28.855</sub>	0.426 <sup>+0.035</sup> <sub>-0.185</sub>	539.967 <sup>+20.384</sup> <sub>-38.284</sub>	218.297 <sub>-178.969</sub>	7.412 <sup>+0.985</sup> <sub>-0.230</sub>	
10735519	...	...	...	...	...	...	...	...	...
10789421	...	...	...	455.994 <sup>+10.275</sup> <sub>-18.197</sub>	0.517 <sup>+0.281</sup> <sub>-0.180</sub>	903.600 <sup>+184.665</sup> <sub>-97.340</sub>	8.881 <sup>+17.913</sup> <sub>-7.311</sub>	9.258 <sup>+0.345</sup> <sub>-0.448</sub>	-0.010 <sup>+0.001</sup> <sub>-0.000</sub>
10815379	...	...	...	...	...	...	...	...	...
10818544	...	...	...	1892.800 <sup>+120.088</sup> <sub>-78.434</sub>	0.967 <sup>+0.011</sup> <sub>-0.030</sub>	1050.905 <sup>+160.062</sup> <sub>-328.243</sub>	356.844 <sup>+2.560</sup> <sub>-3.514</sub>	1.808 <sup>+0.153</sup> <sub>-0.093</sub>	0.000 <sup>+0.000</sup> <sub>-0.000</sub>
10858720	...	...	...	...	...	...	...	...	...
10979669	...	...	...	1532.272 <sup>+54.987</sup> <sub>-20.992</sub>	0.974 <sup>+0.008</sup> <sub>-0.013</sub>	1995.936 <sup>+218.291</sup> <sub>-463.016</sub>	356.030 <sup>+1.424</sup> <sub>-2.425</sub>	-0.022 <sup>+0.008</sup> <sub>-0.002</sub>	0.000 <sup>+0.000</sup> <sub>-0.000</sub>
10991769	...	...	...	...	...	...	...	...	...
10991989	0.974	554.8 ± 64.1	0.000 ± 0.018	...	...	...	...	...	...
11071278	...	...	...	...	...	...	...	...	...
11122789	...	...	...	...	...	...	...	...	...
11135978	...	...	...	...	...	...	...	...	...
11180361	...	...	...	...	...	...	...	...	...
11244501	...	...	...	4715.408 <sup>+411.622</sup> <sub>-203.023</sub>	0.269 <sup>+0.112</sup> <sub>-0.143</sub>	674.638 <sup>+58.702</sup> <sub>-38.804</sub>	331.369 <sup>+16.426</sup> <sub>-9.484</sub>	2.895 <sup>+0.342</sup> <sub>-0.914</sub>	-0.002 <sup>+0.000</sup> <sub>-0.000</sub>
11255667	...	...	...	...	...	...	...	...	...
11295347	...	...	...	...	...	...	...	...	...
11403032	...	...	...	...	...	...	...	...	...
11409673	...	...	...	5483.304 <sup>+199.637</sup> <sub>-143.780</sub>	0.972 <sup>+0.009</sup> <sub>-0.011</sub>	1566216.412 <sup>+259342.620</sup> <sub>-189283.693</sub>	1.82.402 <sup>+1.92</sup> <sub>-1.396</sub>	...	...
11447053	...	...	...	...	...	...	...	...	...
11453915	...	...	...	...	...	...	...	...	...
11560447	...	...	...	...	...	...	...	...	...

Table 3 continued

Table 3 (*continued*)

KIC	$P_{bin}$ (days)	$P_3$ (days)	$e_3$	$P_3^*$ (days)	$e_3^*$	$a^*$ (min)	$\omega^*$	$A$	$B$
11572643	...	...	...	2290.326 <sup>+48.331</sup> <sub>-46.637</sub>	0.503 <sup>+0.314</sup> <sub>-0.198</sub>	1129.003 <sup>+56.179</sup> <sub>-112.310</sub>	15.912 <sup>+39.195</sup> <sub>-14.694</sub>	...	...
11616594	...	...	...	...	...	...	...	...	...
11649962	...	...	...	...	...	...	...	...	...
11769801	...	...	...	...	...	...	...	...	...
11859811	...	...	...	...	...	...	...	...	...
11929266	...	...	...	...	...	...	...	...	...
11923629	...	...	...	...	...	...	...	...	...
11973705	...	...	...	...	...	...	...	...	...
12066630	...	...	...	...	...	...	...	...	...
12157387	...	...	...	...	...	...	...	...	...
12216817	...	...	...	1508.869 <sup>+27.582</sup> <sub>-41.085</sub>	0.619 <sup>+0.071</sup> <sub>-0.084</sub>	533.169 <sup>+48.895</sup> <sub>-41.912</sub>	323.187 <sup>+7.506</sup> <sub>-10.828</sub>	...	...
12255108	...	...	...	...	...	...	...	...	...
12257908	...	...	...	...	...	...	...	...	...
12268220	...	...	...	...	...	...	...	...	...
12305537	...	...	...	2039.912 <sup>+9.942</sup> <sub>-11.011</sub>	0.736 <sup>+0.086</sup> <sub>-0.038</sub>	2946.364 <sup>+654.431</sup> <sub>-207.403</sub>	5.025 <sup>+1.976</sup> <sub>-2.009</sub>	-0.757 <sup>+0.015</sup> <sub>-0.025</sub>	0.001 <sup>+0.000</sup> <sub>-0.000</sub>

## REFERENCES

- 944 Almeida, L., Sana, H., de Mink, S., et al. 2015, The  
 945 Astrophysical Journal, 812, 102
- 946 Almeida, L., Sana, H., Taylor, W., et al. 2017, Astronomy  
 947 & Astrophysics, 598, A84
- 948 Applegate, J. H. 1992, The Astrophysical Journal, 385, 621
- 949 Applegate, J. H., & Patterson, J. 1987, The Astrophysical  
 950 Journal, 322, L99
- 951 Borucki, W. J., Koch, D., Basri, G., et al. 2010, Science,  
 952 327, 977
- 953 Cehula, J., & Pejcha, O. 2023, MNRAS, 524, 471,  
 954 doi: [10.1093/mnras/stad1862](https://doi.org/10.1093/mnras/stad1862)
- 955 Conroy, K. E., Prša, A., Stassun, K. G., et al. 2014, The  
 956 Astronomical Journal, 147, 45
- 957 Correia, A. C., Boué, G., & Laskar, J. 2016, Celestial  
 958 Mechanics and Dynamical Astronomy, 126, 189
- 959 Czesla, S., Schröter, S., Schneider, C. P., et al. 2019, PyA:  
 960 Python astronomy-related packages.  
 961 <http://ascl.net/1906.010>
- 962 Foreman-Mackey, D., Hogg, D. W., Lang, D., & Goodman,  
 963 J. 2013, Publications of the Astronomical Society of the  
 964 Pacific, 125, 306
- 965 Gimenez, A., & Garcia-Pelayo, J. M. 1983, Astrophysics  
 966 and Space Science, 92, 203
- 967 Hulse, R. A., & Taylor, J. H. 1975, The Astrophysical  
 968 Journal, 195, L51
- 969 Irwin, J. B. 1952, The Astrophysical Journal, 116, 211
- 970 Lightkurve Collaboration, Cardoso, J. V. d. M., Hedges, C.,  
 971 et al. 2018, Lightkurve: Kepler and TESS time series  
 972 analysis in Python, Astrophysics Source Code Library.  
 973 <http://ascl.net/1812.013>
- 974 Lomb, N. R. 1976, Astrophysics and space science, 39, 447
- 975 Martin, D. V., & Triaud, A. H. 2015, Monthly Notices of  
 976 the Royal Astronomical Society: Letters, 455, L46
- 977 Pietrzyński, G., Gieren, W., Graczyk, D., et al. 2012,  
 978 Proceedings of the International Astronomical Union, 8,  
 979 169
- 980 Prša, A., Guinan, E., Devinney, E., et al. 2008, The  
 981 Astrophysical Journal, 687, 542
- 982 Ricker, G. R., Winn, J. N., Vanderspek, R., et al. 2014,  
 983 Journal of Astronomical Telescopes, Instruments, and  
 984 Systems, 1, 014003
- 985 Scargle, J. D. 1982, The Astrophysical Journal, 263, 835
- 986 Sterken, C. 2005, in The Light-Time Effect in Astrophysics:  
 987 Causes and cures of the OC diagram, Vol. 335, 3
- 988 Tout, C. A., & Hall, D. S. 1991, Monthly Notices of the  
 989 Royal Astronomical Society, 253, 9
- 990 VanderPlas, J. T. 2018, The Astrophysical Journal  
 991 Supplement Series, 236, 16